INFORMATION TO USERS

This manuscript has been reproduced from the microfilm master. UMI films the text directly from the original or copy submitted. Thus, some thesis and dissertation copies are in typewriter face, while others may be from any type of computer printer.

The quality of this reproduction is dependent upon the quality of the copy submitted. Broken or indistinct print, colored or poor quality illustrations and photographs, print bleedthrough, substandard margins, and improper alignment can adversely affect reproduction.

In the unlikely event that the author did not send UMI a complete manuscript and there are missing pages, these will be noted. Also, if unauthorized copyright material had to be removed, a note will indicate the deletion.

Oversize materials (e.g., maps, drawings, charts) are reproduced by sectioning the original, beginning at the upper left-hand corner and continuing from left to right in equal sections with small overlaps.

Photographs included in the original manuscript have been reproduced xerographically in this copy. Higher quality 6" x 9" black and white photographic prints are available for any photographs or illustrations appearing in this copy for an additional charge. Contact UMI directly to order.

Bell & Howell Information and Learning
300 North Zeeb Road, Ann Arbor, MI 48106-1346 USA
800-521-0600

The Effect of Flotation Deinking Process Parameters on Air Bubble Size and Deinking Efficiency

by

Christopher Patrick Sauvé

A thesis submitted to the Faculty of Graduate Studies and Research in partial fulfillment of the requirements for the degree of Master of Engineering

Department of Chemical Engineering
McGill University
Montreal, Quebec, Canada

September 1999

ACKNOWLEDGEMENTS

First and foremost, I wish to thank my co-supervisors, Dr. Theo van de Ven and Dr. Gil Garnier, for their support, guidance and insight. I would also like to give thanks to Dr. Gilles Dorris and his staff, particularly Natalie Pagé, for their tremendous help in Chapter 3's experiments.

I would also like to extend a great deal of appreciation to my colleagues whose suggestions were very valuable. In particular, I wish to thank: Dr. Jerzy Petlicki, Yanjun An, Christopher Hammock, Alois Vanerek, Craig Murphy and Roger Gaudreault.

I would like to very much thank Alois Vanerek for his photography assistance.

I would like to thank the personnel of the McGill Pulp and Paper Research Center as well as the Machine Shop of the McGill Chemistry Department for their assistance. In addition, I would like to express my gratitude to the personnel at Paprican for their very valuable help, in particular, the Machine Shop, the Photography Department and Library Services.

I greatly appreciate the financial support attained from the National Centres of Excellence.

I would like to thank my family whose constant encouragement was invaluable to me throughout the attainment of this degree.

To my wife, Kathleen Whittaker, I cannot overemphasize how much your love and support meant to me throughout this work.

ABSTRACT

Many traditional laboratory-scale flotation cells lack the attribute of being hydrodynamically similar to the actual industrial flotation process. A device was built that simulated solely the air-injection section of an industrial flotation cell, in which industrial Reynolds numbers can be achieved. It was found that fluid velocity has a moderate effect on the bubble size distribution and surfactant concentration has a large effect. In addition, the presence of 0.2 % consistency TMP fibres or fines was found to have a small effect on the bubble size distribution.

The air-injection unit was then expanded into a functioning lab-scale flotation cell. The objective of these experiments was to investigate the effect of furnish type, air volume fraction and slurry velocity on the deinking efficiency. The 100% aged newsprint runs had considerably lower initial brightness, considerably higher initial ERIC, as well as a much lower Speck Removal after 30 minutes of flotation, compared to the runs using 70% fresh newsprint and 30% fresh magazine. Increasing the air volume fraction while keeping the suspension velocity constant, did slightly improve the deinking efficiency for the 100% aged NP case, however, did not result in any significant improvement for the 70% NP/ 30% MG case. It is believed that the increased shear forces associated with increasing the suspension velocity broke-up ink agglomerates that were in suspension into a larger number of smaller ink particles. Increasing the suspension velocity increased the rate of flotation.

RÉSUMÉ

La plupart des cellules de flottation utilisées en laboratoire ne reproduisent pas les conditions hydrodynamiques des systèmes de flottation industriels. Un appareil a été construit pour simuler la section d'injection d'air d'une cellule de flottation industrielle dans laquelle le nombre de Reynolds peut atteindre des valeurs comparable à celles de l'industrie. Les expériences ont montré que la vitesse du fluide affecte de façon modérée la distribution de tailles des bulles dans le fluide alors que la concentration en surfactant a un effet important. De plus, la présence de fibres ou de fines de pâte thermomécanique (PTM) a peu d'effet sur la distribution de tailles des bulles.

A partir de l'unité d'injection, un système de flottation complet a été monté en laboratoire. Le but des expériences est d'étudier l'effet du type de pâte, de la fraction de l'air dans le fluide ainsi que de la vitesse du fluide sur l'efficacité de désencrage. Le papier journal vieilli utilisé lors des expériences avait une blancheur initiale moindre et une valeur d'ERIC initiale bien plus élevée que celles d'un mélange de 70% papier ournal jeune et de 30% papier magazine jeune. L'enlèvement des points noirs après 30 min de flottation est bien plus bas pour le papier journal vieilli. L'augmentation de la fraction d'air pour une vitesse du fluide constante a légèrement amélioré l'efficacité de désencrage du papier journal alors qu'aucune amélioration significative n'a été remarqué pour le mélange. Nous croyons que l'augmentation des forces de cisaillement reliées à l'augmentation de la vitesse de la suspension permet de briser les agglomérats d'encre en suspension en une grande quantité de petite particules. De plus, l'augmentation de la vitesse de la suspension a augmenté la vitesse flottation.

TABLE OF CONTENTS

LIST OF FIGURES

Page

CHAPTER 1

Page

CHAPTER 1 (cont.)

CHAPTER 2

Page

CHAPTER 2 (cont.)

Page

CHAPTER 2 (cont.)

CHAPTER 3

LIST OF TABLES

CHAPTER 1

INTRODUCTION

1.1 JUSTIFICATION

Flotation deinking is a selective separation process in which hydrophobic (water-repellant) ink particles are removed from a wastepaper stream by becoming attached to gas bubbles, most commonly air, enabling them to be transported upward into a froth in the flotation cell. In a flotation cell design, three separate stages can be identified as aeration, mixing and separation.

Laboratory flotation deinking cells are commonly used for recycling research. A thorough comparative study of laboratory cells has not been done in the literature thus it is not known which best simulates the industrial process. As a result, no standard laboratory deinking cell or operating conditions exist in order to simulate mill conditions in the lab. There is a need for a laboratory flotation deinking cell that convincingly operates under industrially similar hydrodynamic conditions. Laboratory results attained with such a device could closely match those attained in industry.

Laboratory flotation deinking studies found in the literature have concentrated on the effects of various ink types, deinking chemicals and related studies. Not much information is available in the literature concerning the effect of physical parameters such as air volume or air bubble size on the deinking efficiency, although a few papers have been found [1,2]. Based on the lack of research in this area, a suitable study would be to investigate the effect of process parameters on the bubble size distribution attained within the air injection section of a flotation cell and on the overall deinking efficiency.

The overall objectives of this thesis are:

1) Develop and construct a laboratory-scale flotation cell which operates under industrially similar hydrodynamic conditions in the air injection section.
2) Investigate the effects of suspension velocity, the presence of fibres or fines, and deinking chemicals on the air bubble size distribution in the air injection section.
3) Investigate the effects of suspension velocity, aeration rates, and pulp type on the deinking efficiency of this novel laboratory-scale flotation cell.

1.2 LITERATURE REVIEW

1.2.1 Basic Deinking Principles

The term deinking is a general term referring to the removal of printing ink from a slurry of wastepaper in the recycling process. The ink is about 0.5-2% of the mass of the waste paper [3]. A second aim of the deinking process is to remove other objectionable non-fibrous contaminants such as coatings, adhesives and wet-strength resins [4]. The deinkability of a recycled pulp furnish will depend on the paper grade, on the nature and amount of ink in the waste paper and on the ink setting and printing processes.

Crow and Secor [5] describe the ten basic steps in the deinking process, including pulping, pre-washing heat and chemical loop, screening (coarse and fine), through-flow or reverse cleaning, forward cleaning, washing, flotation, dispersion, bleaching, and water recirculation and makeup. Not all of these steps are used in all recycled fibre plants, and the sequence in which they occur can vary. One possible deinking system that incorporates all of the basic ten steps is shown in Figure 1. In-depth descriptions of each of these ten basic deinking steps are available in the literature [3,5].

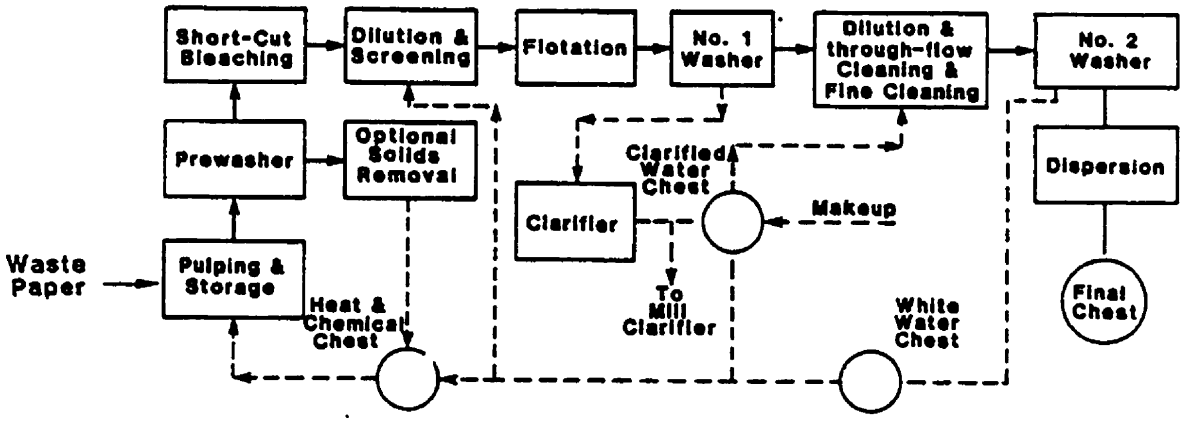

Figure 1. One possible arrangement of the ten basic deinking steps [5]

A simplistic description of the deinking process would be to break it down into two primary steps [6]. The first step occurs in the pulper in which ink is detached from

pulp fibres. The pulper acts essentially as a large blender to disperse pulp into an aqueous slurry. The removal of ink from the surface of cellulose fibres is promoted by mechanical action, chemical treatment, and thermal energy. Pulping may be done at low consistency (4-8%) or high consistency (>12%) using different rotors. The trend is towards high consistency pulpers due to improved contaminant removal efficiencies [7,8] and substantial savings in chemical, steam, electrical energy and to a reduced pulping time [4]. Also during the pulping process various mechanical devices separate unwanted contaminants from the recycled pulp. Such contaminants include long materials (e.g. baling wire, tapes, and plastic sheeting) and large heavy items (e.g. nuts, bolts and rocks). Both batch and continuous repulping processes are available. The batch repulping process is by far more common and some of its advantages include: better overall process control, easy effective blending of batches ensuring uniform pulp quality and mixing of chemicals, the ability to handle changes in incoming furnish quality, and lower chemical cost. The most attractive attribute of the continuous repulping process is a significantly greater production capability for a given unit size of pulper [9].

Step two follows in which the ink, which is dispersed in the aqueous phase, is separated from the pulp slurry. The challenge for the deinking mill is to remove these particles efficiently and in a cost-effective manner. There are two deinking processes by which this can be done: washing and flotation.

Washing is a process that mechanically rinses ink particles and other contaminants out of the pulp. Basically, the process is based upon the large difference in size between the fibres and the ink particles and consists of a series of alternating pulp dilution and thickening operations. These operations are carried out enough times to produce a clean pulp. During thickening of the pulp on a screen, the fibres are retained on the screen and the small contaminant particles pass through the filtration medium with the water phase. Almost all washing systems are based on a countercurrent flow so as to minimize water usage and chemical consumption. Washing equipment may take on a variety of forms such as rotary vacuum washers and double belt washers.

The second type of deinking process is flotation deinking and is the subject of this

research. Flotation deinking is a selective separation process in which hydrophobic (water-repellant) ink particles are removed from a wastepaper stream by becoming attached to gas bubbles, most commonly air, enabling them to be transported upward into a froth in the flotation cell. A basic schematic for a flotation deinking cell is presented in Figure 2.

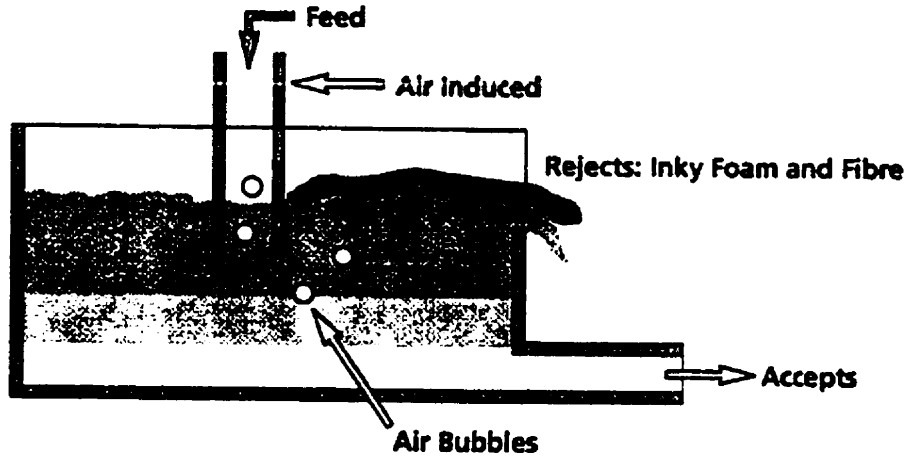

Figure 2. Schematic of a flotation deinking cell [11]

Flotation chemicals are used to make the ink or contaminant particles sufficiently hydrophobic to adhere to air bubbles introduced into the suspension. These air bubble/ink particle complexes then float to the surface where they are removed as a dirt-laden layer of froth in the rejects stream. So-called "cleaned" fibres exit the flotation cell in the accepts stream which is often fed into another flotation cell to undergo further deinking. During the flotation process some percentage of good fibres exit with the rejects stream. Most flotation systems recover some of these good fibres from the rejects stream in a subsequent secondary flotation stage. Typical volumetric flowrates of pulp suspension entering an industrial flotation cell vary upon model type, however, one unit operates at 20 000 L/min. The Reynolds number of the flow in the air injection pipe of one industrial flotation cell, the Escher Wyss CF cell, is 60 000 which indicates a turbulent flow regime. In a later section many industrial flotation deinking cells will be described.

As will be discussed later, washing is more effective than flotation in removing particles of small size (less than 10 microns). Due to this fact washing is an effective method to remove clay and other filler particles, thus making it a good process for the production of low ash content products, such as pulp for tissue production.

Also, the contaminant surface properties required for efficient removal also differ for washing and flotation. In wash deinking, small hydrophilic particles (e.g. flexographic inks) are preferred which remain well dispersed and have little tendency to associate with fibres or with each other. These attributes allow the particles to be carried-out with the water, flowing between fibres, during the dewatering or consistency-raising washing step. Completely opposite surface properties are required for flotation deinking. Required particle sizes for efficient removal by flotation are larger (10-100 microns) and the contaminant must be hydrophobic to adsorb at the air/water interface of a bubble. Flotation chemicals are used to heighten the ink particles' hydrophobicity.

New deinking mills may optimize ink removal efficiencies by using combined ink flotation and washing. The most common configuration is to use flotation first to remove the bulk of the ink, followed by a washing stage to remove the residual ink. This process utilizes the best of both worlds and is particularly effective for wastepaper containing various types of ink formulations. Approximately 10-20% of mills worldwide using a dual system use washing as the first stage followed flotation [3]. One disadvantage of this configuration is that many large ink particles that might have been removed by flotation would be dispersed prior to flotation. To further improve the removal of ink from wastepaper, mills primarily in Europe and Japan use flotation-wash-flotation systems.

1.2.2 Development of Flotation Technology

The original flotation deinking cells were designed on the basis of the equipment used in the mineral flotation industry. In flotation deinking the desired product are clean, hydrophilic fibres which settle on the bottom of the cell, whereas in mineral flotation the desired product are hydrophobic minerals that are concentrated in the froth. Due to the

fact that mineral flotation is a much older and larger industry than flotation deinking, a very large body of useful technical knowledge exists in the literature.

Mineral flotation became a patented process more than 120 years ago. On July 2, 1877, the Bessel brothers were granted a patent for "a process for purifying graphite". This is generally accepted as being the birth of modern froth flotation. As a result of this process, most sulphide ores, a large proportion of the salt minerals, and also raw materials such as iron ore and pit coal are currently enriched by flotation. It was not until 1955 that the first industrial flotation deinking cell became commercial in North America. In 1959, the first European installation started up.

Flotation deinking is more popular than wash deinking in Europe and Japan due to its much lower water consumption and minimal effluent. In contrast, the majority of deinking systems used in North America use washing technology because this separation technique traditionally produced cleaner pulps. Currently, due to increased awareness of environmental issues related to deinking effluent, and the production of improved flotation cells, new deinking installations in North America are predominantly of the flotation deinking type or a combination of both flotation and washing processes.

Flotation deinking has experienced a tremendous growth since the early 1970s. The world production of deinked pulp (DIP) increased four-fold during the period 1972-1981, from 1.5 million tons per year to 5.9 million tons per year. By 1991, the world DIP production experienced a three-fold increase to 17.6 MTY. By 2001, it is estimated that this figure will increase to 31.0 MTY [10].

Deinked pulp is utilized in the production of the following three main paper grades: newsprint, tissue, and printing and writing. The 1991 statistics dictate that of the 17.6 million tons of DIP produced that year, 46% was used in newsprint, 25% in tissue, 13% in printing and writing, with the remainder being used in other paper board grades and in market pulp [11].

Numerous reviews of flotation deinking technology have been written including Dr. H.E Ortner's which was published in the 1981 TAPPI Recycled Fibre Monograph [12]. Since then there have been a number of other review articles published [11, 13-19].

In addition to being a separation process for ink from wastepaper and for minerals in metallurgy, froth flotation and modifications of the flotation process have many applications in other fields. These include the recovery of bitumen from tar sands, flotation of solids from white water in papermaking, and the removal of oil or organic contaminants from water or aqueous solutions [19].

1.2.3 Flotation Theory

Numerous approaches have been followed in the literature for creating a useful model of the flotation process. One common flotation model is referred to as the *Probabilistic Model* in which the flotation process is reduced to its essential elementary steps. Schumann [20] based his probability theory on Gaudin's [21] hypothesis that the flotation process can be divided into three major steps. Schumann expressed the probability of the successful flotation of a particle as being the product of the probabilities of the three main flotation steps. It is assumed that the individual probabilities for a given particle are not correlated:

$$P_{flotation} = P_{(C)}P_{(A)}P_{(R)} \qquad (1)$$

where $P_{(C)}$ is the probability of successful ink particle-bubble collision, $P_{(A)}$ is the probability of adhesion of the ink particle and the bubble, and $P_{(R)}$ is the probability of stabilization and removal of the ink particle-bubble complex from the pulp. During a successful collision between an ink particle and an air bubble a thin film is created between them. For attachment to be accomplished the thin film must rupture, and the three-phase contact expand within this *contact time*. Therefore the *induction time*, which is the sum of the rupture time and possibly the time for three-phase contact expansion, must be smaller than the contact time [28].

The flotation model by Tomlinson and Fleming [22] redefined the last probability in equation (1) leading to an overall probability in the following form:

$$P_{flotation} = P_{(C)}P_{(A)}P_{(E)}P_{(F)} \qquad (2)$$

where $P_{(E)}$ is the probability of retention and elevation of the ink particle through the liquid, and $P_{(F)}$ is the probability that the particle is retained by the froth.

Some models simply define $P_{(E)}$ as being equal to $(1-P_{(D)})$ where $P_{(D)}$ is the detachment rate [23].

Other flotation models are referred to as *Chemical Kinetic Models*. These models are based on an analogy between chemical reaction kinetics and flotation due to the fact that bubble-particle aggregates form as a result of collisions. Similarly, in chemical reaction kinetics the elementary action is a collision between two spheres. Examples of Chemical Kinetic Models can be found in the literature [24-26].

Mixed Models of the flotation process try to combine the concepts used in the Chemical Kinetics Model with those in the Probabalistic Models. One commonly accepted model of this nature can describe ink floatability by expressing the variation of the ink particle number per unit time in a given volume of apparatus. Such variation depends on the number of particle/bubble collisions per unit volume, per unit time (represented by

$z_c \cdot n_p \cdot n_b$, where z_c is a rate constant and n_p and n_b are the number of particles and bubbles, respectively) and on the individual probabilities of interaction, mentioned previously $P_{(C)}$, $P_{(A)}$, and $P_{(R)}$:

$$dn_p / dt = - z_c\, n_p\, n_b\, P_{(C)}\, P_{(A)}\, P_{(R)} \qquad (3)$$

$P_{(C)}$ is dependent on particle size and bubble size as well as system hydrodynamics; $P_{(A)}$ on the ratio of ink and bubble size, hydrophobicity and contact time; and $P_{(R)}$ on particle weight, contact angle, consistency, and flow hydrodynamics [4]. As a result of such dependencies, the efficiency of the flotation process is influenced by the surface and colloidal chemistry of the system as well as the types of equipment used for the gas dispersion, mixing and froth separation. Excellent papers exist that go into detail describing the probability of each elementary step [27,28]. The reader is referred to the literature for further reading on modelling methods of the flotation deinking process [28-31].

1.2.4 Industrial Flotation Cells

A flotation cell is essentially comprised of three major zones: aeration, mixing and separation. The amount of air and bubble size distribution is adjusted within the aeration zone. In the mixing stage, microturbulance is created to increase collision frequency between air bubbles and ink particles. Air bubbles rise to form a froth in the separation zone which is subsequently removed from the cell. Due to the increasing importance of flotation deinking, cell manufacturers continually update the design of their cells to reduce energy, save space, improve deinking efficiency and reduce the loss of valuable fibres.

The ink removal efficiency has been shown to improve if a combination of dissolved and dispersed air is used [32]. Flotation is usually operated using a number of cells connected in series through which the suspension passes in a steady flow [16]. In addition, there are typically two stages to the flotation process. The primary stage is used for deinking, while in the secondary stage the fibres from the froth of the primary stage are retrieved.

Numerous reviews of modern flotation deinking cell technology exist in the literature detailing their principles of operation, configuration and performance [11,16,18,33-35].

The major developments in flotation deinking cell technology have occurred since the end of the 1970's. This evolution is well documented in the literature [11].

Flotation deinking cells are currently being manufactured and distributed worldwide by the following nine companies: Beloit, Comer, Kamyr, Kvaerner Hymac, Lamort Fiberprep, Shinama, Thermo Black Clawson, Voith Sulzer, and Wemco.

Table 1 summarizes the primary features of some of the mainstream flotation cells. Please note that since the production of Table 1, Black Clawson has come to be known as Thermo Black Clawson; and Voith and Escher Wyss have merged to become known as Voith Sulzer.

A description of the eight cells included in Table 1 plus six additional leading flotation deinking cells follows.

Beloit PDM

The Beloit Pressurized Deinking Module (PDM) design is shown schematically in Figure 3. The PDM was the first flotation cell to operate under pressure. In conventional atmospheric cells, as the air bubbles collapse to form the inky foam, the air escapes into

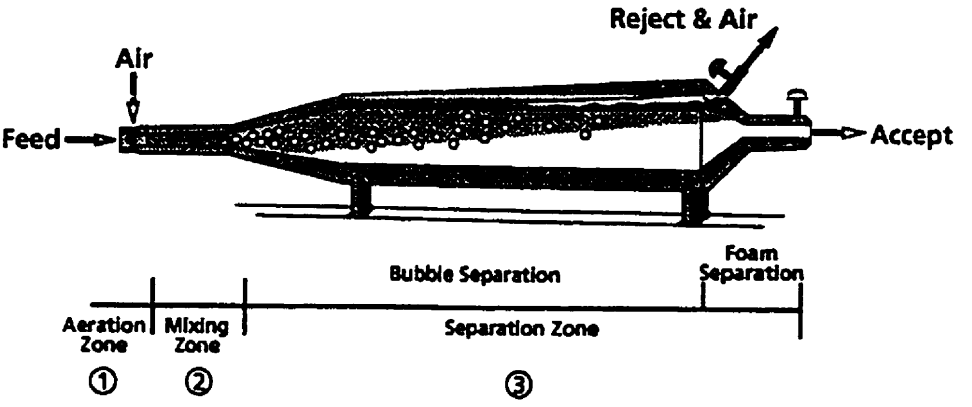

Figure 3. Cross-section of a Beloit PDM Flotation Cell [11]

the atmosphere. The foam is then commonly removed by a weir overflow.

Due to the fact that a moving body of pulp is used to transport the foam over the weir, fibre losses are increased and secondary reject treatment stages are required to recover this good fibre. The novel feature of the PDM is that the air is captured and the foam is removed in the separation zone by the internal pressure of the unit. This foam removal system greatly reduces fibre rejects and therefore no reject stages are required. Also, the air in the rejects stream can be directed out of the building eliminating air pollution problems.

In a flotation cell design, three separate stages can be identified as aeration, mixing and separation. In order to maximize ink removal, the PDM design separates and optimizes each stage independently of each other.

Finally, air is introduced into the PDM with the use of compressed air, eliminating any possible plugging problems that occur with conventional venturi-style injectors. A paper by McCool and Carrol [36] on the PDM mentions that the pressurized air injector

also causes some of the air to be dissolved into the pulp which may come out of solution and be attached to the ink particles. This phenomenon may increase the ink removal rate.

Table 1. Summary of Features for Some Common Flotation Deinking Cells [11]

Supplier	Beloit	Black Clawson	Escher Wyss	Kamyr	Lamort Fiberprep	Voith
1. Cell Name	PDM	IHI/BC	1) CF 2) CFS 3) CFC	Gas Sparged Cyclone	Verticel DA	Elliptical Multi Injector
2. Year Introduced	1987	1991	1) 1984 2) 1989 3) 1992	1991	1985	1990
3. Shape of Body	Tubular	Rectangular	Cylindrical	Cyclone	Cylindrical	Elliptical
4. Pressurized	Yes	No	No	Yes	No	No
5. Vessel Body	Sealed	Enclosed	Open CFC-Enclosed	Sealed	Open	Enclosed
6. Internal Agitator	No	Yes Turbine	No	No	No	No
7. Stock Feed Line	Single	Single	Multi	Single	Multi	Multi
8. Air Feed	Compressed	Compressed	Induced	Compressed	Induced	Induced
9. Reject Removal	Pressurized	Gravity + Scrappers	Gravity	Pressurized	Vacuum	Gravity
10. No. of Stages Primary Secondary	1-4 0	1-2 0-1	1-6 0-2	1-3 0-1	2 0	4-6 1-2
11. Deinked Grades	All	Mainly News	Mainly White	White	All	Mainly News
12. Estimated No. of Systems (April 1992)	25	4	50	1	50	20

Thermo Black Clawson IHI/BC

The Thermo Black Clawson IHI/BC flotation cell consists of a large vessel with rounded corners and has a very large volume (50 m^3 or 13 000 US gal). The cell design is

shown in Figure 4. The cell combines long retention time, large volume of air and high shear mixing to maximize ink removal.

Pulp stock is fed in at the bottom of the cell and the accepts leave the cell at the opposite corner. A blower feeds air into two high-speed turbines located near the bottom of the cell and run its entire length. The turbines mix a large volume of air into the stock with high shearing forces. Internal baffles force the stock to pass around the turbines a number of times, aerating it repeatedly. This flow of air helps to push the foam, which is normally 12-24 inches deep due to the high amount of aeration, to the rejects outlet,

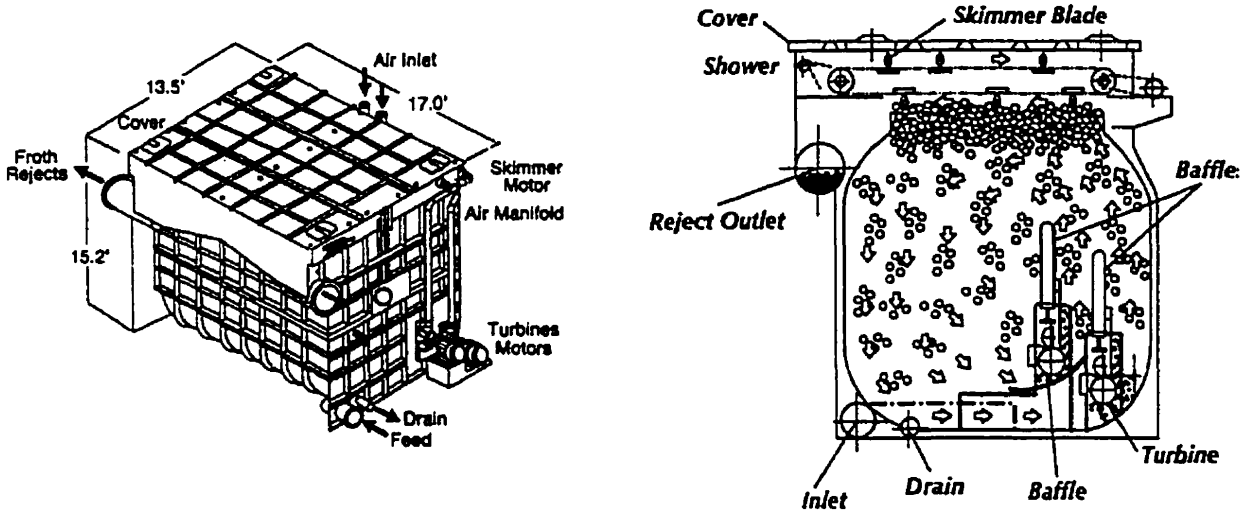

Figure 4. Top and cross-sectional views of the Thermo Black Clawson IHI/BC [11]

where it is skimmed by mechanical paddles into a rejects trough. The deep foam level ensures efficient ink removal, minimizes fibre loss and allows for precise level control. Within the trough, showers are used to break up the foam. These cells operate using an extremely high air:pulp volume ratios (up to 10:1). Increased flotation efficiencies are claimed to be attained due to this fact and the system requires only one primary stage and one or no secondary stage.

Escher Wyss CF/CFS/CFC Cells

The CF (Compact Flotation) Cell is designed for the removal of small ink particles,

and the CFS (Compact Flotation-Speck Removal) Cell was designed for the removal of large ink particles. Both cells are cylindrical with tangential stock feed through multiple lines, and foam is removed by gravity overflow. The primary differences between these cells are in the aeration sections and in the tank construction.

The CFC cell introduced in 1992 is a modification of the CF and the CFS cells. It is a totally enclosed modular design. It may be installed in either a single cell or a stacked two-cell arrangement. Because it's stacked design is self-supporting, it is easier and less expensive to install and also saves floor space. A schematic of the CFC is shown in Figure 5.

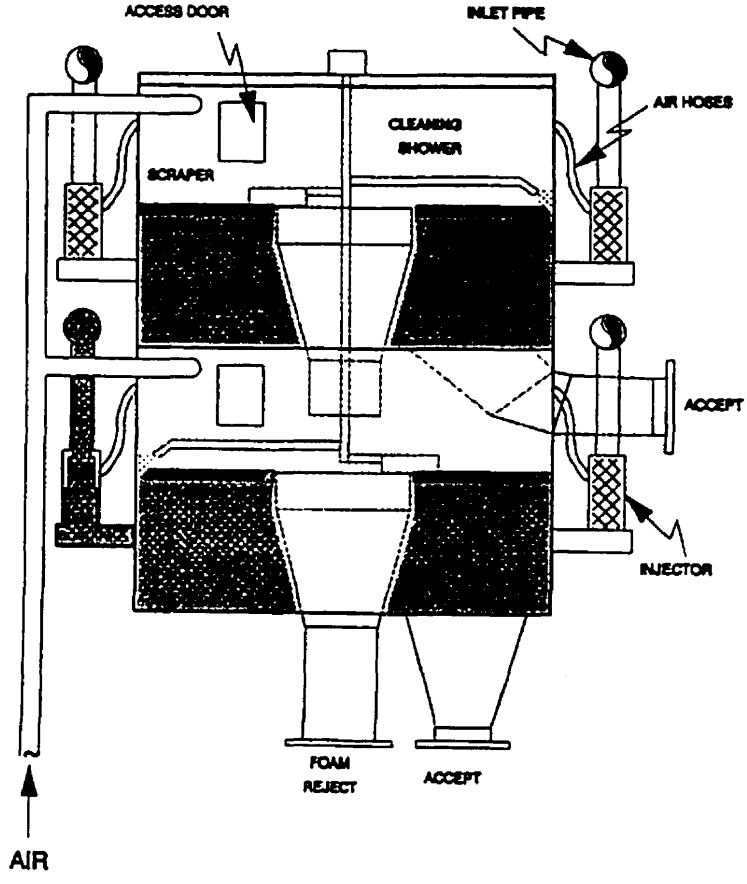

Figure 5. Escher Wyss CFC cell [11]

Two factors are claimed by the manufacturer as being the keys to the efficiency of

Escher Wyss cells. Firstly, the mixing section uses a patented, step-diffuser aeration element based on Escher Wyss headbox technology, shown in Figure 6. As the grey stock flows past the air inlet, air is aspirated into the pulp slurry.

As stock travels through the diffuser and approaches the tank inlet, turbulence grows, creating improved stock/air mixing and increasingly larger bubbles. This controlled, sequential coalescing removes ink particles to as small as ten microns and up to 500 microns in size. Varying numbers (depends on cell size) of step diffusers are located vertically around the circumference of the cell.

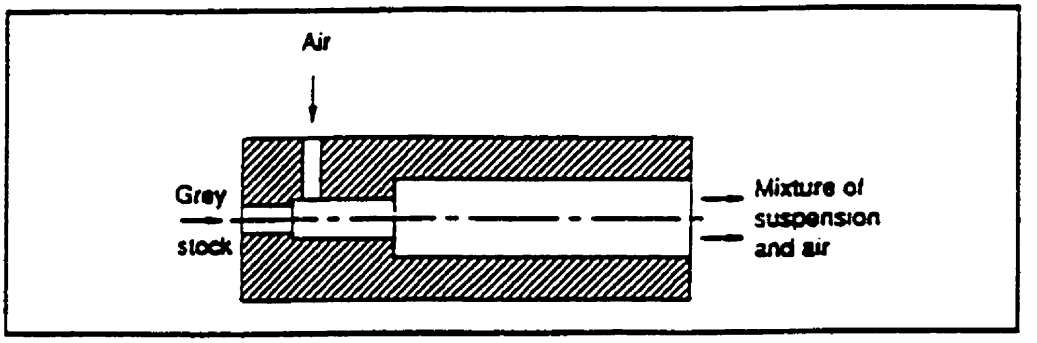

Figure 6. The Escher Wyss step diffuser design [18]

Secondly, the aerated stock is fed into the cell just below the surface of the pulp, allowing air bubbles carrying ink particles to quickly rise to the surface. The tangentially fed stock enters the cell with a slight circular motion to ensure that the foam created in the cell is directed to a central overflow. Showers are located above the central overflow to breakdown the foam. Secondary cells may be required with larger systems.

The CFC Flotation Cell comes in 12 models, either as space saving, stacked systems, or in single units. Capacities range up to more than 8000 GPM.

Kamyr Gas Sparged Cyclone (GSC)

The Kamyr Gas Sparged Cyclone (GSC) is a pressurized flotation cell developed at the University of Utah originally for mineral flotation. The cell design is shown in

Figure 7.

The stock enters the unit tangentially at the top, and the accepts leave at the bottom apex. The stock spirals down the cell against a porous wall. The thin layer of pulp reaches a maximum thickness of less than 5 centimetres.

Compressed air forced through the porous wall produces bubbles that become attached to ink particles. These complexes migrate to the central air core and produce an inky froth that exits via the top of the unit. The short bubble path to the reject area increases the probability of successful ink transport to the reject area before particle detachment from the bubble can occur. Also, thin layer pulp flotation allows for successful deinking at higher consistencies, up to 3%.

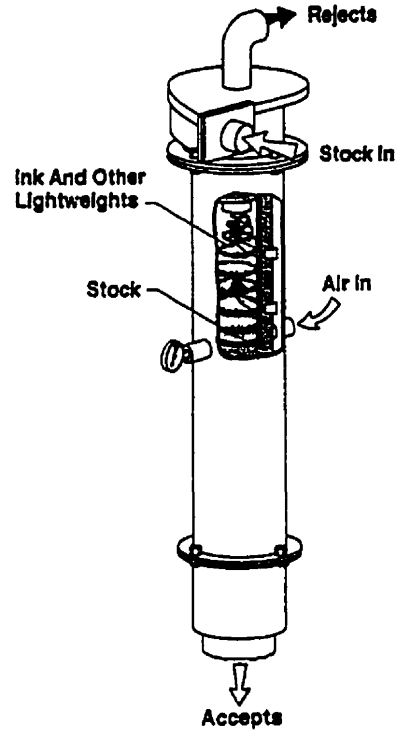

Figure 7. The Kamyr GSC (gas sparged cyclone) [11]

Lamort Fiberprep Double Action (DA) Verticel

The Lamort Fiberprep Double Action (DA) Verticel is a cylindrical cell with a tangential feed. A cross-sectional view of the cell is shown in Figure 8. The typical

system consists of two cells installed in series. The Verticel was the first cell to divide the feed stock into separate streams and apply multi-aeration to each of the streams. This design, which improves the mixing of pulp and air, was later implemented in Escher Wyss and Voith cells.

Another unique feature of the Verticel is that it uses double aeration. That is, the accepts stock is returned to the cell, and more air is added in the process with the use of venturi-type injectors. This improves the deinking efficiency of the cell.

The Verticel was also the first flotation cell to use vacuum to remove inky foam rejects. This increased the yield of the cell and eliminated the need for secondary cells.

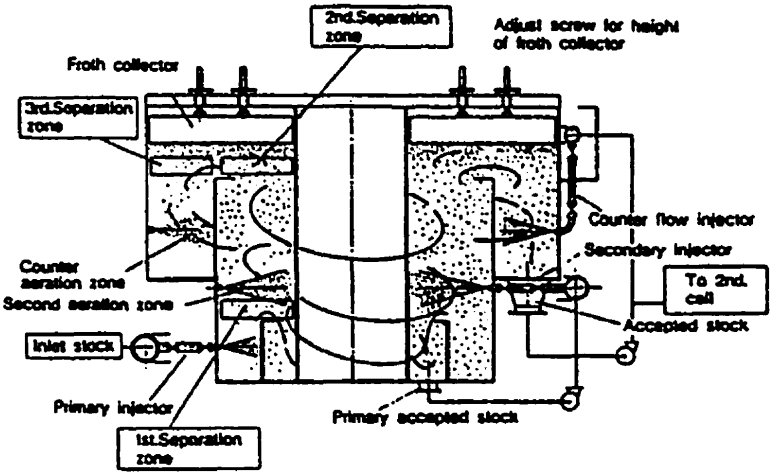

Figure 8. Cross section of the Lamort Fiberprep DA Verticel [11]

Voith Multi-Injector Elliptical Cells

These cells are comprised of single flotation cells arranged one after the other. The cell, shown in Figure 9, has the form of a horizontal elliptical cylinder with an integrated accepts outlet and controllable foam overflow. The number of these cells required is dependent on the raw material and throughput desired.

The accepts of each cell are pumped into the vertical injectors of the next cell. Air at atmospheric pressure is drawn into these injectors, mixed with the pulp slurry and dispersed into the flotation cell. The ink-laden froth that forms flows into a collecting

channel. Some stock overflow is usually required to maintain a constant movement of foam toward the foam channel, which usually results in the need for secondary cells. Shower pipes are also located in the foam channel to breakdown the foam for easier handling.

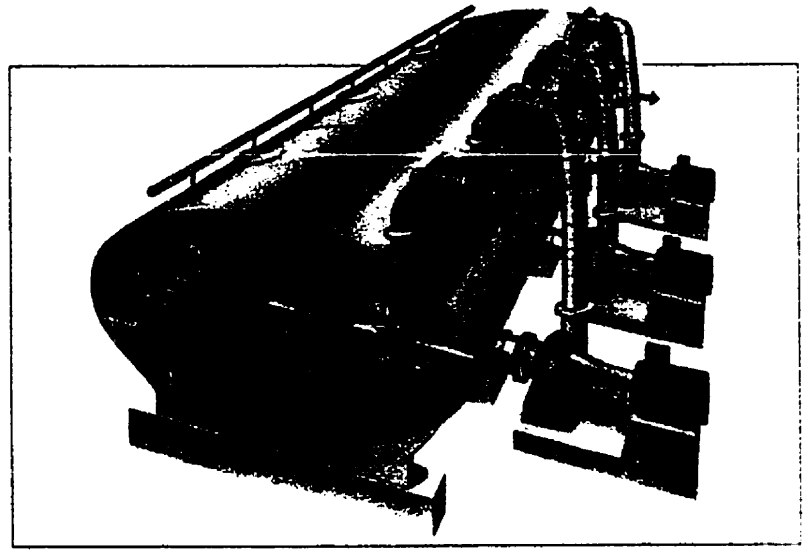

Figure 9. The Voith Multi-Injector Elliptical Cells [11]

Wemco

The Wemco cell was originally designed for the mineral industry and is now used for pulp deinking. The Wemco cell generates the air bubbles through a rotor which is submerged into the stock. The rotor speed and submergence depth can be altered to attain the optimum bubble size distribution for ink removal. The 1000 cubic foot cell model occupies 140 square feet of floor space and utilizes 60-75 hp while circulating the stock at 330 feet per minute [18].

Shinhama Hi-Flo

Another flotation cell in use is the Shinama Hi-Flo flotation cell [37]. This Japanese cell is a hydrocyclone similar to the Kamyr GSC, however, the Hi-Flo is larger and does not have a porous media. A Hi-Flo unit is shown in Figure 10.

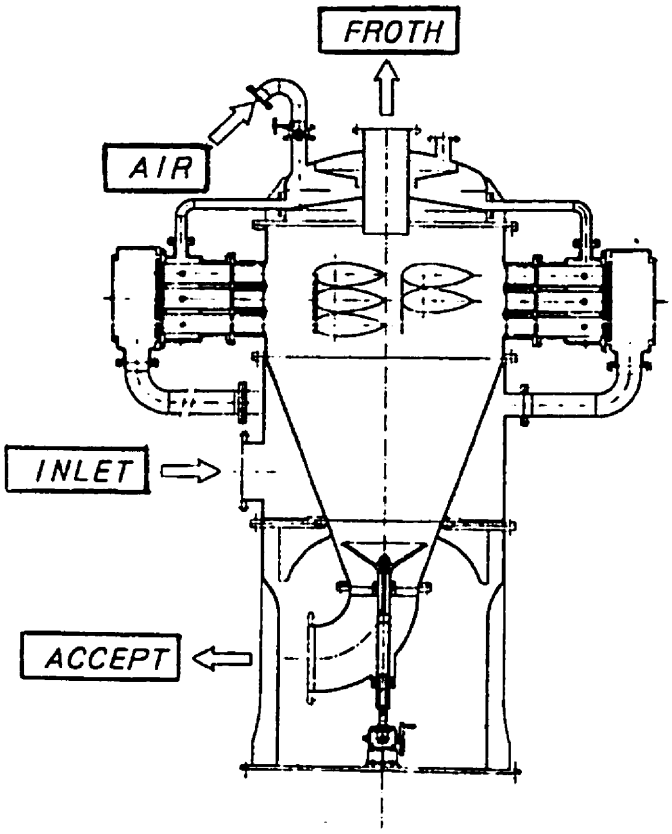

Figure 10. The Shinhama Hi-Flo Flotation Cell [11]

Recent Flotation Cell Designs

Comer Spidercel

The Comer Spidercel, shown in Figure 11, offers a unique approach to deinking. It utilizes reactor technology combined with multi-level air:stock injection applied to flotation deinking. This is said to yield higher ink particle removal efficiencies over a much wider range of particle sizes [38].

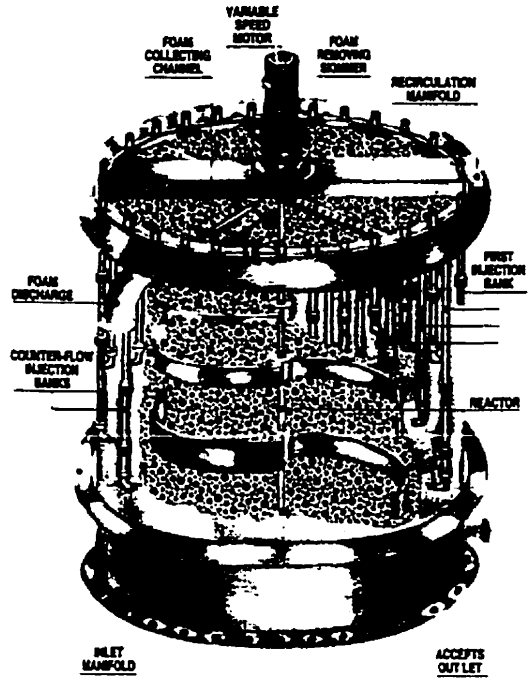

Figure 11. The Comer Spidercel [39]

The body of the Spidercel is cylindrical with a conically-shaped bottom to ensure adequate blending before recirculation. The reactor consists of a variable-speed rotating shaft with blades situated just below three injection levels. The blades help to release additional micronized bubbles at each level. The foam removal system is a scraper and discharge trough situated at the top of the cell. The Spidercel is manufactured in seven different sizes ranging from about 15 to 225 bone dry tonnes per day [38].

Kvaerner Hymac Flotation Column

The Kvaerner Hymac Flotation Column, shown in Figure 12, uses technology extensively used in the mining industry and has adapted it for use with wastepaper deinking. The pulp slurry is injected about one-third from the top of the cell and it travels down in the column while the air injected from the base rises counter-currently to the stock. An ink-laden foam forms at the top of the column and is removed by a scraper.

The cell is typically 5-7 meters high and 1.5 - 4.6 meters wide [40]. The cell manufacturers claim that flotation column technology provides low operating and capital costs (electricity, yield loss, space requirements, possibilities for outside building) and leads to a simplification of the whole flotation process in deinking plants [41]. Air is injected into the cell with the use of uniformly distributed porous spargers which produces a wide range of bubble sizes for high ink removal efficiency and low chemical consumption. The cell is totally enclosed to capture air emissions.

Thermo Black Clawson MAC Cell

The MAC Cell, shown in Figure 13, is the successor of the Verticel previously discussed. The manufacturer claims that one MAC Cell's increased flotation efficiency is equivalent to the use of two or three Single-Aerated (SA) or Double-Aerated (DA) Verticels in series. A single MAC cell contains internally the required number of flotation stages in series. As a result, the Mac Cell is a space-saving cell having a maximum height of 3.8 m and a maximum diameter of 7.8 m. Air is added into the cell using Autoclean injectors, which the manufacturer claims are unpluggable. The cell is also marketed as requiring 40% less power than the Verticel [42].

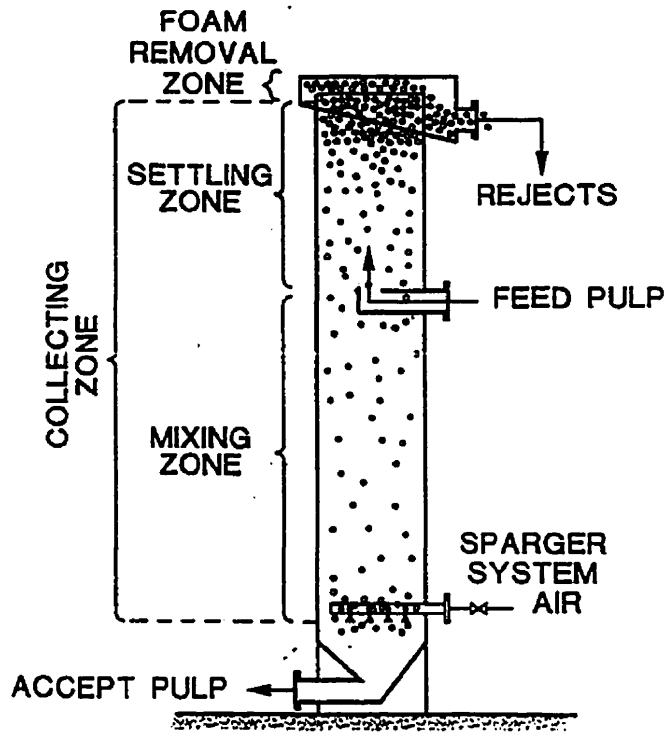

Figure 12. The Kvaerner Hymac Flotation Column [40]

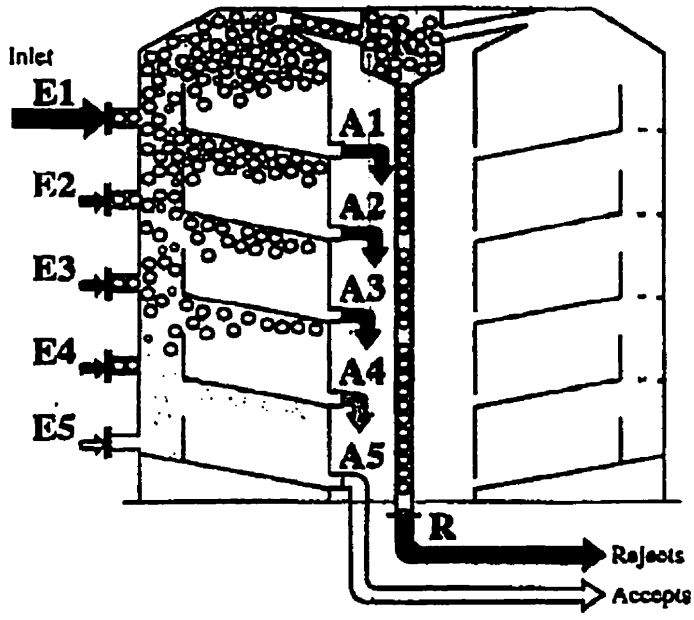

Figure 13. The Thermo Black Clawson MAC Cell [42]

Voith Sulzer Ecocell

The Voith Sulzer Ecocell, shown schematically in Figure 14, operates very similarly to the Voith Elliptical Multi Injector but incorporates some technological advantages of the Escher-Wyss CF cell. It is claimed to effectively remove a wide range of printing ink particle sizes (approximately 5-500 micrometers). The cell is totally closed with an internally located aeration element ensuring a closed process air circuit. The large aeration element in the Venturi-style injectors prevent plugging. A secondary flotation cell is recommended to minimize fibre loss. The EcoCell can be optionally equipped with a FrothVac for the destruction of difficult foam.

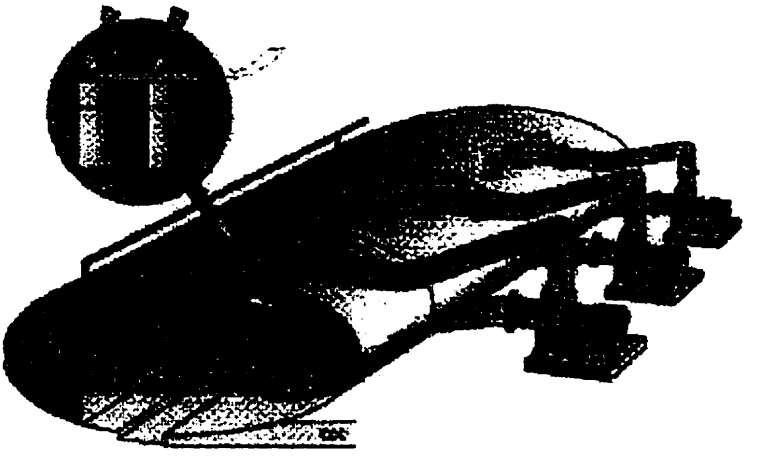

Figure 14. The Voith Sulzer Ecocell [43]

1.2.5 Laboratory-Scale Flotation Cells

Laboratory flotation deinking cells are commonly used for recycling research. Some of the variables that are studied include: residence time in the cell, number of passes through the cell, air volume, air bubble size, temperature, stock consistency, water quality, the type and amount of soaps or surfactants added. There is currently a wide variety of laboratory-scale flotation deinking cells being used. Many of these cells are manufactured by mill-scale equipment suppliers (e.g. Voith, Lamort Fiberprep, Denver). Different brands of laboratory units operate under different conditions, for example, different volumes of pulp are used. The suspension volumes typically used in such cells

is between 1.3 and 28 L, although one 250 L unit exists. Even when the same brand and model of laboratory units are used, the operating conditions may be different, when operated by different research groups. Therefore, because no standard cell or operating conditions have been established, comparisons of results from different groups are difficult.

The majority of laboratory cells have a turbulent zone at the base of the cell, which prevents the sedimentation of dispersed particles and promotes particle-bubble collision frequencies and thus particle-bubble adhesion. However, it has been found that excessive mixing may lead to the detachment of the particle from the bubble [44]. At the top of most laboratory cells is a quiescent zone, which allows for effective froth removal either manually or by a powered skimmer. The quiescent zone also discourages recirculation of the inky froth into the suspension being deinked. A thorough comparative study of laboratory cells has not been done thus it is not known which best simulates the industrial process. Several papers can be found in the literature that discuss current laboratory deinking practices [1, 2, 45, 46].

Laboratory flotation experiments have concentrated on the effects of various ink types, deinking chemicals and related studies. Not much information is available in the literature concerning the effect of physical parameters such as air volume or air bubble size on the deinking efficiency, although a few papers have been found [1,2]. Some existing cells have inadequate control of various physical parameters such as volume of air intake, air bubble size, and air bubble size distribution.

Air is introduced into most laboratory cells by a rotor-stator principle. The air for flotation is taken in by a rotating stirrer (rotor) and distributed by static elements (stator). Some existing systems also use pressurized air for the flotation process, commonly in combination with a rotor for air distribution within the pulp.

The presence of an internal rotor in many laboratory flotation cells, and the lack of them in the vast majority of industrial cells, can lead to differences in flotation efficiencies. For example, variations of the rotor rotation speed significantly affects the flow pattern in the cell. Increasing the rotation speed increases the turbulence in the cell

and may hinder the successful flotation of air bubble/ink particle complexes to the froth. High turbulence in the flotation cell can also lead to a partial recirculation of the froth into the pulp suspension, thus decreasing the flotation efficiency. In addition, increased shear caused by the rotor could break ink particles down into a smaller size, which may be more difficult to float. Also, this increased shear may release ink particles that were still attached to fibres, which might not have occurred in an industrial flotation unit due to the lack of rotor shear. For these reasons, the presence of an internal rotor within a laboratory cell may make comparisons with industrial cells difficult.

Based on some of the above arguments, Ackerman et al. [1] listed the requirements of a laboratory flotation cell as being: **(1)** simple, sturdy, and self-cleaning design **(2)** aeration without any stirrer **(3)** control of air supply, bubble size, and bubble-size distribution **(4)** formation of froth not affected by counter-mixing with the suspension **(5)** continuous froth removal.

A brief description of six commercially available laboratory deinking cells now follows.

Voith E Cell

The Voith E cell, shown in Figure 15, is made of plexiglass and is a scaled-down version of Voith's industrial flotation cells. Air is introduced into the cell from the air Venturi plexiglass injector. The froth is manually removed by scraping it across the overflow weir. The cell is available in two sizes, 18 litres (type E-18 V) and 250 litres (type E-250 V).

Lamort Fiberprep LAM'DEINKIT Cell

The Fiberprep/Lamort LAM'DEINKIT is a laboratory unit which combines a

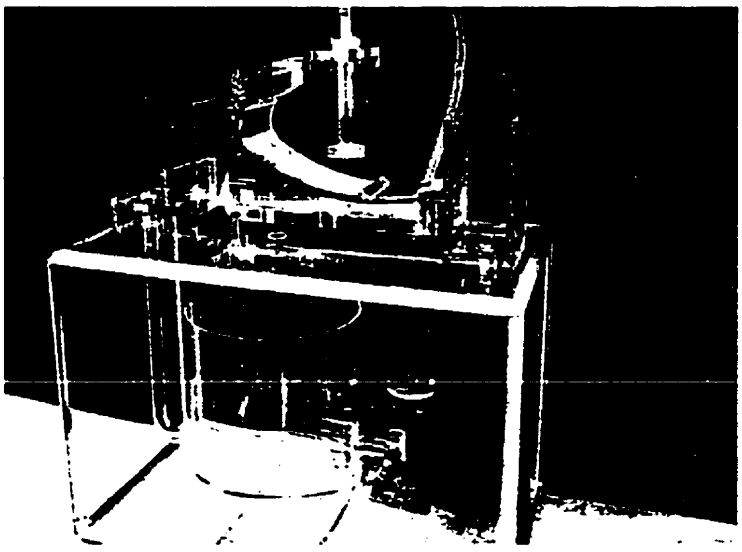

Figure 15. The Voith E Laboratory Flotation Cell (type E-18 V) [47]

laboratory sized high consistency pulping unit with a laboratory flotation deinking unit. With this unit it is possible to evaluate the pulping action as well as the ability to float this material after pulping. The unit is easily converted from a pulper to a deinking unit in a matter of minutes. To convert the unit to a flotation cell, the cover is removed, a low profile, flat rotor is installed designed to mix air with stock, a perforated air-suction column is installed over the flat rotor, and a froth collection collar is placed over the top rim of the pulper tank. The speed of the motor is switched to high speed for the flotation operation.

Flotation experiments are run with pulp suspension having a consistency between 0.8-1.3%. During flotation the rotor speed is 1440 rpm. The froth which forms during the experiment is continuously scraped into a froth collection collar and water (at the same temperature as the suspension) is added to maintain a constant level in the cell throughout the test. Hyperflotation is typically achieved after 12-13 minutes and represents the maximum attainable removal of ink.

Denver Cell

The Denver laboratory cell, shown in Figure 16, operates in much the same manner as its industrial counterpart which originated in 1950 and was the first flotation deinking cell. The cell is a rectangular tank containing a central agitator which is located within a shaft. When the agitator is turned on, air is drawn down the shaft and is dispersed through the stock. The froth is manually removed by scraping it across the overflow weir into a collection vessel.

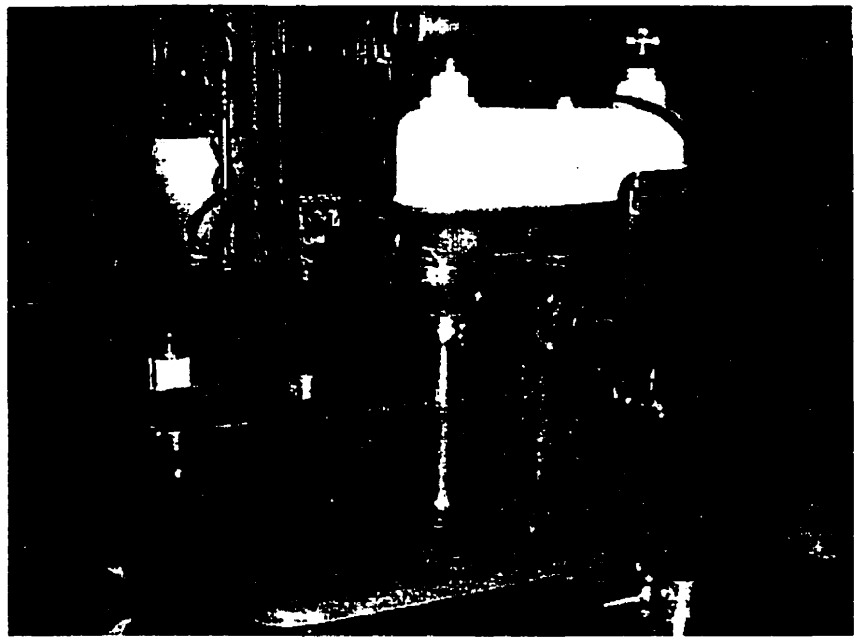

Figure 16. The Denver Laboratory Flotation Cell [49]

Adirondack Formax Cell

The Adirondack Machine Corporation Formax laboratory flotation deinking cell was developed to be as flexible as possible for evaluating process variables as well as to produce deinked pulp sample sizes large enough for further processing, such as thickening or displacement washing [48]. Such processes have fibre losses associated with them and require sufficient sample size for handsheet preparation. The cell, shown in Figure 17, is constructed from stainless steel as opposed to plexiglass. The disadvantage of using plexiglass is that ink particles tend to adhere to the walls of the cell

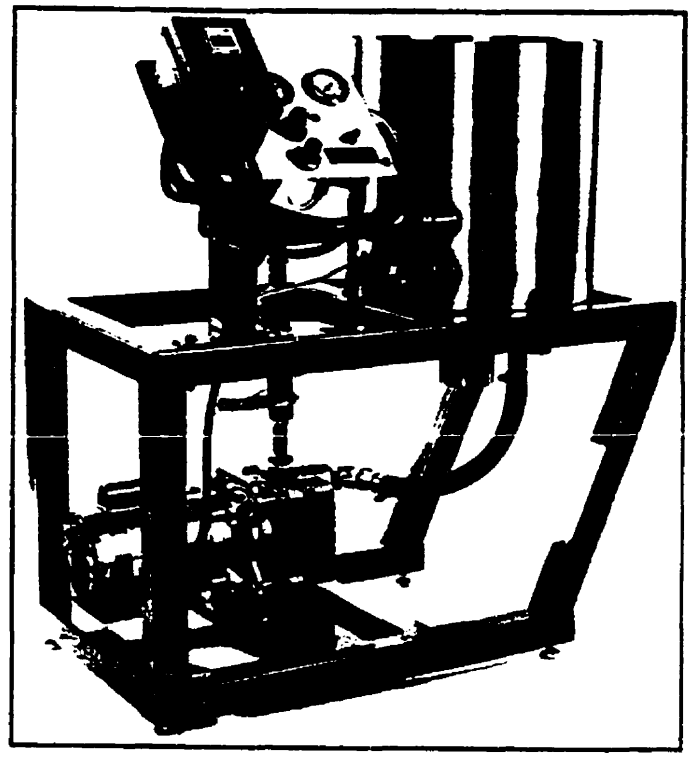

Figure 17. Adirondack Formax Laboratory Flotation Cell [48]

which affects the reproducibility of experiments.

The cell is designed to operate with 28 liters of stock at 1% consistency. The stock is circulated through the deinking tank and a 3/4 inch PVC circulation loop by a centrifugal pump. Compressed air is introduced just before the stock enters the cell at a maximum rate of 2 cubic feet per minute (@ 15 psi). Bubble size is controlled through regulation of both air pressure and air flow. This method for producing air bubbles allows for a variety of bubble sizes at equal air volumes and is easily adjusted [48].

A reject tube is located in the center of the cell. The stock and reject tube heights are adjusted so the reject foam spills into the tube. Typically, the reject tube is 11 inches from the tank bottom.

Leeds Cell

Figure 18 depicts the Leeds cell which is used by Gil Dorris et al. at the Pulp and Paper Research Institute of Canada (PARICAN), Pointe-Claire, Quebec, Canada. The body of the cell is made of plexiglass and is mounted on top of a base unit which houses an impeller assembly and a variable-speed motor. The square cell has a main volume of 5 L with a removable sloped extension that adds 1.5 L to the total cell. The sloped extension channels the froth to facilitate its manual removal with a scraper.

Gas is fed into the cell at flow rates of 1.5 to 3 L/min by a low-pressure gas supply to the base of the cell via a sloping pipe which passes through the back of the cell. Gas bubbles emerge from the pipe and are immediately broken down into smaller bubbles by a variable speed impeller which typically operates at above 1000 rpm. The impeller consists of a disk with vertically-oriented rods equally spaced around the periphery. Baffles are placed around the impeller to prevent a swirling motion within the cell. In order to dampen turbulence in the upper portion of the cell, corner pieces are placed above the baffles and held in place by bowed stainless steel wires. The cell temperature is adjusted with a temperature controller connected to a heater and thermistor located

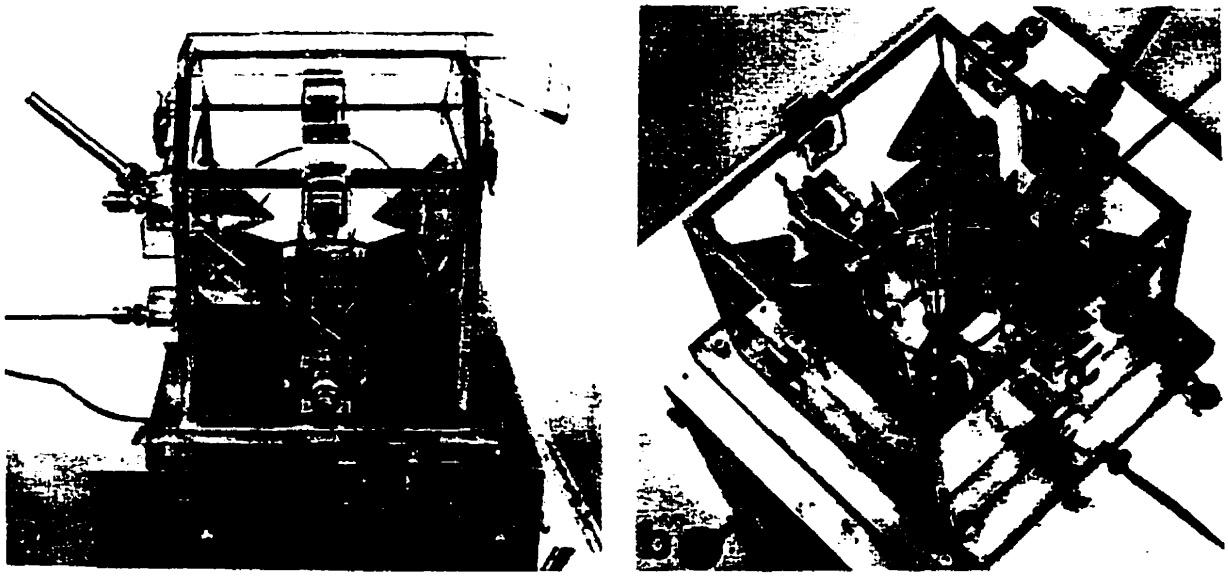

Figure 18. Side and top view of a Leeds Laboratory Flotation Cell [45]

inside the cell.

Injector-Aerated Cell

With the Injector-Aerated laboratory flotation cell, developed by the Institute of Paper Technology/ Darmstadt, Germany, it is possible to study the effects of physical parameters, such as, air volume fraction and bubble size, as well as deinking chemicals. This cell produces fibre yields of approximately 90% which is similar to the yield obtained in the primary stage of industrial flotation units [1].

The flotation cell consists of a plexiglass cylinder 30 cm in diameter with a concentrically situated reject discharge tube, 9 cm in diameter. The height of the rejects tube is adjustable. The suspension volume varies between 10 and 20 L. The deinked stock exits in the accepts stream and enters one of two storage tanks which are equipped with a stirrer and impact plates to keep the stock well mixed and avoid the formation of deposits. Air is introduced just prior to the inlet of the cell with the use of a Venturi injector.

Since two storage tanks are provided, the flotation cell can be operated under different conditions, see Figure 19. In continuous, single-stage flotation, the suspension is circulated through a loop consisting of the cell and one tank until the desired flotation time is reached. Alternatively, single-pass flotation can be implemented in which all of the pulp is pumped from the bottom storage tank, through the flotation cell, and all the accepts are collected in the upper storage tank. This completes one pass. The stored accepts can now be transferred back to the empty bottom storage tank and the process can begin again for a second pass. This can be repeated until the desired number of flotation passes is achieved.

It is known that the vertical distance which an air bubble/ink particle aggregate must travel to reach the suspension surface affects the flotation efficiency. In order to investigate this, the cell is equipped with three alternative stock inlets positioned at various heights, see Figure 19.

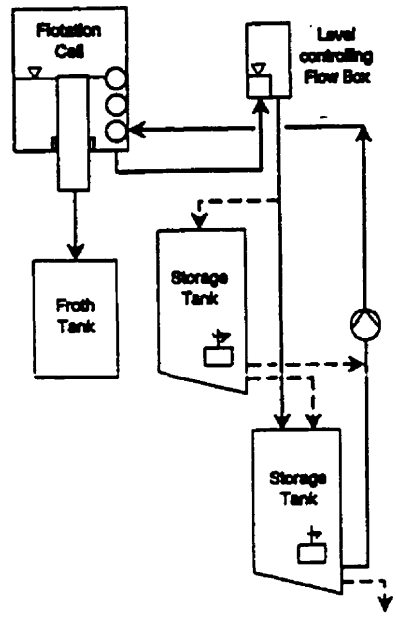

Figure 19. Scheme of the Injector-Aerated Laboratory Flotation Cell Unit [1]

1.2.6 Factors Affecting Flotation

Numerous papers have been written describing the factors that affect flotation deinking [36, 50-55]. These factors can be divided into two groups: those related to the incoming grey stock properties and those related to the equipment.

The incoming stock typically has the following characteristics: consistency 0.5-2.0 %; pH 8-11; temperature 40-55 °C; and water hardness 110-130 ppm Ca^{++}. The optimum pH, temperature, and water hardness are dependent on the choice of flotation chemicals used. For instance, water hardness is a factor only if fatty acid soaps are used. Flotation efficiency has been found to improve if the incoming grey stock has a significant ash content. A clay content of 8 - 10 % is considered a minimum requirement, and 12-14 % is preferable [17]. This level can usually be maintained by blending in coated waste with the greystock. Approximately 25-30 % of the clay is removed in the rejects stream.

The optimum stock consistency is dependent on the type of flotation cell used but is typically within the 0.5-2% range. However, it stands to reason that if the fibres are

present at too high a stock consistency, they will decelerate the rise of the air bubble/ ink particles complexes. Too high a stock consistency may result in a decreased flotation efficiency because the increased frictional resistance of the stock suspension may loosen the ink particles from the air bubbles thus preventing their discharge with the froth.

When considering the optimum equipment attributes for a flotation cell, four principal factors can be identified and summarized as: **(i)** ink particle attributes - number, size distribution, shape, and surface chemistry; **(ii)** air bubble attributes - the number and size distribution; **(iii)** the role of mixing and foam removal; and **(iv)** chemistry.

(i) Role of Ink Particles

Ink particle size has been shown in the literature to be an important aspect in flotation [56,57]. The particles must be large enough in order for an adequate amount of bubble/particle collisions to occur yet they must be small enough so that the bubble/particle agglomerate may ascend to the flotation cell surface. Ink particles must also be sufficiently hydrophobic, or are able to be made so through chemical addition, in order to attach to the bubbles. For example, the hydrophilicity of water borne inks has been identified as the key factor responsible for the poor floatability in some [57]. Finally, the relative velocity of ink particles before collision with the air bubbles will play an important role in the interfacial contact step of particle/bubble interaction [58,59].

The number, shape and size distribution of the ink and contaminant particles delivered to the flotation cell will depend primarily on the type of deinking stock being treated and on the treatment imposed in the repulping stage. Figure 20 shows the classic particle size distribution versus removal curve. This figure illustrates the particle size distributions that are generally suitable for washing and flotation. Washing is best suited for the removal of small particles generally below 10 microns, whereas flotation is more suitable for particles between 10 and 100, and cleaners and screens will remove particles that can be seen visually (above 35 microns). These numbers are not to be interpreted as absolute values but rather general trends of the deinking industry. For instance, many of the flotation cells discussed above can, and do, handle particles beyond the size range

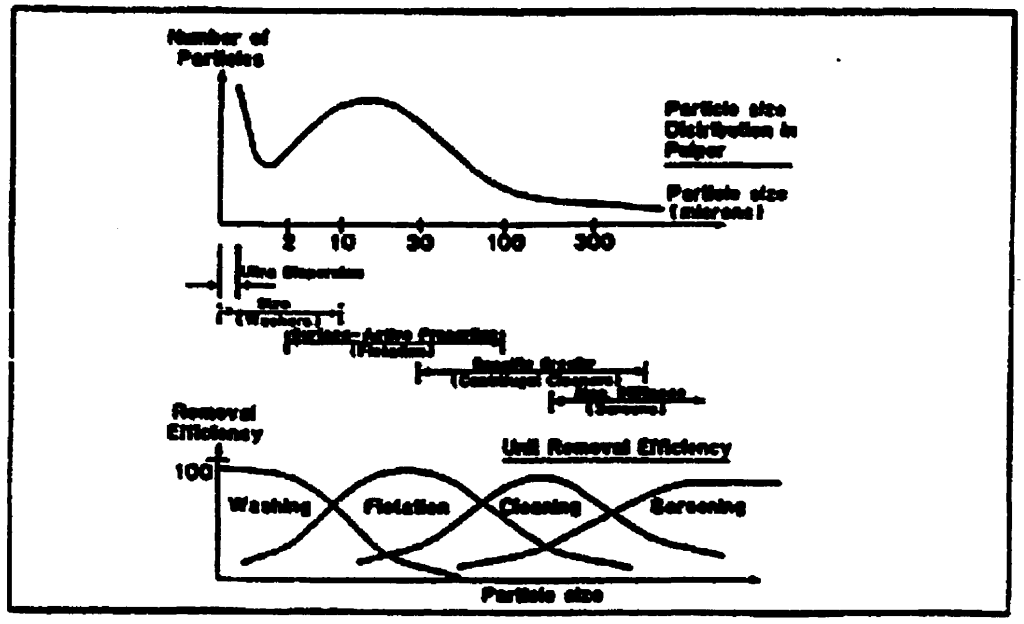

Figure 20: Particle size distribution and removal [18]

indicated.

Effective removal of ink particles from the repulped fibre slurry is only possible if the ink particles are completely detached from the fibres prior to flotation. This is achieved in the repulper at an appropriate temperature using mechanical action and the addition of chemicals. Ineffective repulping results in printing ink trapped inside fibre bundles, as shown in Figure 21. Flotation using pulp in this condition will not be effective in removing the ink particles from the fibre stock suspension. Figure 22 depicts another sign of ineffective repulping. In this case the fibre bundles have been opened up, however, ink particles still are adhered to the individual fibres. Such pulp can never yield optimum flotation efficiency because the ink-laden fibres will always cause some kind of mottling. Figure 23 shows a well prepared stock. All the ink particles are detached from the fibres and can now be effectively floated from the fibre stock suspension.

Table 2 shows the ink particle sizes generally found after repulping for various printing methods. It is apparent that flexographic inks are generally too small to be

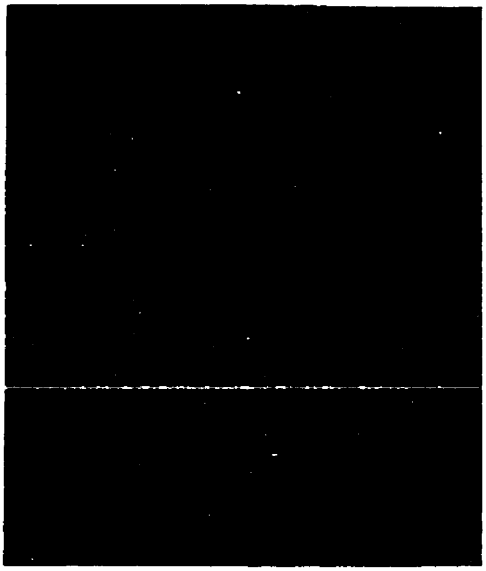

Figure 21. Poorly slushed pulp [16]

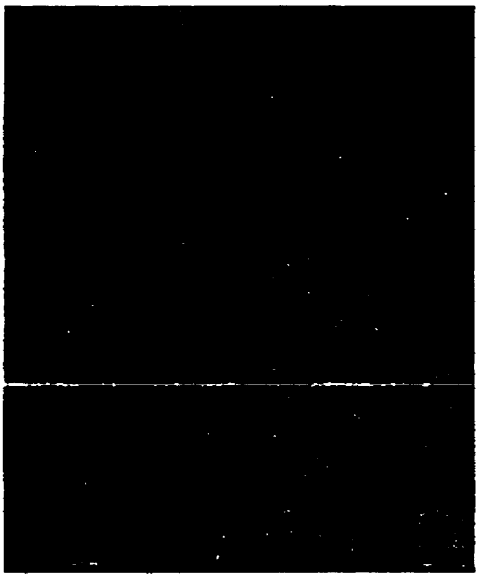

Figure 22. Stock completely defibered but ink particles still adhere to fibres [16]

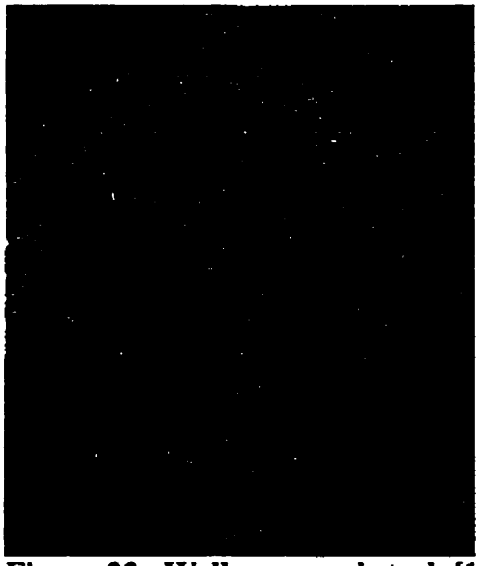

Figure 23. Well-prepared stock [16]

efficiently removed by flotation. However, it has been shown in the literature that a suitable chemical treatment can render flexographic inks suitable for flotation by agglomerating the particles and inducing a hydrophobic surface [61].

Numerous papers have been published regarding the effect of particle size on the flotation efficiency. Larson et al. [62] performed flotation experiments using model ink

Table 2. Ink particle sizes after repulping printed papers [60]

PRINTING PROCESS	PARTICLE SIZE (Microns)	PAPER
LETTERPRESS	2-30	UNCOATED
	10-100	COATED
OFFSET	2-30	UNCOATED
	5-50	COATED
GRAVURE	2-30	UNCOATED
	5-30	COATED
FLEXOGRAPHY	0.3-1	UNCOATED
	0.7-2	COATED

particles in soap solutions but in the absence of fibres. Based on their results the flotation process follows first order kinetics with the rate constants being proportional to the particle diameter raised to the power 1.8. This dependence was attributed to an increase in collision efficiency with increasing particle diameter. This phenomenon was later confirmed in ink pulp suspensions [63]. Although other papers have been cited that indicate a similar size dependence to that reported by Larson et al. [62,63], others indicate that particle size plays no role in flotation [33,64] or that flotation efficiency drops with increasing particle size [16].

(ii) Role of Air

A crucial parameter is the ratio of particle size to air bubble diameter. Linck [50] has shown that bubbles must have a minimum diameter of 0.3 mm in order to have sufficient buoyancy to push through the fibre slurry. Isler [65] has shown if bubbles are too small (diameters smaller than 0.1 mm) they will tend to stick to pulp fibres, causing their removal during flotation. Such a phenomenon is applicable to dissolved air flotation clarifiers due to the fact that they utilize bubbles of this magnitude. Particles which are too big for the size of an air bubble have a small contact surface in comparison to the

particle length, thus allowing high turbulence in a flotation cell to dislodge the particle from the surface of the bubble.

Dongming et al. [66] describe that if the particle is too small, surface tension and the electrostatic double layer forces come into effect and the particle cannot adhere to or penetrate the surface of the bubble. Szatkowski and Freyberger [54] have shown that the optimum bubble size to particle size ratio should be approximately 5:1. This paper also discusses that the mechanism for the flotation process is controlled, in part, by the rate of bubble coalescence and buoyancy of the particle-laden bubbles.

If the ink particles to be removed have a large size distribution, the 5:1 bubble size to particle size ratio requires that a range of bubble sizes be produced for the successful flotation of all particle sizes. The bubble diameter and number of bubbles in a flotation system are controlled by the injectors. Thus, the injector design and operation could be described as the heart of any flotation unit. The efficiency of the injector is described by Pfalzxar [52] as being dependent on the specific intake of air, the specific energy, and the throughput through the injector. The efficiency of an injector can be increased by increasing the air flow and thereby increasing the bubble surface area per unit time passing through the cell. Beyond a certain point, however, the air flow is no longer dispersed into discrete bubbles. Typically, the air flow rate ranges from 30 % to 50 % of the pulp flow rate, however, some of the cells previously discussed operate with much higher air:pulp ratio. The optimum flow rate must take into account the size and number of ink particles and contaminants to be removed in addition to the design of the flotation cell. The majority of the flotation cells worldwide introduce air into the system using atmospheric air injectors similar to the Escher Wyss design discussed earlier.

The effects of using other gases, rather than air, for flotation deinking has been investigated in the literature. In one particular study the gases evaluated were oxygen, nitrogen, and carbon dioxide. Only carbon dioxide was found to have any advantages over conventional air flotation. It increased the acidification of the system leading to better optical properties but reduced mechanical properties [67].

(iii) Role of Mixing and Foam Removal

Effective mixing between the inky stock and the air bubbles is essential in order to attain a maximum rate of collision between the bubbles and the particles to be removed.

The act of air injection and the subsequent mixing that occurs results in the formation of foam. A few different systems are in use in order to separate the ink-laden foam from the deinked stock. Most commercially available systems use some sort of overflow mechanism, whereby the inky foam overflows to a weir. As previously described, the Lamort Verticel systems use vacuum-assisted foam removal and the Beloit Pressurized Deinking Module (PDM) uses the pressure in the flotation chamber to force the rejects from the unit. Once the foam is created it is stabilized by the chemical environment. It should be stable enough to carry the ink and other particulates from the flotation cell, however, the foam must break down upon entering the weir or else it may excessively build-up within the reject handling system.

(iv) Role of Deinking Chemicals

Deinking chemicals are used to achieve the following four objectives [11]: **(1)** separation of ink from fibre (wetting) and prevention of redeposition of ink on fibre (detergency) **(2)** increase the hydrophobicity of ink particles to facilitate their removal by flotation **(3)** bleaching of fibre **(4)** clarification and sludge dewatering

Chemistry is involved in many of the key processes in a deinking mill: pulping, flotation, washing, bleaching, water clarification and sludge treatment. A list of chemical types and their application is presented in Table 3. Table 4 goes on to describe function of some the key deinking chemicals. One paper [68] explains in detail the function of the various chemicals in Table 3. One interesting paper [7] gives six examples of the appropriate selection of deinking chemicals for six realistic deinking operations.

It is important to remember that some of the chemicals have more than one action, not all of which may be desirable. For example, caustic soda makes fibres more flexible and helps to remove the ink; but, in newsprint furnishes, it will cause alkali darkening, or

Table 3. Deinking System Chemicals [11]

Chemical	Pulper	Flotation	Bleaching	Clarification and Sludge Treatment
1. Sodium Hydroxide	X		X	
2. Sodium Silicate	X		X	
3. Chelating Agents	X		X	
4. Surfactants	X	X		
5. Dispersants	X			
6. Detackifiers	X			
7. Agglomerators	X			
8. Flotation Collectors	X	X		
9. Calcium Chloride	X	X		
10. Hydrogen Peroxide	X		X	
11. Sodium Hydrosulphite			X	
12. Formamidine Sulfinic Acid			X	
13. Sulphuric Acid			X	
14. Alum				X
15. Flocculation Polymers				X

undesirable yellowing of the stock.

Flotation chemicals are generally known as collectors and can be classified into two main groups: soaps and synthetic collectors.

The traditional flotation deinking chemicals are soap and calcium ions (calcium chloride), however, recently many deinking plants have turned to using synthetic surfactants (surface-active-agents). Soaps and surfactants have similar chemical natures in that both are molecules that have a spherical hydrophilic body and a long hydrophobic tail. Figure 24 presents the structure and classification of the most commonly used surfactants.

Soaps

A soap is a salt, usually the sodium salt, of a fatty acid. The soap collector systems used in deinking processes today are blends of fatty acid derivatives with chain lengths of C-14 to C-18 [69]. Soap is normally added in amounts of 0.5 - 1.0 % based on

the mass of moisture-free pulp. In order for soap to be an effective flotation agent, calcium ions must be present in the suspension. Such ions are typically introduced into

Table 4. Functions of Deinking Chemicals [70, 71]

DEINKING CHEMICAL	FUNCTION
Sodium hydroxide (NaOH)	Swells fibers Loosens ink Activates hydrogen peroxide
Sodium silicate ($NaSiO_x$)	Removes ink particles from fibers Prevents ink redeposition (dispersion) Stabilizes peroxide
Sodium carbonate ($NaCO_3$)	Water softening Buffering Alkalinity
Complexing agent (e.g.. DTPA)	Stabilizes peroxides by chelating metallic ions (Mn, Mg, Sr) Allows reduction of silicate use
Non-ionic Surfactants (e.g. Alkyl Phenyl Ethoxylates)	Wetting Emulsification Ink removal
Collector (Flotation)	Binds to ink particles Attaches to air bubble for froth separation
Dispersant (Washing)	Disperses ink particles Ink particles can be removed with wash water
Hydrogen peroxide (H_2O_2)	Bleaching agent for the fiber Prevents alkaline yellowing

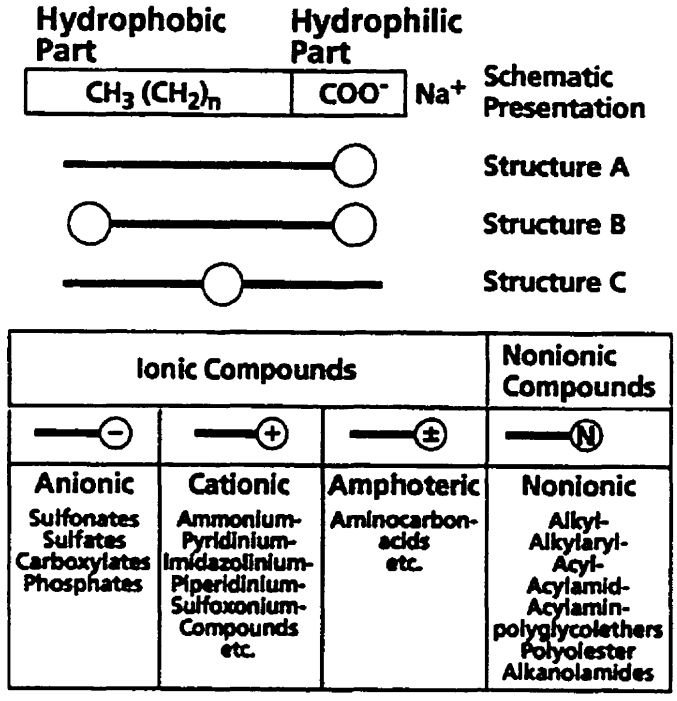

Figure 24. Structure and Classification of surfactants [72]

the system with the use of calcium chloride. Enough calcium chloride is normally added to the system to give a hardness of 180-200 ppm (as $CaCO_3$). Overdosing can induce higher losses of some types of fibre in the flotation cell. Other authors have stated that there must be an excess of soap to allow it to act as a frothing agent [73].

Larson et al. [62] proposed a mechanism for the collector action of calcium soaps during the attachment of ink particles to gas bubbles. Ink particles alone tend to have a highly negative zeta potential. When soap is added, the zeta potential becomes even more negative. Such a decrease favours the release of the inks from the fibre and the formation of stable colloidal suspensions. However, these freed ink particles do not attach to air bubbles at this stage due to their highly negative charge. When calcium ions are introduced into the system, the charge is reduced and the soaps precipitate as calcium soaps on the surfaces of the ink particles. The charge reduction leads to the formation of aggregates, which are hydrophobic due to the presence of precipitated calcium soaps, and

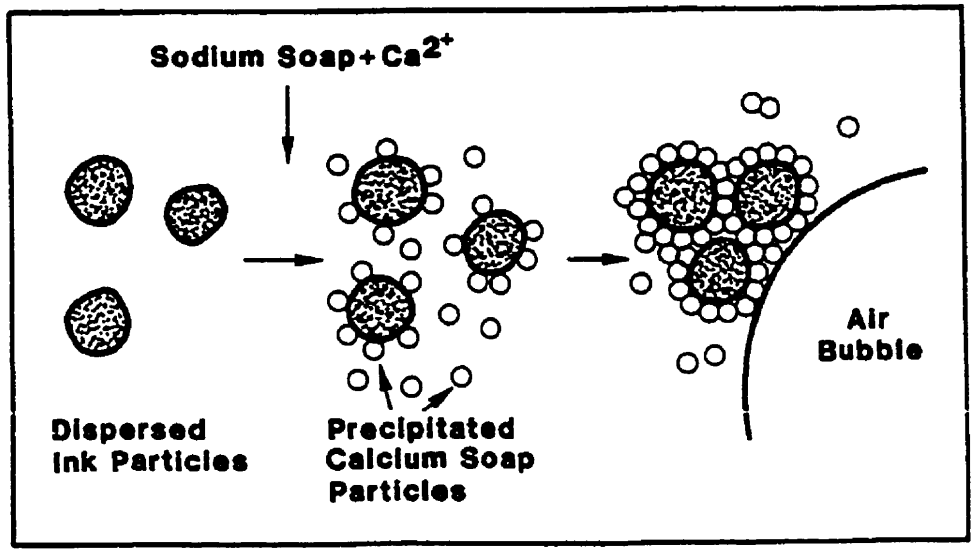

Figure 25. Mechanism for the collector action of calcium soaps during flotation [62]

to the attachment of ink particles to gas bubbles. This mechanism is shown in Figure 25. This mechanism was also confirmed by Harwot et al. [118]. Soaps are supplied to mills either as a liquid or a solid. Liquid soaps, typically a 50% solution, is usually added just before the flotation cell. Mills using soaps in solid form often utilize a make-up preparation system.

Synthetic Collectors (Surfactants)

In many flotation deinking units surfactants are currently replacing the traditional flotation deinking chemistry of soap and calcium chloride. These synthetic collectors do not require calcium ions for flotation of ink particles. Surfactants are typically classified as ionic or non-ionic in nature, depending on whether or not they are electrolytically dissolved in water. The ionic type surfactants are further classified as anionic, cationic and ampholytic types depending on the polarity of the ion. They are often referred to as displectors because they involve both dispersion and collection mechanisms. The ratio of the long chain hydrophilic group and the spherical hydrophobic group, which is known as the HLB or the hydrophobic/hydrophilic balance, determines the dispersion/collection behavior of the surfactants.

The following advantages have been claimed for the use of synthetic surfactants

over soaps [74]: **(1)** because calcium ions are not required, these surfactants can reduce chemical deposits in the paper making process, increase the pulp brightness, and be used in soft water **(2)** the displector mechanism makes them more suitable for systems that combine flotation with washing **(3)** they float flexographic ink particles more efficiently **(4)** because they are liquid, they are easier to handle **(5)** smaller amounts (0.1-0.3 %) are required compared with soaps (0.5-1.0 %).

The reader is referred to the literature [75] for further information on surfactant properties, such as, the critical micelle concentration (CMC), the hydrophobic:lipophilic balance (HLB), the micellar aggregation number, the surfactant cloud point, and surfactant foaming.

pH and Temperature Effects

Alkaline pH and elevated temperatures cause fibre swelling and subsequent ink release. Nonionic surfactants are essentially independent of flotation cell pH, however, the stearates, or soft soaps, are highly affected because of their ionizable nature [9]. Bubbles tend to be too large for efficient flotation when the pH is 5 or below. Low pH levels also convert acids at the fibre surfaces to their unionized forms, making the fibres more hydrophobic and hence, more susceptible to flotation [9]. Also, beyond a pH of 11 the bubbles tend to be extremely small have been shown to increase fibre yield loss [9].

1.2.7 Effect of Flotation On Paper Quality

It is common knowledge that the flotation process tends to have adverse effects on some of the paper qualities [76]. When comparing the qualities of deinked fibres to those of virgin fibres, the most important parameters to consider are the physical and optical properties plus runnability and printability.

Howard and Bichard [77, 78] showed that the greatest change in fibre physical properties is caused by the first recycle and after four recycles the physical properties have essentially stabilized. This is reflected in Figure 26, which illustrates the basic effect of recycling on unbleached softwood kraft pulp.

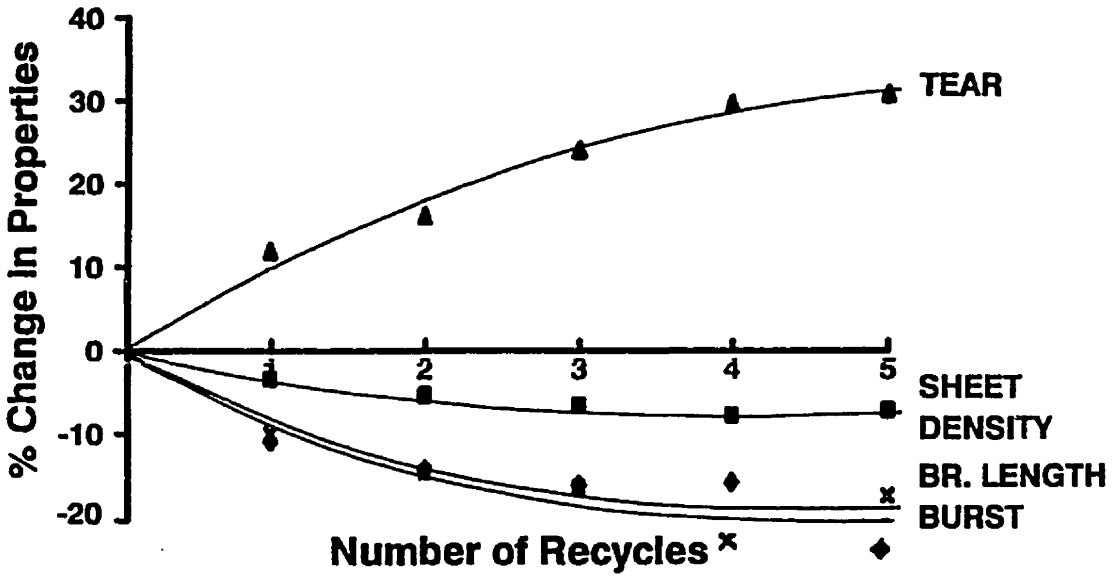

Figure 26. Stabilization of paper physical properties following recycling [60]

One study has shown that the flotation process does not seem to alter fibre strength significantly [79]. Other studies by Wultsch and Maier [80] and Eriksson [81] stated that due to the chemico-thermal treatment of the fibre material the strength properties increased by at least 14%. In other studies, however, friction coefficients have been reported to decrease [82]. These effects have been attributed [83] to the phenomenon known as hornification. Hornification refers to the hardening of pulp due to the collapse of the fibre wall during sheet consolidation and drying which results in a less conformable wet fibre after reslushing. The primary change in fibre properties by recycling is the loss of bonding ability, which can be counteracted to a certain extent by refining, chemical additives, fractionation and blending with virgin pulp [11].

In general, the runnability of recycled newsprint and other printing papers that contain secondary fibre is not significantly different than that of virgin fibres. However, the runnability of deinked pulps is affected by the concentration of residual contaminants and the nature of the pulp. Sticky deposits can cause significant runnability problems.

Some of the approaches that can be taken to solve this problem include the addition of talc and other chemicals [84], efforts to improve the "electrostatic" climate of the paper-machine back-water system [85], the addition of a profile correction system, the reduction of open draws, and the adjustment of reel and winding parameters [86].

Discrepancies in printability and appearance are more apparent. This is primarily due to the fact that recycled sheets tend to be more absorbent because of higher sheet porosity. This requires the use of more ink during printing which causes poorer printing resolution and higher rub-off. Secondary fibres tend to be less white than virgin fibres due to remaining ink spots and other dirt specks. This leads to a lower sheet brightness. Recycled fibres usually cannot be used as a furnish component in the most critical paper grades.

1.2.8 Efficiency of Flotation

The design of a flotation unit aims at the maximum ink removal and minimum reject rate as shown in Figure 27 below.

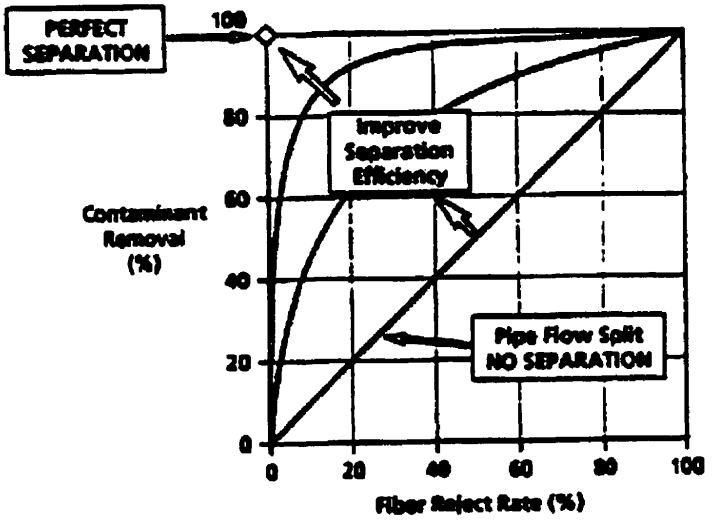

Figure 27. Perfect separation of contaminants and fibre [11]

The closer a system approaches perfect separation (100% ink removal at 0% rejects rate), the better its deinking efficiency. The efficiency of a flotation cell is measured by three major parameters: brightness, ink removal, and rejects rate.

Table 5 shows the type of data required for the complete evaluation of the efficiency of a deinking system. The analysis of feed, accepts and rejects should be performed in terms of volume flow, fibre fraction, brightness, ink concentration and stickies concentration.

Table 5. Flotation Deinking Efficiencies Based on Data from Feed, Accepts, and Rejects Streams [11]

	FEED	ACCEPT	REJECT	BALANCE
A. MEASURED DATA 1. Volume Flow 2. Consistency (%) 3. Ash (%) 4. Fiber Fraction 5. Brightness 6. Ink Particles 6.1 Concentration by number 6.2 Concentration by area 6.3 Particle size distribution 7. Stickies 7.1 Concentration by number 7.2 Concentration by area 7.3 Particle size distribution				
B. CALCULATED DATA 8. Flow Balance 8.1 Volume 8.2 Solids 8.3 Ash 8.4 Fiber fractions 9. Brightness 9.1 Delta brightness 10. Ink Removal Efficiency 10.1 By number 10.2 By area 10.3 By particle size 11. Sticky Removal Efficiency 11.1 By number 11.2 By area 11.3 By particle size				

In order to calculate deinking efficiency both the removal efficiencies for ink particles of different sizes and brightness increase (or Delta brightness) should be reported. Measurement of ink particle size requires the use of image analysis equipment. In general, image analysis equipment is limited by particles greater than 2 microns in size. Thus the removal of smaller particles can only be assessed in terms of brightness.

Solvent extraction of deinked pulp is one method to quantitatively measure the amount of ink removal providing all interfering compounds have been removed. A second possible method would be to appropriately select spectroscopic method of analysis (IR, UV, VIS, NMR, etc.) of the extract.

Definition of Brightness

Brightness refers to the lightness or overall reflectivity of the paper sheet measured at a wavelength of 457 nm. Reflection is the portion of the incident light that is returned from the sheet surface. The portion of the light which is not reflected from the sheet surface can be either transmitted, scattered or absorbed as heat. Brightness is measured at 457 nm wavelength because the brightness increase between unbleached and bleached pulp reaches its maximum at this wavelength.

The brightness of the paper surface depends on: **1)** the optical characteristics of the paper **2)** the wavelength of the light **3)** the geometry of the instrument that makes the measurement **4)** the reflectance of the object used as a backing for the sheet of paper.

Brightness as a Measure of Flotation Efficiency

Brightness has been a key chemical parameter used to gauge overall deinking efficiency [87]. The more ink gets removed out of the pulp furnish, the higher the brightness. The data collected can also be used to compare mill efficiencies with the efficiencies generated in the laboratory flotation cells. To obtain the efficiency of laboratory flotation cells the samples are subjected to prolonged flotation until no more ink can be removed. This is known as infinite flotation, ultimate flotation, hyperflotation,

or laboratory flotation. Typically, commercial mills can remove 90-95% of the ink that gets removed by infinite flotation [11].

There are four important limitations with the use of brightness as a deinking efficiency indicator:

1) The finest size ink particles tend to travel to the bottom of pulp samples such that it makes the top side of the pads much brighter. Depending on which side the measurement is performed, there is a potential for discrepancies between tests.

2) The TAPPI standards for brightness pad preparation require extensive washing which may result in the removal of fine ink particles present in the pulp [88]. Thus ink removed by such washing may be interpreted as if it were removed during the flotation process, resulting in overly optimistic flotation efficiencies.

3) There is no direct correlation between brightness and the amount of ink present in the sample. It has been suggested that smaller ink particles will have a greater effect on brightness than larger ink particles [87]. This is due to the increased surface area to volume ratio of the smaller particles. In a flotation system that recycles newsprint which contains small ink particles, the brightness will increase about 10-15 points. In contrast, a deinking system that recycles white grades where ink particles are larger will only achieve a brightness increase of about 5-10 points [11]. Therefore, brightness is not only affected by total amount of ink, but also by the ink particle size distribution.

4) Brightness is a composite measurement of all components of the recycled sheet. If ink is removed, the brightness will increase because ink has a lower brightness than fibres. On the other hand, if ash is removed, brightness may decrease because ash can have a higher brightness than fibre. For this reason, brightness change across a deinking module is determined by the proportional change in ink content and furnish components.

Limitations 3 and 4 have led to the development of image analysis techniques in order to measure directly the concentration of ink particles and their size distribution. Another measure of deinking efficiency is edge brightness, also known as unprinted brightness. This is the brightness of the unprinted edge of the recovered paper to be recycled. The efficiency of flotation can then be attained by comparing the brightness of a handsheet made from the recycled pulp to the edge brightness. For newsprint deinking systems the final brightness obtained (without high-consistency bleaching) is typically one to two points less than the edge brightness [11].

Ink Removal as a Measure of Flotation Efficiency

Ink removal is usually calculated from measuring ink concentration in the pulp by image analysis. In fact, image analysis has now become the standard tool for counting and sizing contaminant particles. The application of Automated Image Analysis to measure ink particles emerged in the late 1970's and early 1980's. It has since become the standard analytical tool for measuring not only ink particles but also other contaminants since it can measure directly the particle area, largest diameter, total number of particles and total area of particles. Figure 28 depicts an example of image analysis test results.

Since the development of image analysis, automated image analysis techniques have evolved so rapidly that there are now instruments that apparently eliminate subjective human limitations such as the new ASA-2000 instrument from Applied Vision Systems [89]. However, even though the superior resolution of the scanner allows it to easily discriminate particles as small as 0.02 sq. mm, there is still a need for future developments in order to enable the instrument to differentiate between different types of contaminants. Image Analysis techniques have been discussed extensively in the literature [90-93].

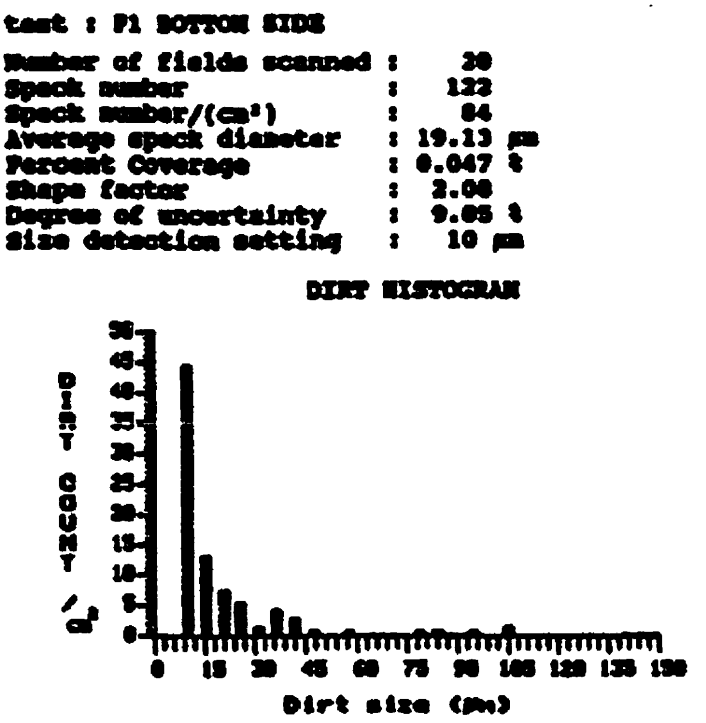

Figure 28. Output of a dirt analysis count apparatus [94]

1.3 SHORTCOMINGS OF EXISTING LAB-SCALE FLOTATION CELLS

The first major shortcoming of the majority of available laboratory flotation cells is that they are unable to adequately control various physical parameters such as volume of air intake, air bubble size, and air bubble-size distribution [1]. This is because air is introduced to these cells by a rotor-stator principle, or by pressurized air commonly in combination with a rotor for air distribution within the pulp. For reasons explained in Section 1.2.5, the presence of internal rotors within these laboratory cells make comparisons difficult with industrial flotation cells, where the vast majority lack internal rotors. Thus it was desirable to construct a lab-scale cell that introduces air without the use of an internal rotor, in a similar fashion to a typical industrial cell.

The second major short-coming of many lab-scale flotation deinking cells is that many do not convincingly attain hydrodynamic conditions in the air-injection section similar to that attained in typical industrial cells. Two of the parameters the hydrodynamic conditions do affect are the air bubble size distributions and

air bubble/ink particle collision frequencies. Both of these parameters have an effect on the flotation kinetics. It was desired to build a lab-scale flotation cell that had industrially similar hydrodynamics in the air-injection.

The third major short-coming is that the majority of lab-scale cells are not equipped with an accurate method of measuring air bubble size distributions. It was desired to build a lab-scale cell with this capability in order to investigate the effect of various operating parameters on the air bubble size distribution.

1.4 GENERAL OBJECTIVES

The overall objectives of this thesis are:

1) Develop and construct a laboratory-scale flotation cell which operates under industrially similar hydrodynamic conditions in the air injection section.
2) Investigate the effects of suspension velocity, the presence of fibres or fines, and deinking chemicals on the air bubble size distribution in the air injection section.
3) Investigate the effects of suspension velocity, aeration rates, and pulp type on the deinking efficiency of this novel laboratory-scale flotation cell.

1.5 ORGANIZATION OF THE THESIS

Chapters two and three are written in the format of separate manuscripts. Chapter two contains a description of the laboratory set-up that simulates the air-injection section of an industrial flotation cell, much like the Escher Wyss CF cell design, and presents various bubble size distribution results for various operating conditions. Chapter three contains a description of the laboratory flotation cell that has been developed, which is an evolution of the apparatus described in Chapter two. Flotation deinking efficiency results are presented and the feasability of this novel design to simulate the industrial reality is discussed. There is a logical continuation between these chapters and the necessary links are drawn within the introductory sections.

CHAPTER 2

THE EFFECT OF FLOTATION DEINKING PROCESS PARAMETERS ON THE AIR BUBBLE SIZE DISTRIBUTION

ABSTRACT

Laboratory-scale flotation deinking cells are useful in that the fundamental principles of the industrial process can be investigated in order to improve the flotation efficiency. Many traditional laboratory-scale flotation cells lack the attribute of being hydrodynamically similar to the actual industrial flotation process. The first objective of this research is the development of a laboratory-scale flotation cell in which industrial Reynolds numbers can be achieved in the air-injection section. The construction of the lab-scale flotation cell proceeded in two stages. First, a device was built that simulated solely the air-injection section of an industrial flotation cell. The air-injection unit has a loop configuration and is comprised of a custom-built centrifugal pump, injection sections for air and deinking chemicals, a glass optical analysis section, and connecting pipe made of polyvinylchloride. The experiments performed with this device are presented in this chapter and investigate how air bubble size is affected by process parameters and deinking chemicals. This device was later expanded into a functioning lab-scale flotation cell. Deinking efficiency results attained with it are the topic of Chapter 3. In this chapter, it was discovered that fluid velocity has a moderate effect on the bubble size distribution and surfactant concentration has a large effect. In addition, the presence of 0.2 % consistency TMP fibres or fines was found to have a small effect on the bubble size distribution.

2.1 INTRODUCTION

The objective of this chapter is to investigate the effect of several process parameters (suspension velocity, the presence of fibre or fines, and deinking chemicals) on the air bubble size distribution in the air-injection section of an industrial flotation deinking cell. This work is of interest because it is known that air bubble size does effect the flotation efficiency of ink particles from a repulped fibre suspension [95]. A brief background of some relevant findings from the literature now follows.

A crucial parameter is the ratio of ink particle size to air bubble diameter. Linck [50] has shown that bubbles must have a minimum diameter of 0.3 mm in order to have sufficient buoyancy to push through the fibre slurry. Isler [65] has shown if bubbles are too small (diameters smaller than 0.1 mm) they will tend to stick to pulp fibres, causing their removal during flotation. Szatkowski and Freyberger [54] have argued that the optimum bubble size to ink particle size ratio is approximately 5:1. If the ink particles to be removed have a large size distribution, the 5:1 bubble size to particle size ratio requires that a range of bubble sizes be produced for the successful flotation of all particle sizes. Ahmed and Jameson [96] have also argued the fact that a wide size distribution of bubbles is preferred for efficient removal of particles of all sizes.

Of all flotation deinking process parameters, surfactants have the most pronounced effect on the air bubble size distribution. Both the dynamic and equilibrium surface tension of the air bubbles are affected by the molecular size and hydrophobic/hydrophilic balance of the surfactant. Rao and Stenius [97] have shown that the surface tension of a surfactant at its critical micelle concentration (cmc) decreases with increasing hyrophilicity of the surfactant. At the same time, as surface tension decreases the air bubble size decreases. In the presence of surfactants, Rao and Stenius [97] showed that the air bubble size distribution is unimodal and has a sharp maximum, and that as the surfactant concentration increased, the average bubble size decreased and the distribution became narrower. The relationship between decreasing surface tension and decreasing bubble size follows from the Young-Laplace equation.

The air bubble size has been shown to increase during the course of flotation deinking experiments [2]. This was explained by the loss of surfactant with time and thus an increasing surface tension of the fluid or by the decreasing stock consistency due to

permanent foam removal.

The amount of shear on air bubbles has been shown to have an effect on the bubble size. For example, Milanova and Dorris [45], using a Leeds flotation cell, were able to have some degree of control on bubble size by varying the speed of the impellar that brokedown bubbles. Milanova and Dorris [45] indicated that the major factor affecting bubble size was the presence of a surfactant that reduced the coalesence of bubbles.

The air flow rate, defined as the ratio of air flow versus pulp flow, in a flotation cell also effects the air bubble size. Experiments using pulp-free water by Gottsching et al. [2] showed that the average bubble size increased with increasing air flow rate for a fixed water flow rate. Gottsching et al. [2] also saw that despite the fact that the average bubble diameter changed at different water and air flow rates, the shape of the bubble size distribution was identical. A bimodal shape was constant with peaks at 1 and 2 mm, and the maximum air bubble size was approximately 4 mm.

The type of air injector has also been seen to affect the air bubble size distribution in water [2]. When using pulp at 0.5% consistency, however, all average bubble size distributions of different injector types and air flow rates showed almost identical peaks. The contention of the authors was that the effect of stock consistency on air bubble size is thus larger than the effect of injector type or air flow rate.

Bubble column experiments [98] indicate that even low consistencies of 0.1% can have an effect on the air bubble size. These experiments indicated that fibres act as barriers to upward bubble motion and increase bubble coalescence, leading to larger bubbles.

Work by Ajersch and Pelton [99] and Drabek et al. [100] indicate that, in the absense of deinking chemicals, air bubbles do not adhere to fibres or fines.

In order to perform this chapter's experiments a lab-scale air-injection unit was designed and built that simulates the air-injection section of an industrial flotation deinking cell. Prior to describing the details of the experimental design used for this chapter's research work, the industrial flotation cell that is the most similar to our design will first be reviewed, the Escher Wyss CF (Compact Flotation) Cell.

Figure 1 below shows a photograph of an Escher Wyss CF Cell (model number CF5B-A1). Seventy-two pipes supply this flotation cell with stock suspension to be deinked. These seventy-two pipes are divided into six groups of twelve pipes. From the perspective of the photograph in Figure 1, three of these groups of twelve pipes are visible.

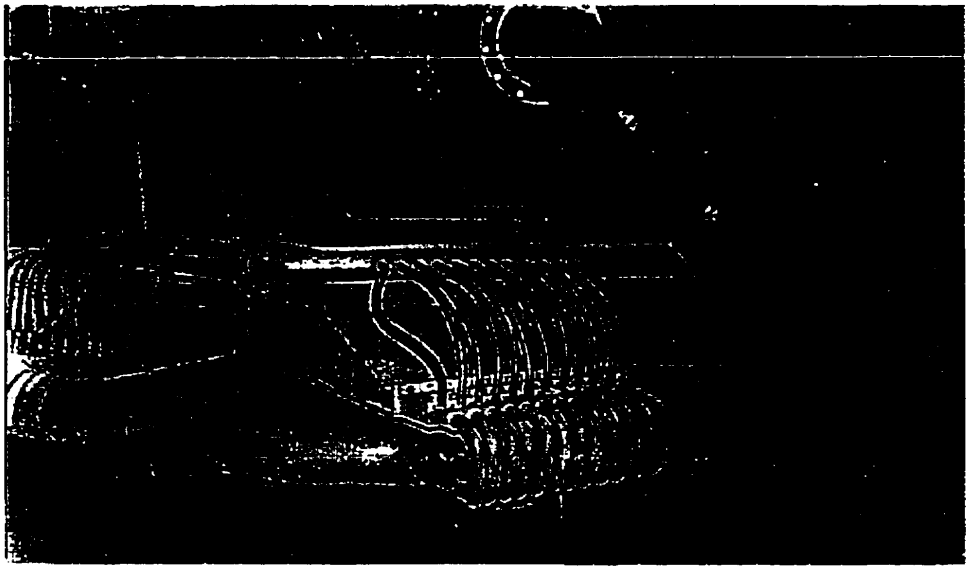

FIGURE 1. The Escher Wyss CF Flotation Cell [101]

Figure 2 shows a close-up picture of one of the sets of twelve pipes entering the cell. The pulp suspension, typically having 0.8-1.2% consistency, is fed to the twelve smaller pipes (4 cm interior diameter or I.D.) from a large main pipe. Typical volumetric flowrates and linear velocities of the pulp suspension in the smaller pipes are 150-225 L/min and 2-3 m/s, respectively. The Reynolds number in the smaller pipes can therefore be calculated as being approximately 76 000-114 000, indicating a turbulent flow regime.

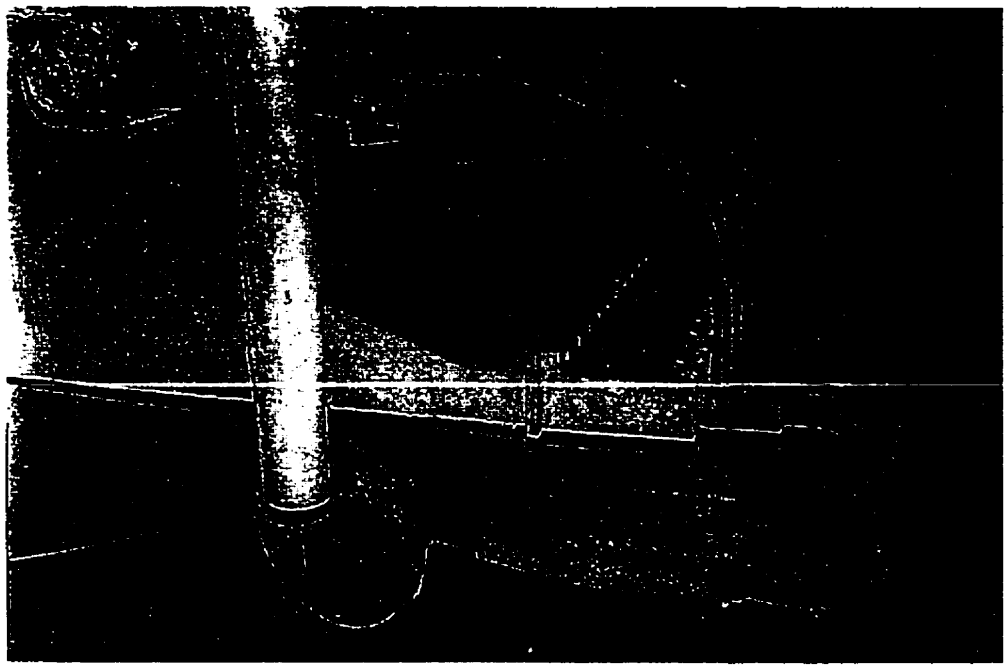

Figure 2. The Escher Wyss CF Cell Air-Injection Section [101]

Following a sharp bend in the pipes, air is aspirated into the pulp streams with the use of step-diffusers. The typical volume fraction of air in these streams is 20-40%. Figure 3 is a schematic of the air-injection section.

The aerated stock is then fed into the diffusing section of the flotation cell where the velocity decreases significantly. Because the stock is fed into the cell at a relatively shallow depth with respect to the surface of the pulp, air bubbles carrying ink particles quickly rise to the surface. The tangentially fed stock enters the cell with a slight circular motion to ensure that the foam created in the cell is directed to a central overflow. A photograph of the central overflow is shown in Figure 4.

2.2 EXPERIMENTAL DESIGN

The first objective of this project was to build a laboratory scale flotation cell in which industrial Reynolds numbers can be achieved in the air-injection section. Attaining hydrodynamics similar to the industrial reality is intended to facilitate the

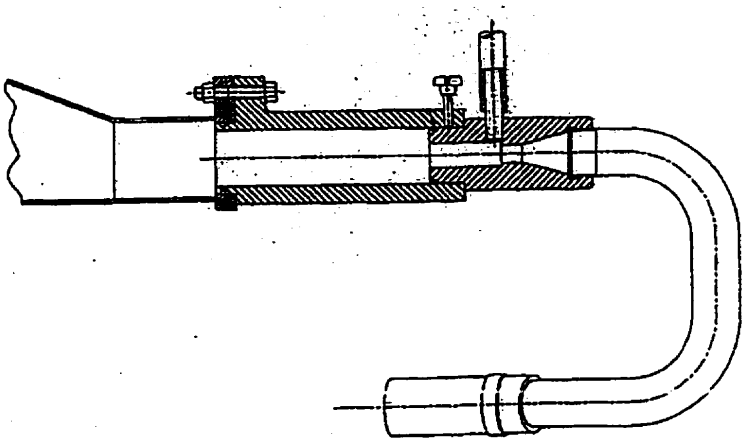

Figure 3. Schematic of the Escher Wyss Step Diffuser [102]

Figure 4. Escher Wyss CF Cell Central Overflow for Foam Removal [101]

comparison of our results to the actual industrial process. The construction of the lab-scale flotation cell proceeded in two stages. First, a device was built that simulated solely the air-injection section of an industrial flotation cell. Results attained using this device are presented in this chapter. In Chapter 3, an expansion of this basic design will be discussed which is a functioning laboratory flotation deinking cell in which effective separation of ink can be attained.

Figure 5 is a schematic of the air-injection unit used to characterize bubble size distributions under various operating conditions. Figure 6 is a corresponding photograph. A flotation cell is comprised of three major zones: **(i)** aeration; **(ii)** mixing; and **(iii)** ink separation. The intent of this unit is to simulate the aeration and mixing stages of industrial flotation cells.

The air-injection unit has a loop configuration made primarily from polyvinylchloride (PVC). The unit is mounted on a ½ inch aluminum base. Pulp suspension is circulated within the loop by a centrifugal pump, and air is injected into the loop using a compressed air cylinder. This simulates the aspiration of air into the inlet pipe of an industrial flotation cell as shown in Figure 2. Still images of air bubbles moving in suspension can be taken from an image cell using a video camera. Bubble size distributions were obtained from these images using image analysis.

The typical volume of liquid or suspension used in the loop for this chapter's experiments was 6.6 liters. However, the loop size can be lengthened with the use of extension pieces to provide an additional 2048 ml of volume. Appendix B discusses two lengthened loop configurations.

Industrial Reynolds numbers can be attained in the loop because the pipe interior diameter (I.D.=4 cm) is the same as the Escher Wyss CF cell inlet pipe and industrial fluid velocities of 2-3 m/s and beyond can be attained. The step-diffuser used in Escher Wyss CF cell induces vigorous mixing of the air and pulp. Due to the fact that a step-diffuser was not used for Chapter 2's experiments, less vigorous mixing of the air and pulp was attained in comparison to the industrial reality.

The unit sits within a drainage basin made from ¼ inch polyvinylchloride (PVC). The rectangular basin (2.55m by 0.62m) collects any liquid should a spill occur during an experiment. The four main loop components are: **(i)** a custom-built stainless steel centrifugal pump **(ii)** injection sections for air and deinking chemicals **(iii)** an image cell to attain air bubble images **(iv)** clear pipe made from PVC.

2.2.1 Centrifugal Pump

The heart of this air-injection unit is a unique centrifugal pump. The pump is a slightly modified version of one designed several years ago by Dr. Tadeuz Dabros, a former member of Dr. Theo van de Ven's research group at the Pulp and Paper Research Centre of McGill University. A photograph of the original pump used by Dr. Dabros is shown in Figure 7.

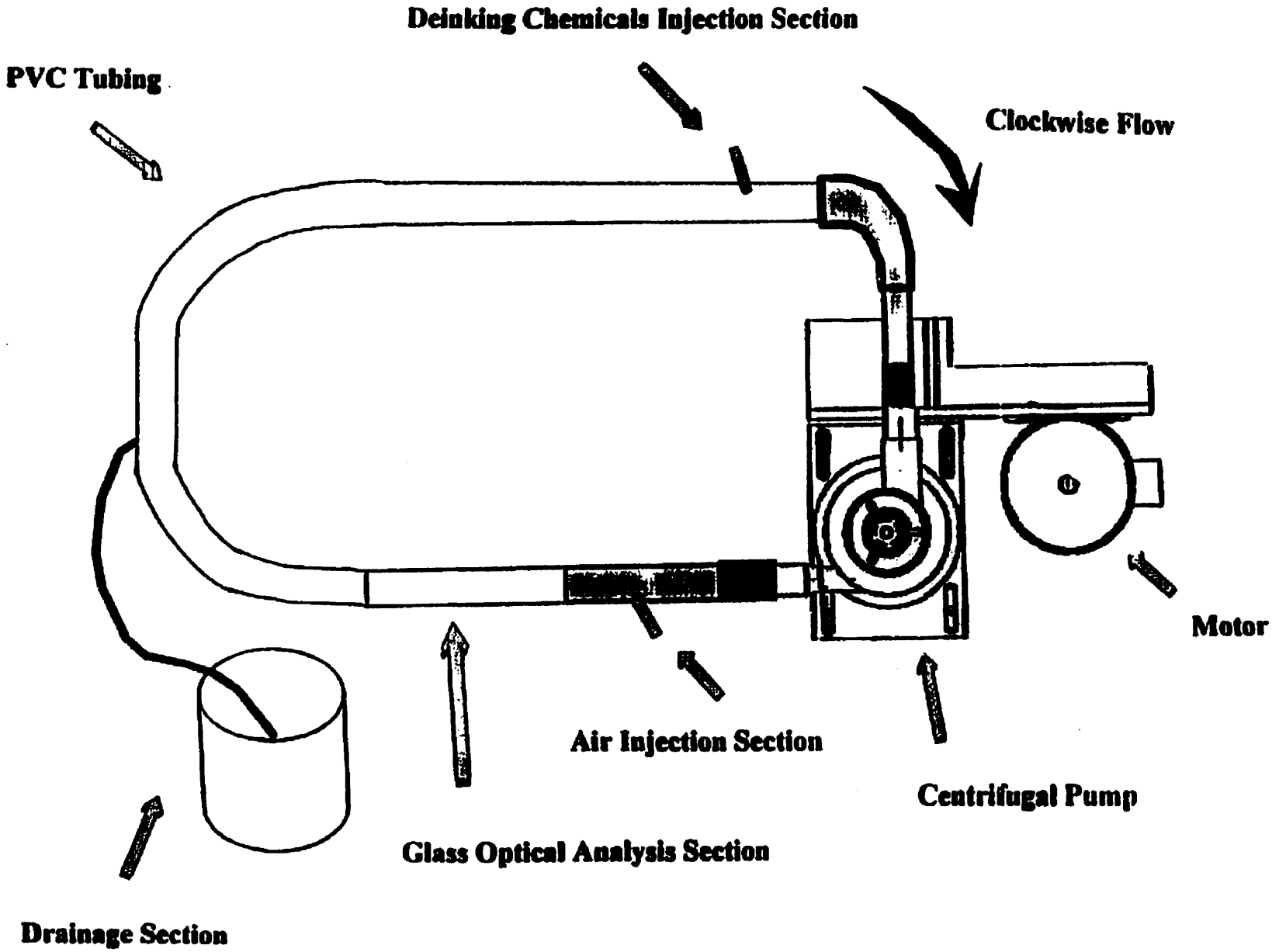

Figure 5. Overhead View of the Air-Injection Unit

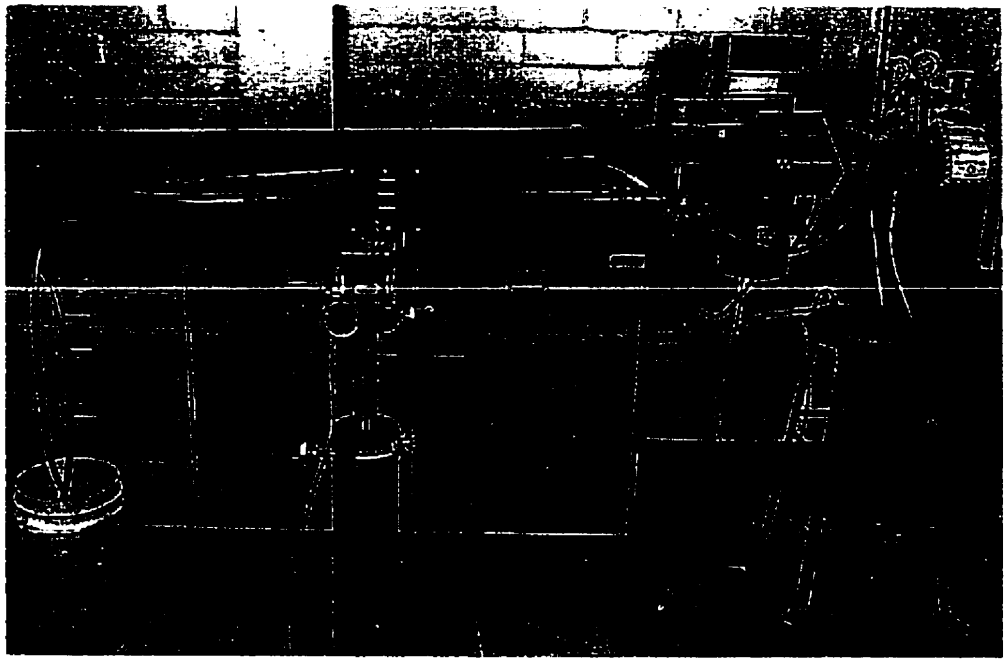

Figure 6. The Air-Injection Unit [103]

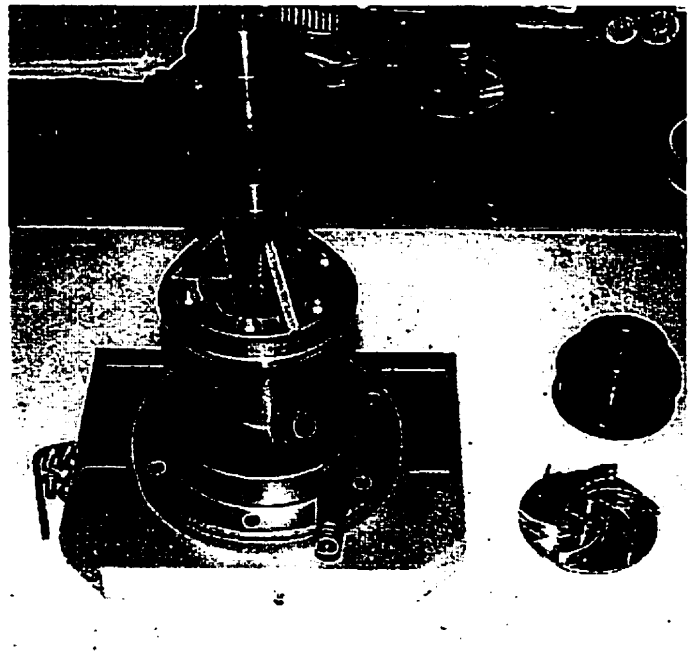

Figure 7. Basic Pump Design [104]

The pump shown in Figure 7 was designed and built to circulate mixtures of sand and oil. In addition, the pump was designed not to entrain air, a common problem in many centrifugal pumps. The slurry is pumped into the center of the pump down an inclined pipe (I.D.=1 inch or 2.54 cm) where it comes into contact with an assembly of circulating blades (shown dismantled and lying to the right of the pump in Figure 7). The slurry is then pumped out through the outlet pipe (I.D.=1 inch or 2.54 cm). The assembly of blades in the pump is attached to a central shaft. The pump shaft is rotated by a motor with the use of a rotating belt, which is covered by a protective metal shield. Any air bubbles that enter the inlet pipe with the incoming slurry can float up through the central cone-portion of the pump, which is open to the air. In this fashion the pump releases any entrained air.

The pump used for these experiments is shown in Figure 8. It operates in a similar manner as the pump described above, however, a few alterations have been made.

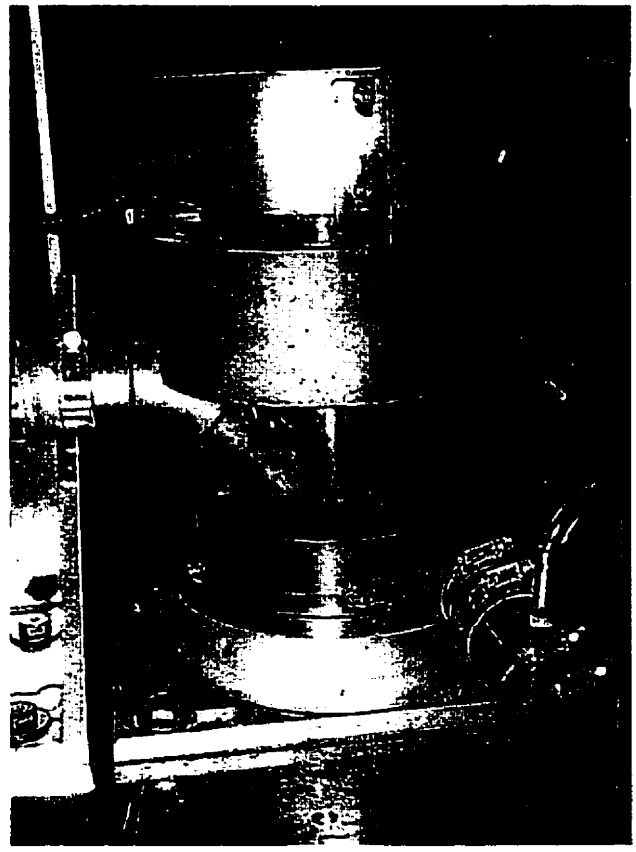

Figure 8. Pump Used in This Study [103]

The four major changes from the initial pump design that have been made are (please refer to Appendix A for a cross-sectional blueprint of the pump): **(i)** The interior diameter of the inlet and outlet pipes have been enlarged from 2.54 cm to 4 cm to connect with the 4 cm I.D. PVC pipe. **(ii)** The inlet has been rotated approximately 90 degrees clockwise from the outlet to facilitate the construction of a loop around the pump. **(iii)** The inlet pipe feeds approximately 1 inch off from the center of the pump as opposed to directly into the pump's center as the initial design did. This was done to ease the flow of fluid through the pump from the inlet to the outlet. **(iv)** A 2.4 liter (approximately 20.5 cm in diameter by 8.1 cm deep) reservoir section has been added to the top of the pump. The reservoir section was added because a higher liquid level in the pump was desired. The loop can easily be filled by pouring a suspension directly into the pump's reservoir section. Figure 9 below shows how the loop is filled with liquid.

Figure 9. Fluid Being Poured Into the Loop Via the Pump [103]

The revolution speed of the pump shaft is measured using a tachometer. A RPM digital display is mounted above the motor. The linear velocity of fluid circulating in the loop has been calibrated with the RPM readings. Fluid can be circulated within the loop to 3 m/s and beyond (the pump has not been tested to its maximum power).

2.2.2 Injection Sections for Air and Deinking Chemicals

Air and deinking chemicals are introduced into the loop with the use of small ¼ inch 2-way ball valves. Air is introduced into the loop through one needle valve located 9 cm from the beginning of the outlet pipe of the pump. Air is fed from a compressed air cylinder and the flowrate is regulated with an Omega Rotameter (model FL-1808).

Deinking chemicals are introduced into the loop through another ¼ inch 2-way ball valve located 12 cm before the 90 degree bend leading to the pump inlet. Deinking chemicals are fed from a 4 liter beaker by a Cole-Palmer Masterflex peristaltic pump.

Figure 10 below depicts the air-injection valve in the foreground and the deinking chemicals valve in the background.

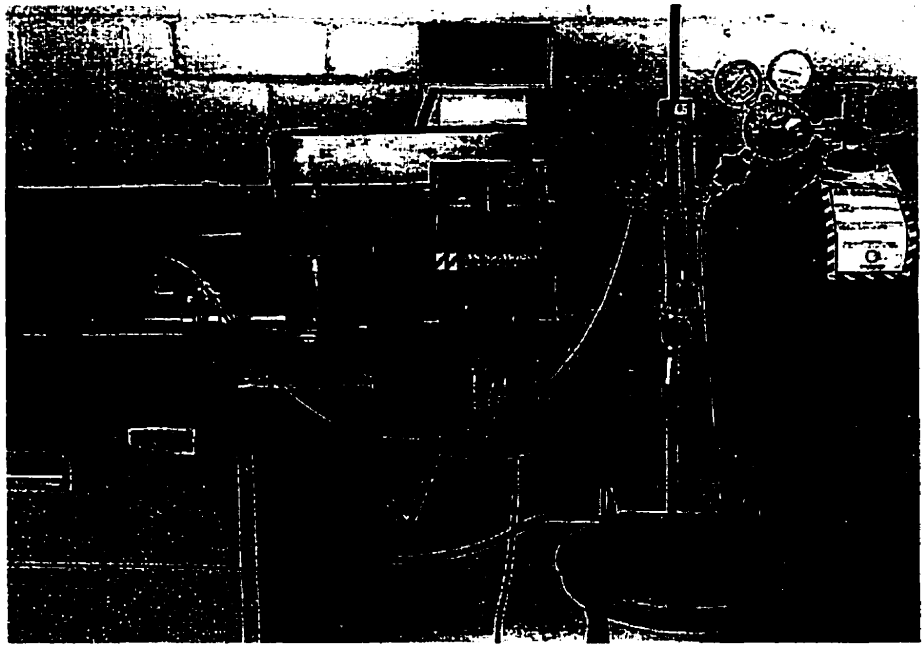

Figure 10. Close-up of the injection sections [103]

2.2.3 Image Cell

The image cell was designed to obtain clear video images of bubbles moving in suspension at industrial linear velocities (i.e. 2-3 m/s). Images can be taken directly through the 4 cm I.D. clear PVC pipe, however, a tremendous amount of bubble overlap occurs making it difficult to discern bubbles from one another.

In order to alleviate this problem, an image cell with a rectangular cross-section was constructed having a spacing of 1 cm between two glass faces. A 1 cm spacing would definitely reduce the amount of bubble overlap in the images, and it was expected and shown not to significantly alter the shapes of bubbles (which are typically smaller than 3 mm in size). Figure 11 depicts the image cell and camera set-up.

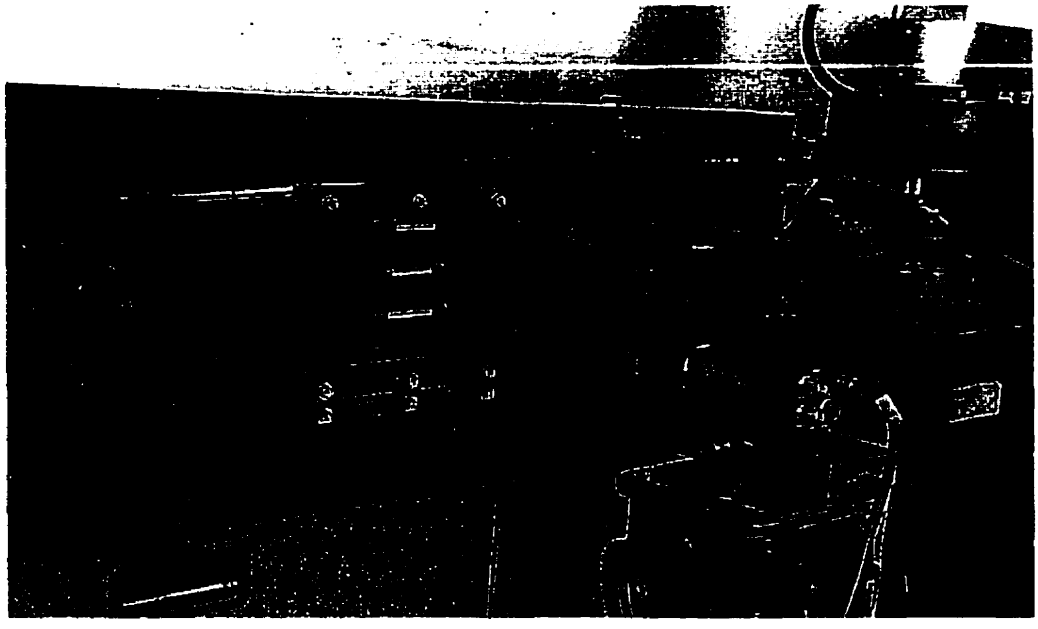

Figure 11. Image Cell/Camera Set-Up [103]

The image cell was designed to have the same cross-sectional area as the 4 cm I.D. PVC pipe (12.6 cm^2) in order to minimize velocity fluctuations in this section. Thus with the spacing between the two glass faces chosen to be 1 cm, the height was set at 12.6 cm. Tempered glass was chosen due to its high strength properties. The rest of the image cell is comprised of PVC. The image cell can be dismantled by undoing six bolts should a replacement of the glass faces be required. At either end of the image cell are PVC unions (Nibco 1½ inch) which allow for quick and easy placement and removal of the image cell from the loop. The total length of the image cell (including female union-halves) is 59.5 cm and the length of the rectangular cross-section is 15 cm.

2.2.4 Clear PVC Pipe

Clear polyvinylchloride (PVC) pipe was chosen as the connecting pipe for the loop instead of other clear piping alternatives (e.g. glass, acrylic). PVC was chosen because it is shatter resistant, it has high strength properties (rated to 330 p.s.i.), and standard fittings (e.g. elbows, unions, valves, etc.) are readily available.

In order to reduce the pressure losses in the loop, a u-shaped length of continuous PVC pipe was fabricated and installed, replacing two 90 ° elbows. This u-shaped section is equipped with a drain to quickly empty the loop of its contents.

2.3 IMAGE ANALYSIS SYSTEM

The image analysis system for these experiments consisted of three elements: **(i)** a video camera **(ii)** appropriate lighting **(iii)** an image analysis software.

2.3.1 Video Cameras

In order to attain crisp images of bubbles moving quickly (i.e. 1-3 m/s) in suspension, a video camera with a fast shutter speed was required in order to minimize motion blur.

Two CCD (charge coupled device) video cameras were used interchangeably to obtain images for this research work, the Sony Color SSC-C374 and the Co-Star Black and White Progressive-Scan CV-M10. The range of shutter speeds for the Sony and Co-Star video cameras are 1/60s to 1/10 000 and 1/60s to 1/800 000, respectively. Thus the Co-Star can operate at shutter speeds 80 times faster than the Sony camera. With the Sony color camera set at its fastest shutter speed of 1/10 000s, clear images were captured which could effectively be analyzed by image analysis.

The Co-Star camera was purchased midway through the project and was chosen because it has much faster shutter speeds and its "Progressive-Scan" technology improves the image quality of fast-moving objects. The optimum shutter speed for the Co-Star camera was found to be 1/20 000s. Operating at faster shutter speeds than 1/20 000s resulted in images which were too dark. This is due to the fact that increasing the shutter speed lessens the amount of light available to expose the image. Images attained

using the Co-Star camera were slightly sharper than those obtained using the Sony, and also could be readily analyzed by image analysis.

All images were stored on S-VHS tapes and were later transferred to a computer using a frame-grabber board and analyzed by image analysis.

2.3.2 Lighting

In order to attain high-quality images, high-powered lighting was required as well as an appropriate background color. Two Unomat LX801 Multi-Power (300/150 Watt) halogen light sources were used.

In order to provide good contrast between air bubbles and the fluid, a yellow cardboard sheet was used as background for the images. The color yellow provided a better contrast than all other colored sheets tested. The 8.5" by 11" sheet was positioned approximately four inches behind the image cell. The image cell was lit from behind by reflecting light off the yellow sheet into the back glass pane of the cell. Lighting the cell in this fashion provided superior images as compared to when the cell was lit from the same direction the camera was facing.

These light sources release a tremendous amount of heat during use. Due to the fact that PVC melts at 60 °C, it was necessary to cool the image cell and surrounding pipes during experiments. This was done with the use of a table fan set at maximum power.

2.3.3 Image Analysis Software

The image analysis software used to attain the bubble size distributions was Image Pro Plus for the Macintosh. Images stored on S-VHS tapes were transferred onto a PowerMac 7500 computer using a frame grabber. These images were then analyzed to obtain the bubble size data. This data was then imported into Microsoft Excel where the bubble size distributions were plotted.

2.4 MATERIALS

2.4.1 Water Grade

For these experiments tap water was used.

2.4.2 Pulp

Newsprint grade Thermal Mechanical Pulp (TMP) was used for these experiments. The freeness of the pulp was 120 and the brightness was 60.

2.4.3 Deinking Chemicals

The flotation deinking chemicals used in these experiments were Calcium Chloride and Sodium Oleate.

2.5 EXPERIMENTAL METHODS

2.5.1 Calibration of Pump RPM and Fluid Velocity

In order to calibrate the pump RPM with the fluid velocity in the loop, a small plastic tracer particle, weighing 0.118 g, was used. The time was recorded for the particle to circulate 20 times in the loop containing tap water at room temperature with the pump set at a specific RPM. With the loop length measured as being 3.78 m, the velocity for that RPM setting could easily be calculated. The velocity was measured in this fashion 5 times and the average value was taken as being the fluid velocity for that RPM setting. Table 1 includes the calibration data.

Table 1. Calibration of Pump RPM and Fluid Velocity

RPM	Distance Traveled (m)	Average Time for 20 Revolutions (s)	Velocity Calculated (m/s)
526	75.5	76.1	1.00
593	75.5	65.3	1.16
910	75.5	39.6	1.91
949	75.5	37.7	2.00
1260	75.5	27.6	2.73
1372	75.5	25.2	3.00

From the data contained in Table 1, the following linear relationship with an R^2 value of 0.999 can be obtained which is valid until a fluid velocity of 3 m/s:

$$\text{Fluid Velocity [m/s]} = (2.36*10^{-3})\ (\text{Pump RPM}) - 0.24 \qquad (1)$$

2.5.2 Air Volume Fraction Control

In order to perform well-characterized experiments with the air-injection unit, it was necessary to be able to control the air volume fraction. In order to do this a tape measure was placed on the inside wall of the pump's reservoir section, as shown in Figure 12 below.

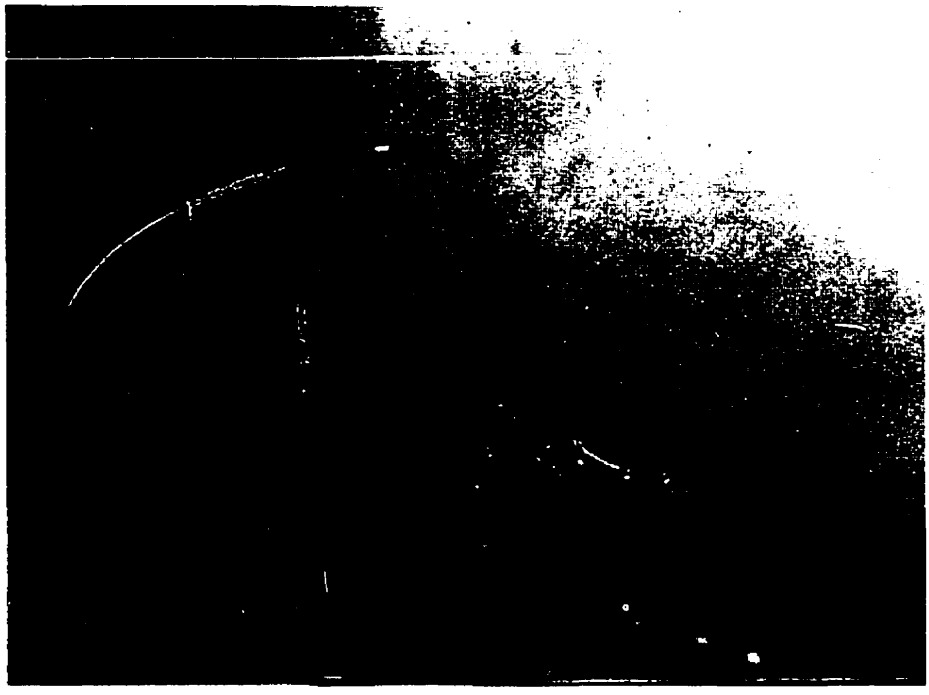

Figure 12. The Pump Reservoir Section with Measuring Tape [103]

The volume of the loop contents was calibrated with the increments on the tape measure by pouring known volumes of tap water into the loop. Appendix C contains the loop volume calibration data. From this data the following linear relationship with an R^2 value of 0.999 can be obtained:

$$\text{Loop Volume [mL]} = (291.46)(\text{Tape Measure Mark [cm]}) + 5296.97 \qquad (2)$$

Any air bubbles in the loop were removed during this volume calibration because their volume would have corrupted the data. Air bubbles were removed from the loop by circulating the water at approximately 0.8 m/s for at least 10 minutes. In Figure 12 some

air bubbles can be seen reaching the water surface in the pump's reservoir section. At a moderate fluid velocity of 0.8 m/s, air bubbles can effectively float up through the pump and escape into the atmosphere when they reach the liquid surface. At very low or very high fluid velocities air bubbles are removed less efficiently. At low fluid velocities there is not enough shear to break up pockets of air which tend to form and remain at various locations in the loop. Increasing the fluid velocity increases the shear and the air pockets are broken down into dispersed air bubbles. These dispersed bubbles can then be removed as they circulate through the loop. At high fluid velocities, however, dispersed air bubbles travel with so much momentum that they tend to pass through the pump rather than float up within it. The buoyancy of the bubbles is offset by their momentum and they circulate within the loop for a much longer period of time than at more moderate fluid velocities.

The definition of air volume fraction used in this research is: *the volume of dispersed air divided by the total volume of aerated fluid or suspension*. For all the experiments presented in this chapter, the air volume fraction used was 6 %. This value is low compared to air volume fractions used in industry (e.g. 20-40% for the Escher Wyss CF Cell), however, the intention for these experiments was to minimize bubble overlap in images so that they could be readily analyzed by image analysis.

Attaining the desired air volume fraction was achieved by filling the loop with tap water or suspension to the 4.5 cm mark on the reservoir's tape measure with all dispersed air removed. The liquid is then circulated at the desired velocity for that specific experiment and air is injected into the loop at an appropriate flowrate to achieve a steady liquid level height in the reservoir section at 6.0 cm. This liquid level increase indicates that 438 ml of dispersed air is present in 7050 ml of aerated liquid present in the loop, which is equivalent to an air volume fraction of 6 %.

During any experimental run operating at steady state, the amount of air being injected into the loop is equal to the amount of air floating up and escaping from the pump. For various liquid velocities, different air flowrates must be injected into the loop in order to attain the same volume fraction of air. This is because, in general, as the liquid velocity is increased, air is less efficiently removed through the pump as was discussed earlier. For this reason, as the liquid velocity is increased, less makeup air is

required to be injected in order to maintain the same liquid level height in the reservoir section.

2.5.3 Vertical or Horizontal Image Cell Configuration

Figures 6 and 11 have shown the image cell oriented in a vertical configuration. The unions at either end of the cell also make it possible to orient the cell in a horizontal configuration, as shown in Figure 13. A level is used to ensure that the cell is perfectly horizontal.

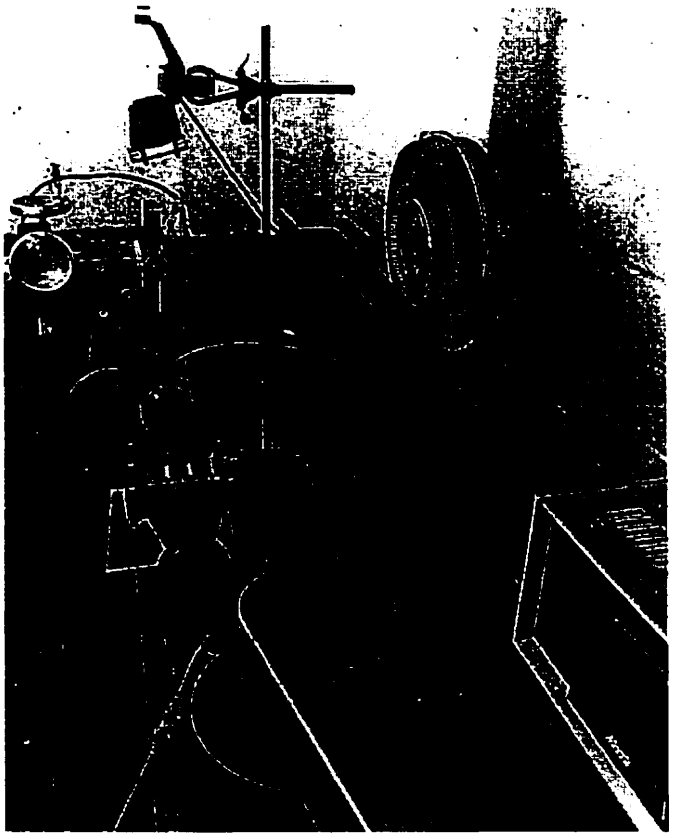

Figure 13. Horizontally Configured Image Cell [103]

Preliminary experiments, without the use of deinking chemicals, were performed with the image cell oriented in the vertical configuration. When operating the air-injection unit at low fluid velocities (e.g. 1 m/s and below), it was found that air would agglomerate as a layer of air at the top of the image cell. Meaningful bubble size distributions could not be attained under such conditions due to the fact that dispersed air bubbles were no longer present in that section of the cell. This difficulty was

circumvented by performing the same runs with the cell oriented in the horizontal configuration. A layer of air no longer formed and a meaningful bubble size distribution could now be obtained because air bubbles remained dispersed.

Figure 14 is an image of air bubbles in tap water moving at 1 m/s taken from the top portion of the image cell oriented in the vertical configuration. Numerous bubbles have congregated at the top of the cell and have clearly formed a layer of air. Figure 15 is an image also taken from the top portion of the cell of air bubbles in tap water moving at 1 m/s, however, the cell is now oriented in the horizontal configuration. A layer of air no longer forms and the air bubbles remain well dispersed.

Figure 14. At 1 m/s fluid velocity, a layer of air forms at the top section of the image cell when it is configured vertically

Figure 15. At 1 m/s fluid velocity, dispersed air bubbles exist at the top section of the image cell when it is configured horizontally

For higher fluid velocities (e.g. 2 m/s), the orientation of the image cell vertically or horizontally was not an issue. At such speeds the high degree of turbulence prevented a layer of air from forming at the top of the image cell when configured in the vertical configuration. Figures 16 is a bubble size distribution histogram for a 2 m/s run of tap water and air having an air volume fraction of 6% with the image cell horizontally oriented. Figure 17 is a bubble size distribution for an identical run except the image cell is vertically oriented.

Figure 16.
(6 % volu

Figure 17.
(6 % volu

It is apparent from Figures 16 and 17 that the trends in the histograms are extremely similar. Bimodal histograms are present in which one peak represents the smaller bubbles and one peak represents the larger bubbles. The average values for the two peaks for both configurations are extremely close, and thus it is found that the orientation of the image cell is insignificant for 2 m/s fluid velocities and beyond. A hypothesis as to the reason bimodal histograms result is discussed in the Results and Discussion section.

As noted in Figures 16 and 17, the number of bubbles used to comprise the vertical and horizontal configuration histograms were 2160 and 1676, respectively. A total of 21 images were analyzed for each run. The reason that the horizontal configuration run had 22.4% less bubbles is simply because the field of view of the bubble images attained using that orientation was 22.8% smaller. Considering this factor, the bubble count per unit volume in both runs was virtually identical. This fact, combined with the strong similarity of the histograms in Figures 16 and 17, proves the reproducibility of the experimental procedure.

Thus, meaningful bubble size distributions were obtained for both low and high fluid velocity cases with the image cell oriented in the horizontal configuration. Based on these findings, the image cell was chosen to be oriented in the horizontal configuration for all experimental runs. All bubble size graphs and results from here onward were obtained with the image cell in the horizontal configuration.

2.5.4 Top, Middle and Bottom Image Cell Sections

With the image cell oriented in the horizontal configuration, it was observed that the bubble size distribution was somewhat different at the top, middle, and bottom portions of the cell. Figures 18, 19 and 20 are the bubble size distributions for the top, middle and bottom sections of the cell, respectively, for the 2 m/s tap water and air run discussed above. Each histogram represents data obtained from 7 images. Combining all the data contained in Figures 18, 19 and 20 results in the histogram shown in Figure 16.

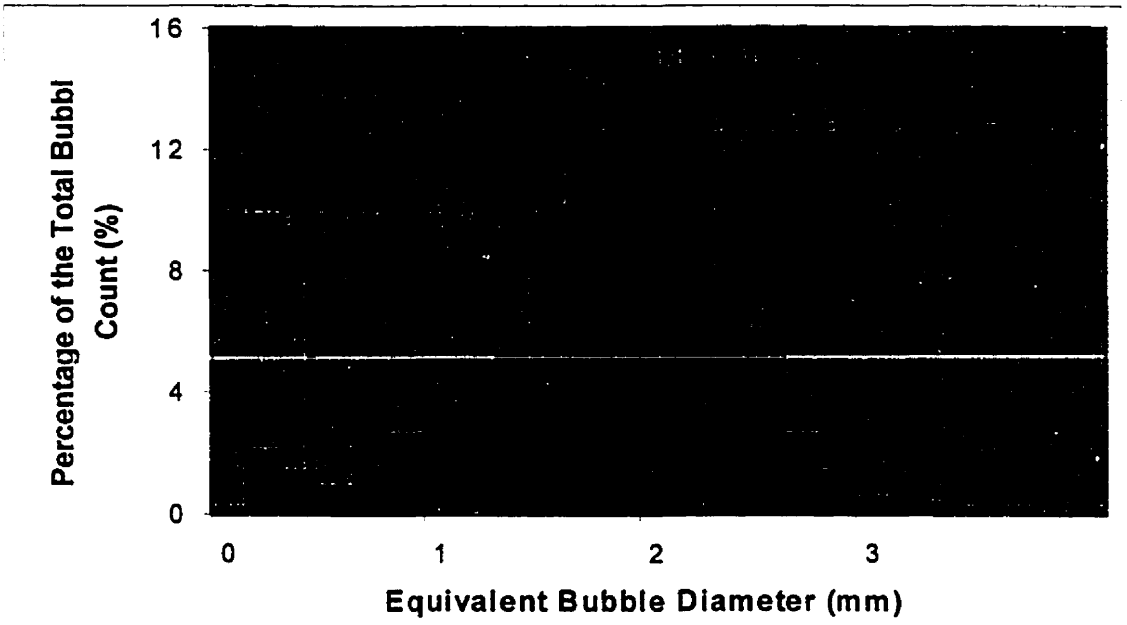

Figure 18. Air bubble size distribution located at the top section of the image cell for a 2 m/s tap water and air run (6 % volume fraction air)

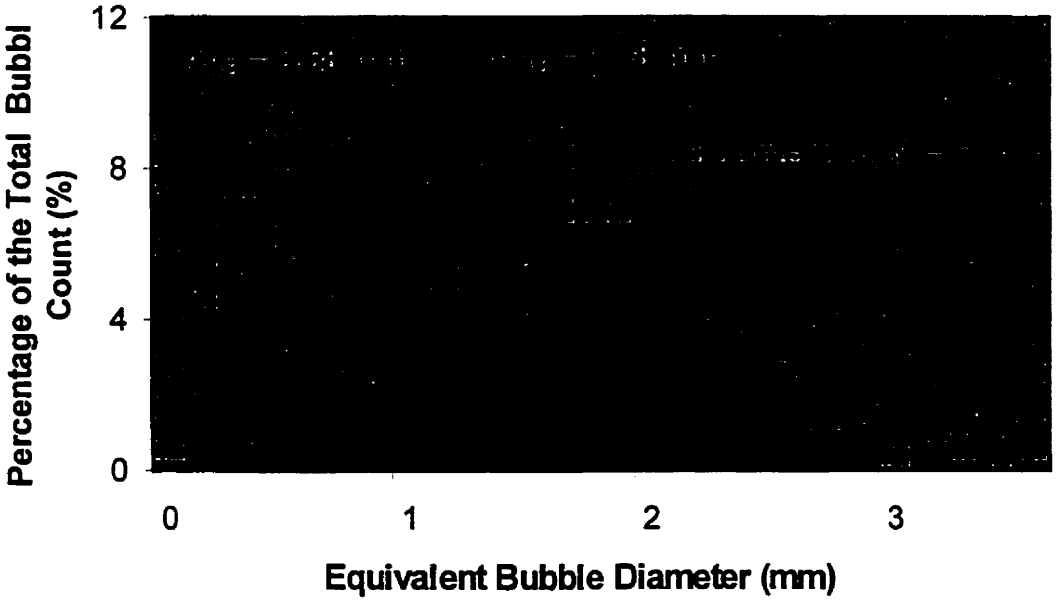

Figure 19. Air bubble size distribution located at the middle section of the image cell for a 2 m/s tap water and air run (6 % volume fraction air)

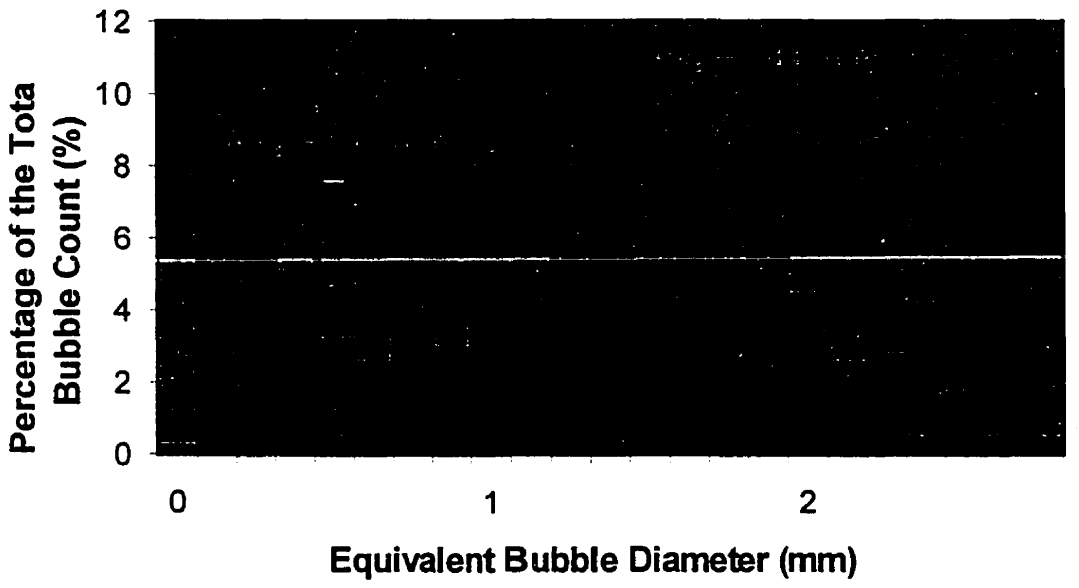

Figure 20. Air bubble size distribution located at the bottom section of the image cell for a 2 m/s tap water and air run (6 % volume fraction air)

The absolute values for the average bubble sizes (i.e. small and large bubble peaks) are not drastically different, however, the overall shape of the histograms do differ. In order to account for the variations in the bubble size distribution across the cell and attain an overall bubble size distribution for an experimental run, 7 images were taken from the top, middle, and bottom sections of the image cell. The data from these 21 images were than merged to form the bubble size distribution histogram for that run. Measuring tapes, shown in Figure 11, were placed on the image cell glass at the three positions. These scales were required when performing image analysis on the images because they provided a reference as to the sizes of the bubbles.

2.5.5 Bubble Size Measurement Using Image Analysis

Image Pro Plus' measurement operations are performed in terms of screen pixel positions. For example, the length of a measurement is determined by the number of pixels along the line, the area of an outlined object is determined by the number of pixels within the outline, and so forth. In order to analyze an image for bubble size data, it first

was necessary to calibrate the pixel-level measurements into meaningful length-scale measurements. The scale was calibrated using the tape measure, which is present in all images, using the *Image* button in the *Spatial Calibration* dialog box.

Bubble size measurements were initially attempted using an automatic counting and sizing image analysis procedure. Using the *Count/Size* command on the *Measure/Analysis* menu you can count and measure multiple objects automatically. For counting purposes, objects are identified by their intensity (for *Monochrome* images) or color (for *True Color*-Class images). Therefore, it is best to begin with an image that contains objects that are clearly distinguishable from the background, and have an intensity range/color different from the other elements in the image. Due to the fact that many images do not initially fit such ideal conditions, there are a number of pre-processing steps that can be taken to correct such deficiencies, such as filtering processes and contrast enhancement.

Automatic sizing and counting of bubbles was determined not to be a feasible method of analysis for our images because of the following two reasons: **(i)** Due to the nature of the images, 100% of the bubbles could not always be made clearly distinguishable from the background, even with the use of pre-processing techniques. This resulted in erroneous size measurements. **(ii)** When bubbles overlapped in an image, it was not possible to automatically measure the entire area of all overlapping bubbles.

Bubble size measurements were performed using a manual tracing procedure available with Image Pro Plus. With this analysis approach all bubbles in an image that are visible to the naked eye can be accurately measured for size. Bubble overlap is also not a concern when using this method. The manual measuring tools are accessed using the *Measurements* command in the *Measure* menu. The only manual measuring tool used was *Area*. This tool is used to measure the area of a polygon that you define by digitally tracing its perimeter using a mouse. The area of the polygon is determined by calculating the number of pixels encompassed by the shape. The area measurement is then reported in mm^2 units due to the spatial calibration done prior to analyzing the image.

Due to the fact that air bubbles were traced one at a time using the manual tracing method, it is much more time consuming than the automatic counting and sizing method,

which takes only seconds to analyze an entire image that contains hundreds or thousands of bubbles. The analysis time required to analyze one image using the manual tracing method varies significantly depending on how many bubbles are contained in the image. An image containing 600 bubbles can be analyzed in approximately 30 minutes, whereas one containing 3600 bubbles may require over two hours of analysis.

2.5.6 Bubble Size Distribution Histograms

In order to attain the bubble size distribution for a run, the Feret diameter (the equivalent diameter of a circle with the same area) was calculated for all of the bubbles from the area data attained using Image Pro Plus. The Feret diameter is calculated using the following basic equation:

$$\text{Feret Diameter} = (4A/\pi)^{1/2} \qquad (3)$$

The bubble size distribution histogram then plots the "Percentage of the Total Bubble Count" versus a range of Feret diameter bins (evenly distributed between the data's minimum and maximum diameter values). A Feret diameter value is counted in a particular bin if it is equal to or less than the bin number but is greater than the previous bin number. All values below the first bin value are counted together, as are the values above the last bin number.

2.5.7 Average Bubble Size Calculations

Some of the bubble size distribution histograms were unimodal (i.e. one peak was present) and others were bimodal (i.e. two peaks were present). The average bubble size for the unimodal case was simply: *the sum of all of the Feret diameters divided by that run's total number of bubbles counted.* For the bimodal cases, two average bubble sizes were calculated, one for the smaller bubble peak and one for the large bubble peak. The average bubble size for each peak was: *the sum of the Feret diameters comprising that peak divided by the number of bubbles comprising that peak.* The bin located between the two peaks having the lowest "Percentage of the Total Bubble Count" marked the division

between the peaks. For "Average Bubble Size" calculations, this dividing bin was interpreted as belonging to the "Small Bubble" peak.

2.5.8 Typical Experimental Run Procedure

In order to attain the bubble size distribution for a given experiment, the air-injection unit is first operated under steady state operating conditions. The general experimental procedure is as follows:

(i) Have the image cell oriented in the horizontal configuration. Use a level to ensure that it is perfectly horizontal.

(ii) Fill the loop with the water or pulp suspension by pouring it into the reservoir section of the pump.

(iii) Remove any entrained air from the loop by circulating the fluid at approximately 0.8 m/s for a sufficient amount of time (approximately 10-15 minutes) at which point no entrained air is visible.

(iv) Inject deinking chemicals into the loop using the peristaltic pump. Allow at least two minutes for thorough mixing and for the removal of any entrained air introduced into the loop while injecting chemicals.

(iv) Pour tap water into the reservoir section of the pump until a liquid level of 4.5 cm on the measuring tape is attained. Allow at least two minutes for thorough mixing of this added water.

(vi) Adjust the pump RPM in order to attain the desired fluid velocity.

(vii) Continuously inject air into the loop at an appropriate flowrate so as to attain a steady liquid level at 6.0 cm on the measuring tape in the pump's reservoir section. The loop is now operating at 6 % volume fraction air.

(viii) Allow one minute to elapse in order to achieve steady state conditions in the loop.

(ix) Using the Sony or Co-Star video camera, a S-VHS recorder and appropriate lighting, attain approximately 1 minute and 20 seconds of footage of bubbles moving in suspension from each of the three sections on the image cell (top, middle, and bottom).

(x) Randomly chose 7 images (typically one every 10 seconds) for each of the

three image cell sections (a total of 21 images) and transfer them from the S-VHS tape to the hard drive of the PowerMac 7500.

(xi) Use Image Pro Plus software to analyze the 21 images and attain the Feret diameters of all the visible bubbles in the images.

(xii) Combine the bubble size data attained from the 21 images. Plot the bubble size distribution histogram for the run using Microsoft Excel.

2.5.9 TMP Fibre/Fines Separation Procedure

Experiments were performed in which the effect of the presence of fibres or fines on the air bubble size distribution was investigated. In order to separate fibres from fines of the TMP stock , a Flygt Float-Wash fractionator equipped with a 100 mesh screen was used. Appendix D includes a schematic of the Float-Wash followed by its operating instructions. Prior to the fractionation, the TMP pulp was hot disintegrated using the Domtar Method in order to remove the latency.

2.6 RESULTS AND DISCUSSION

Seven experimental runs were performed using the air-injection loop apparatus to investigate the effect of various process parameters on the bubble size distribution in the air-injection section of a flotation deinking cell. The four process parameters investigated were: **(i)** fluid velocity **(ii)** the presence of fibres **(iii)** the presence of fines **(iv)** the presence of deinking chemicals (Sodium Oleate alone or with Calcium Chloride).

For all of the runs tap water was used and the air volume fraction used was 6 %. Runs 1, 2 and 3 used only tap water and air and investigated the effect of fluid velocity on the bubble size distribution. The velocities used for runs 1, 2, and 3 were 1, 2 and 3 m/s, respectively. Runs 4, 5, 6 and 7 were all performed at 1 m/s. Run 4 investigated the effect of the presence of 0.2% consistency TMP fibres on the bubble size distribution. Run 5 investigated the effect of the presence of 0.2% consistency TMP fines on the bubble size distribution. Run 6 investigated the effect of the presence of 0.33 mmol/L Sodium Oleate on the bubble size distribution. Run 7 investigated the effect of the presence of 0.2% TMP fibres and 0.07 mmol/L (or 1% based on fibre mass) Sodium

Oleate and 0.09 mmol/L (or 0.5% based on fibre mass) Calcium Chloride on the bubble size distribution.

2.6.1 Typical Bubble Images

Typical bubble images are shown below in Figures 21-25 for Runs 1, 4, 5 , 6 and 7 (images for Runs 2 and 3 are much like that of Run 1 and are thus not shown). Figure 21 depicts a very crisp still image of air bubbles moving at 1 m/s in tap water. The smallest increments on the scale present in the image represent millimeters. Thus, nearly all of the bubbles in the image have diameters larger than 1 mm.

Figure 22 illustrates that air bubbles moving at 1 m/s are still easily discernable despite the presence of 0.2% consistency TMP fibres. This was made possible with the use of the novel image cell whose 10 mm wide flow channel minimized visual blockage of the bubbles by fibres.

Figure 23 depicts an image from Run 5 of air bubbles flowing at 1 m/s in a slurry of 0.2% consistency TMP fines. Due to the fact that fines are very small and have much higher specific surface area than fibres do, they scatter more light than fibres and as a result make the image more cloudy and the bubbles less visible. It is believed that due to the presence of fines, many of the small bubbles present were not visible in the images and thus were not able to be counted and measured. This was not believed to be an issue when fibres alone were used because they did not significantly hinder the visibility of small air bubbles.

Figure 24 depicts an image from Run 6 of air bubbles flowing at 1 m/s in tap water having 0.33 mmol/L of Sodium Oleate (the approximate concentration present in some industrial flotation deinking cells). Due to the fact that Sodium Oleate soap reduces the surface tension of the air bubbles, very small bubbles were created during this run. As a result of this, in order to effectively measure the bubble sizes, a higher image magnification was required. This is the only run in which a higher magnification was used. In Figure 24, 1 mm in length is represented by the white bar. Thus, with the exception of the largest bubble in the image, all of the bubbles present are smaller than 1 mm in diameter.

Figure 21. Typical image for Run 1 (Tap water moving at 1 m/s with 6% volume fraction air)

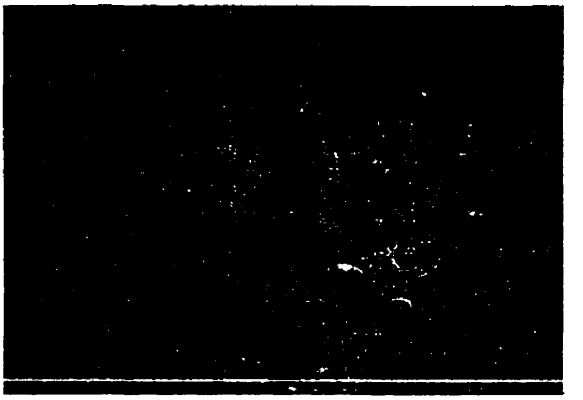

Figure 22. Typical image for Run 4 (Tap water and 0.2% consistency TMP fibres moving at 1 m/s with 6% volume fraction air)

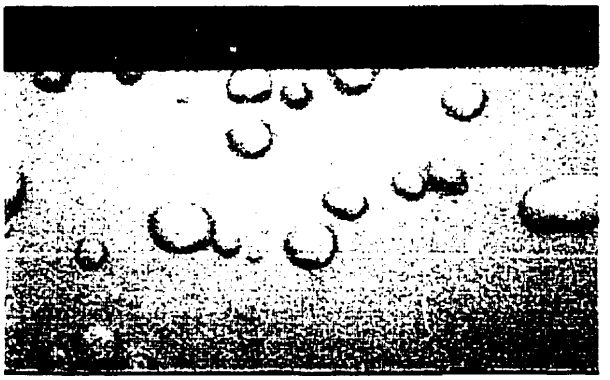

Figure 23. Typical image for Run 5 (Tap water and 0.2% consistency TMP fines moving at 1 m/s with 6% volume fraction air)

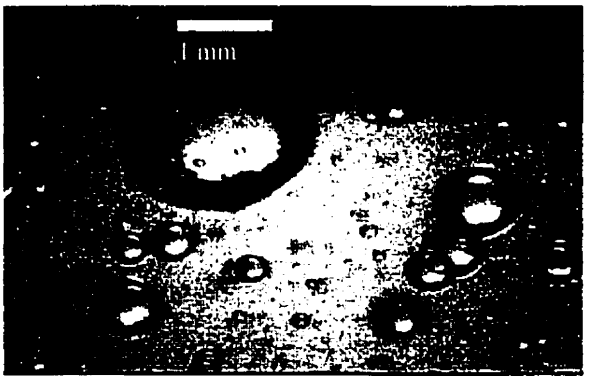

Figure 24. Typical image for Run 6 (Tap water and 0.33 mmol/L Sodium Oleate moving at 1 m/s with 6% volume fraction air)

Figure 25. Typical image for Run 7 (Tap water with 0.2% consistency TMP fibres and 0.07 mmol/L Sodium Oleate and 0.09 mmol/L Calcium Chloride, moving at 1 m/s with 6% volume fraction air)

Not only were the bubbles smaller when surfactant was used, but they were more spherical. The runs which did not use Sodium Oleate had more ellipsoidal bubbles. This deformation is caused by the change in the shear stresses and normal forces acting on the interface between the bubbles and the media. The droplets' form stabilizes when these forces balance on the interface [105].

Figure 25 depicts an image from Run 7 of air bubbles flowing at 1 m/s in 0.2% consistency TMP fibre slurry having 0.07 mmol/L of Sodium Oleate (1% of the fibre mass) and 0.09 mmol/L Calcium Chloride (0.05% of the fibre mass). The Sodium Oleate's concentration was approximately one-fifth of the concentration used in Run 6, thus the air bubbles were not expected to be as small as in Run 6. Because of this fact, the standard magnification used in Runs 1-5 was used to capture images for Run 7.

2.6.2 Effect of Fluid Velocity

In multiphase flow equipment, the size distribution of bubbles is commonly determined by the dynamics of break-up and coalescence. The coalescence proceeds until the drops are large enough to be broken apart and a dynamic equilibrium will be established between coalescence and break-up [106].

A few general concepts will be discussed which are useful when considering bubble breakage due to shear stresses. First of all, in turbulent flows such as the ones discussed in this work, only the energy associated with eddies with length scales smaller than the bubble diameter is available to cause splitting; larger eddies merely transport the bubble. Secondly, a bubble in a shear field tends to rotate and deform. If the velocity gradients are large enough, interfacial tension forces and viscous stresses inside the bubble are no longer able to maintain the fluid particle intact, and it ruptures into two or more smaller daughter particles [105]. As will be discussed, the relative size of these daughter particles to each other has a large effect on the nature of the bubble size distribution.

The bubble size distribution for Run 1 in which tap water was circulated at 1 m/s is shown in Figure 26 (air-volume fraction was 6% and remains so for all other runs). The 'Percentage of the Total Bubble Count' is plotted versus the 'Equivalent Bubble Diameter'. The histogram is bimodal in nature depicting two peaks, one representing the

Figure 26
moving a

Figure 27
at 1 m/s v

Table 2. Summary of Bubble Size Distribution Data for Runs 1-7

Run Number	Run Description	Small Bubble Avg. Size (mm)	Large Bubble Avg. Size (mm)	Percent Small Bubbles (%)	Percent Large Bubbles (%)	Bubble Count in 21 Images	Type of Bubble Size Distribution
1	H_2O 1 m/s & 6% vol. frac. air	0.4	3.0	44	56	606	Bimodal
2	H_2O 2 m/s & 6% vol. frac. air	0.5	1.8	31	69	1879	Bimodal
3	H_2O 3 m/s & 6% vol. frac. air	0.4	1.4	26	74	3673	Bimodal
4	0.2% Fibres 1 m/s & 6% vol. frac. air	0.6	3.5	59	41	861	Bimodal
5	0.2% Fines 1 m/s & 6% vol. frac. air	<0.9	3.1	>26	<74	>403	Bimodal
6	0.33 mmol/L Sodium Oleate 1 m/s & 6% vol. frac. air	0.3	Not Present	100	0	1511	Unimodal
7	0.2% Fibres + 0.07 mmol/L Sodium Oleate + 0.09 mmol/L $CaCl_2$ 1 m/s & 6% vol. frac. air	0.9	Not Present	100	0	1553	Unimodal

'large bubbles' having an average size of 3.0 mm, and the other peak representing the 'small bubbles' having an average size of 0.40 mm. In Table 2 these peak average values are tabulated as well as the run number; a description of the run; the total bubble count from the 21 images analyzed for the run; the percentage of the total bubble count comprised by each peak, noted as 'Percent Small Bubbles' and 'Percent Large Bubbles'; and a description of the histogram (e.g. 'Bimodal' or 'Unimodal'). Table 2 summarizes the bubble size distribution results for Runs 1-7. *The reader is referred to Appendix E for the bubble size distribution histograms for Runs 2-5, and Run 7 (the histogram for Run 6 is shown in Figure 27).*

It should be noted that the bubble size distributions discussed in this chapter are specific to the experimental apparatus used, and particularly, the air-injector used. One study in the literature has shown that the bubble size distribution for a given set of process parameters is dependent on the nature of the air-injector used, especially in the absence of pulp [2].

Of the 606 bubbles measured for run 1, 44% of them (267) comprised the 'small bubble' peak and 56% of them (339) comprised the 'large bubble' peak. The reason why there exists two peaks is likely due to the fact that when exposed to low amounts of turbulent energy in a pipe (e.g. when traveling in slow moving fluid); it is energetically favorable for bubbles to break up into one small bubble and one large bubble. This is because it requires more energy for a bubble to break up into two equally sized bubbles [107]. This is supported by the experimental results of Hesketh et al. [108] for bubble and drop breakage in turbulent pipe flows. Hesketh et al.'s results show that equal-sized (symmetric) bubble breakage has the lowest breakage probability. This tendency for bubbles to break up into one small bubble and one large bubble (axisymmetric bubble breakage) results in two distinct peaks in the bubble size distribution histogram for Run 1.

When the turbulent energy of the system is increased (e.g. when the fluid velocity is increased), however, the probability of more equal-sized (symmetric) bubble breakage also increases. This trend was exhibited in the results for Runs 2 and 3. When the velocity of the tap water in Run 2 was increased to 2 m/s, the probability of symmetric bubble breakage increased resulting in a reduction of the percentage of 'small bubbles'

counted. The percentage of small bubbles decreased from 44% in Run 1 to 31% in Run 2, and the average size of the small bubbles in both runs were almost identical. Because the probability of symmetric bubble breakage increased, the average size of the 'large bubbles' decreased but their number increased in comparison to Run 1. The 'large bubble' peak had an average value of 1.8 mm and comprised 69% of the total bubble count of 1879. Not surprisingly, by increasing the fluid velocity the total bubble count increased significantly (three fold) from Run 1.

In Run 3, the turbulent energy of the system was increased again by increasing the fluid velocity to 3 m/s. As a result of this, the probability of symmetric bubble breakage also increased. The percentage of 'small bubbles' decreased to 26% and the average size of the 'small bubbles' was the same as in Run 1, 0.4 mm. Again, because the probability of symmetric bubble breakage increased, the average size of the 'large bubbles' decreased and their number increased. The 'large bubble' peak had an average value of 1.4 mm and comprised 74% of the total bubble count of 3673. By increasing the fluid velocity from 2 m/s to 3 m/s the total bubble count essentially doubled from Run 2 to Run 3.

The general trend exhibited is that as the fluid velocity was increased, the percentage of 'small bubbles' decreases. It is speculated that if the fluid velocity were to be increased further, eventually a critical fluid velocity would be reached in which the percentage of 'small bubbles' would become zero and a unimodal bubble-size distribution histogram would be attained. The average bubble size of the bubbles comprising this single remaining peak would accordingly be very small due to the highly turbulent regime. At this critical fluid velocity the subjected shear stress on the bubbles would be strong enough to homogeneously break them up into small bubbles which comprise the single peak.

Similar bimodal and unimodal histogram trends resulting from varying amounts of shear forces acting on bubbles or droplets have been found in the literature. One study involved the use of the Injector Aerated Laboratory Flotation Deinking Cell described in Chapter 1 [2]. One graph in this paper is visually similar to Figure 26. For a water and air system using a step-diffuser air-injector, the air bubble size distribution is

plotted for various water flow rates (7 and 9 m^3/h) and air volume fractions (57-107%). For all experiments a bimodal distribution was attained which is very similar to Figure 26. The general average bubble size values for each of the two peaks is very similar to those attained for our Runs 1-3. The method of bubble size measurement use by the authors was very different from the image analysis techniques employed in this work. Hunold et al. [2] utilized a special probe that measured bubble size based on different optical refraction of light by air and the continuous medium.

Another study found in the literature investigated the effect on the droplet size distribution of Oleic Acid being injected at the base of a bioreactor from a spinning sparger [109]. The shear forces acting on the droplets were controlled by altering the RPM of the spinning sparger. Bimodal histograms were attained when low amount of shear stress was exerted on the droplets (i.e. when the angular velocity of the sparger was low or the sparger was not spinning at all). For the cases in which high amounts of shear stress was exerted on the droplets (i.e. where the sparger was spinning at moderate to high velocities), unimodal histograms were obtained.

2.6.3 Effect of the Presence of Fibres

In Run 3 the effect of the presence of fibres on the air bubble size distribution was investigated. A low TMP fibre consistency of 0.2% was chosen in order for the air bubbles to be adequately visible. The suspension velocity was chosen to be 1 m/s and the air volume fraction held constant at 6%. Thus the only difference between this run and Run 1 was the presence of 0.2% fibres.

The bubble size distribution was bimodal as it was in Run 1, and the average peak values were similar. The percentages of 'small bubbles' to 'large bubbles' was somewhat different, however. This is likely because some of the turbulent energy of the system is dissipated from the translational motion of the fibres. Thus the presence of fibres helps shield bubbles from turbulent eddies in the fluid and thus effectively reduces the shear stress acting on the air bubbles. This reduction of shear stress increases the probability of axisymmetric bubble breakages resulting in very small and very large bubbles.

Due to the heightened production of small bubbles due to this phenomenon, the percentage of small bubbles was 59%, up from 44% in Run 1. It also makes logical sense

that under these conditions, several small bubbles could end up breaking off from one large bubble. Thus the total number of bubbles could increase when the turbulent energy of the system is decreased, with the majority of the bubbles being 'small bubbles'. This occurred in this instance and the total bubble count was 861, up from 606 in Run 1.

Because axisymmetric bubble size breakage was more likely due to the presence of fibres, the average size of the 'large bubbles' increased to 3.5 mm in comparison to Run 1's value of 3.0 mm. A study in the literature states that fibres act as barriers toward upward bubble motion and increase the coalescence of bubbles [98]. This phenomenon is likely a contributing factor in the increase of the average sizes of the 'small' and 'large' bubbles from their values in Run 1.

Work by Ajersch and Pelton [99] indicates that, in the absence of deinking chemicals, air bubbles do not adhere to fibres. This is consistent with this chapter's results which illustrated that the presence of fibres had only a small effect on the air bubble size distribution.

2.6.4 Effect of the Presence of Fines

In Run 5 the effect of the presence of fines on the air bubble size distribution was investigated. A low TMP fines consistency of 0.2% was chosen in order for the air bubbles to be adequately visible. Even at this low fines consistency level, small air bubbles (i.e. smaller than 0.5 mm) were very difficult to distinguish in the still video images. This is because fines are extremely small and thus have very high specific surface area with which to scatter light and make the images very cloudy. The suspension velocity was chosen to be 1 m/s and the air volume fraction held constant at 6%. Thus the only difference between this run and Run 1 was the presence of 0.2% fines.

The bubble size distribution was bimodal as it was in Run 1 and the average peak value for the 'large bubbles' was similar. Due to the fact that the images with fines were very cloudy, it is believed that we were unable to measure many very small air bubbles from the images. Due to the fact that many 'small bubbles' were unable to be counted, it is believed that the average size of the 'small bubbles' peak is actually less than the tabulated value of 0.9 mm. In accordance with this, the total bubble count is greater than

the tabulated 403, and the percentage of 'small bubbles' from the total bubble count is greater than the tabulated value of 26%.

It is believed that the presence of fines, like fibres, may reduce the shear stress acting on air bubbles. Because fines are smaller than fibres, it is believed, however, that they have less of an effect in this regard than fibres do. The presence of fines should slightly increase the likelihood of axisymmetric bubble breakage as compared to when no fines are present. This would lead to a greater percentage of small bubbles than were present in Run 1. Thus the actual percentage of small bubbles is likely slightly higher than Run 1's 44%, and lower than Run 4's 59%. Correspondingly, the actual total bubble count is likely slightly higher than Run 1's 606 and lower than Run 4's 861.

Because axisymmetric bubble size breakage may have been slightly more likely due to the presence of fines, the average size of the larger bubbles slightly increased to 3.1 mm in comparison to Run 1's value of 3.0 mm. This finding is not conclusive however, because this very small difference in average bubble sizes is likely within the experimental error of the analysis.

Fines, like fibres, may act as slight barriers toward upward bubble motion and slightly increase the coalescence of bubbles. This phenomenon may be a contributing factor in the small increase of the average size of the 'large bubbles' from the value in Run 1.

Work by Drabek et al. [100] indicate that, in the absense of deinking chemicals, air bubbles do not adhere to fibres or fines. This is consistent with this chapter's results which illustrated that the presence of fines had only a very small effect on the air bubble size distribution.

2.6.5 Effect of Deinking Chemicals

In Run 6 tap water with 0.33 mmol/L of Sodium Oleate was circulated in the loop at 1 m/s having 6% volume fraction air. This concentration of Sodium Oleate is typically used in some industrial flotation cells and is below its critical micelle concentration of 0.48 mmol/L. The bubble size distribution for Run 6 is shown in Figure 27.

The presence of Sodium Oleate drastically reduces the surface tension of air bubbles, which allowed the bubbles to be easily broken down by the turbulent flow

regime. The air bubbles were broken down to such a degree that a unimodal bubble size distribution was attained having a very small average bubble size of 0.3 mm. The higher magnification used to attain images for Run 6 was essential to accurately measure these small bubble sizes. A large total of 1511 bubbles were counted for this run despite the small image size. Had the image size used in the other six runs been used for Run 6, it is estimated that over 51 000 bubbles would have comprised the bubble size distribution. It is clear that the presence of Sodium Oleate has an extremely large effect on the bubble size distribution.

The objective of Run 7 was to investigate the effect of multiple process parameters on the bubble size distribution. Tap water containing TMP at 0.2% consistency and 0.07 mmol/L Sodium Oleate (1% of the fibre mass) and 0.09 mmol/L Calcium Chloride (0.05% of the fibre mass) was circulated in the loop at 1 m/s having 6% volume fraction air.

The presence of Sodium Oleate resulted in a unimodal bubble size distribution as was similarly achieved in Run 6. Due to the fact that the Sodium Oleate concentration is approximately one-fifth of the concentration used in Run 6, the surface tension of the air bubbles was not as substantially reduced resulting in a larger average bubble size of 0.9 mm. One study in the literature also found that when a surfactant was used, a unimodal bubble size distribution was attained, and that when the surfactant concentration was increased, the average bubble size decreases and the size distribution narrows [97].

The effect of the presence of 0.2% consistency fibres on the bubble size distribution is likely negligible in comparison to the effect of the presence of Sodium Oleate.

A total of 1553 bubbles were counted for Run 7, in comparison to 861 bubbles in Run 4 in which 0.2% consistency fibres were present in the absence of deinking chemicals.

2.7 CONCLUDING REMARKS

A laboratory unit which simulates the air-injection section of an industrial flotation deinking cell has been built. Image analysis has been used to obtain bubble size distributions from still images of air bubbles moving in suspension. The main points of interest from this chapter's work are:

① The presence of Sodium Oleate strongly reduced the air bubble size and produced a unimodal bubble size distribution. The average air bubble increased with a decreased concentration of Sodium Oleate.

② Bimodal bubble size distributions were attained for all experiments except when Sodium Oleate was used.

③ The presence of TMP fibres at 0.2% consistency had a small effect on the air bubble size distribution. It is believed that the fibres reduced the shear stress exerted on air bubbles, increasing the probability of axisymmetric bubble breakage.

④ The presence of TMP fines at 0.2% consistency did not have a significant effect on the air bubble size distribution. Fines, like fibres, may slightly reduce the shear stress exerted on air bubbles, increasing the probability of axisymmetric bubble breakage. This finding was not conclusive, however.

⑤ Increasing the fluid velocity increases the probability of symmetric bubble breakage and has a significant effect on the bubble size distribution.

2.8 RECOMMENDATIONS FOR FUTURE WORK

The following types of experiments are interesting possibilities for continued work concerning the effect of flotation deinking process parameters on the air bubble size distribution:

- the effect of temperature on the air bubble size distribution
- the effect of air injector design on the air bubble size distribution
- the effect of surfactant type and concentration on the air bubble size distribution
- the effect of higher fibre/fine consistencies on the air bubble size distribution

CHAPTER 3

THE EFFECT OF FLOTATION DEINKING PROCESS PARAMETERS ON DEINKING EFFICIENCY

ABSTRACT

The flotation deinking air-injection unit described in Chapter 2 has been developed into a fully functional laboratory-scale flotation deinking cell for experiments discussed in this chapter. The objective of these experiments was to investigate the effect of furnish type, air volume fraction and slurry velocity on the deinking efficiency. The deinking efficiency was gauged by measuring the Ink Speck Count, ISO Brightness and Effective Residual Ink Content (ERIC) of 3.0 gram Buchner pads prepared before and after flotation deinking. Some of the experiments used 100% aged newsprint furnish and others used 70% fresh newsprint and 30% fresh magazine. One run using 70/30 mixture of newsprint and magazine attained a final Brightness of 67.4, an increase of 11 points, indicating that the cell functions well. Increasing the air volume fraction while keeping the suspension velocity constant, did slightly improve the deinking efficiency for the 100% aged NP case, however, did not result in any significant improvement for the 70% NP/ 30% MG case. The 100% aged newsprint runs had considerably lower initial brightness and considerably higher initial ERIC compared to the runs using 70% fresh newsprint and 30% fresh magazine. The 100% aged newsprint runs also achieved much lower Percentage Speck Removal compared to the runs using 70% fresh newsprint and 30% fresh magazine. It is believed that the increased shear forces associated with increasing the suspension velocity broke-up ink agglomerates that were in suspension into a larger number of smaller ink particles. It is not believed, however, that increasing the shear by increasing the suspension velocity dislodged ink from within fibre flocs, and increased the amount of ink available to be floated. Increasing the suspension velocity increased the rate of flotation.

3.1 INTRODUCTION

The objective of these experiments was to utilize a novel flotation deinking cell to investigate the effect of furnish type, air to stock volume fraction and suspension velocity (i.e. effect of shear) on the deinking efficiency. A brief literature review now follows on the effect of various flotation process parameters on the deinking efficiency.

Increasing the air to stock volume fraction has almost always been seen in the literature to improve the deinking efficiency [1, 110]. The degree of increased deinking efficiency achieved by increasing the air to stock volume fraction has been shown in one study to be strongly dependent on the type of air injector used [1]. In that study three different air injectors were tested, and one particular air injector design (Injector A) produced significantly higher pulp brightness increases, at two air to stock volume fractions (40 and 80%). For Injector A, the pulp brightness increase observed when the air to stock volume fraction was increased from 40% to 80% was approximately 2.5 brightness points. For Injector B and C, the pulp brightness increases observed when the air to stock volume fraction was increased from 40% to 80% was only approximately 0.5 brightness points. The authors explained that the poor brightness increase of injectors B and C is that the injector designs resulted in poor air to stock mixing [1].

Pulp consistency has been shown to affect the deinking efficiency. One study using the Injector-Aerated Laboratory Flotation Cell, however, saw similar pulp brightness increases in the pulp consistency range of 0.5% to 1.5% [1]. The data does show a slight trend, however, towards higher brightness increases with increasing pulp consistency. Other studies using the Denver Cell observed the opposite trend. One of such studies found that the brightness increase was greater when the pulp consistency was reduced from 1.0% to 0.5% [46]. Another study using the Denver cell found that when the consistency was increased from 1.0% to 1.6%, the brightness gain decreased from 9.8 points to 1.7 points, or a 82.7% reduction [111]. Based on these findings, the effect of pulp consistency on the deinking efficiency is likely highly dependent on the design of the flotation cell being used.

Flotation time obviously has an effect on the deinking efficiency. One study using the Denver Cell observed that the pulp brightness did not continuously increase

with time but reached a plateau after 6-10 minutes of flotation [46]. The authors theorized that any remaining ink was probably still attached to the fibres and was unavailable for removal by flotation. Another study using the Denver Cell saw that the first 30 seconds of flotation experienced the largest gain in both brightness and ink area removal [111]. Afterwards, improvement on both brightness gain and ink area removal slowed down and hyperflotation was essentially reached after 5 minutes of flotation. In another study using an Adirondack Formax Cell, hyperflotation was achieved within 15 minutes of flotation [41].

Paper ash content and age have been shown to affect the deinking efficiency of the resulting furnish.

Ash content has been shown to play an important role in the flotation process [112]. Clays and other ash components are believed to provide sites for ink attachment and ink particle agglomeration. The ink-coated particle is then trapped in the foam layer and separated from the pulp slurry. Calcium ion, often originating from calcium carbonate paper filler, is believed to improve the effectiveness of fatty acids often used in flotation deinking. Temanex Consulting Inc. reports 'a 70:30 ratio of ONP :magazine (pigmented) grades is recommended, since (flotation) deinking efficiency is maximized by the presence of about 8-10% mineral pigment which acts as a catalyst' [113]. In 1967, Raimondo observed that flotation was more efficient when paper with a substantial filler content was used, such as coated 'illustrated' papers. Raimondo suggested that the attachment of ink to the coating layer, as opposed to the fibres, made the ink more easily removable from these types of papers. He theorized that the coating, rather than the fillers themselves, leads to the improved deinking of 'illustrated' paper [114].

Paper age has been shown to affect the deinking efficiency. In one study by Dorris [115] utilized two pulp samples from 70% ONP / 30% OMG blends obtained by repulping fresh and aged issues of the same ONP, with a single source of OMG. Accelerated aging of ONP was done in a laboratory oven at 60 °C for 18 hours. Aging of the ONP produced a brightness drop of 5 to 7 points (depending on the pad preparation technique used), which corresponded to an increase of ERIC by 350 to 500 ppm.

The amount of shear imposed on a pulp suspension has been shown to effect the deinking efficiency. One study using the Denver flotation cell found that for a fixed air

flowrate, the deinking efficiency was improved with increasing rotor speed [110]. The authors attributed this to the fact that increasing the rotor speed creates a greater and more intense shear field, which breaks the air up into smaller bubbles. The creation of a larger number of smaller bubbles results in a greater overall surface area available for floating particles.

Temperature has been seen in some cases to have an effect on the deinking efficiency. In one study, the overall ink removal decreased from 98.6% at 135 °F to 89.7% at 90 °F [116]. This was found to be at least partly due to the fact that larger (> 300 micron) ink particle removal efficiency was relatively low (< 85%) at 90 °F.

3.2 EXPERIMENTAL DESIGN

The flotation deinking air-injection unit described in Chapter 2 has been developed into a fully functional laboratory-scale flotation deinking cell for experiments discussed in this chapter, which is shown below in Figure 1.

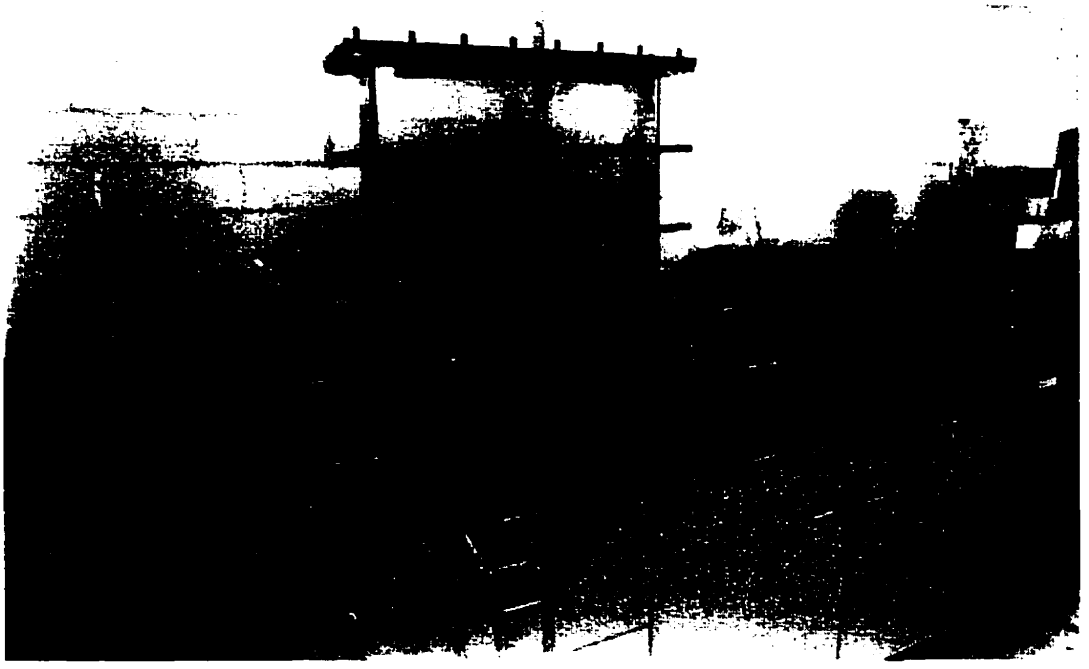

Figure 1. The laboratory-scale flotation deinking cell [103]

The large loop configuration of the air-injection unit used in Chapter 2 (described in Appendix B) has been modified in three ways which will be described in the following three sub-sections.

3.2.1 Air-Injection Step-Diffuser

The first modification is that the air-injection valve positioned 9 cm following the pump is no longer used as the air injection location. It was discovered that the large pipe diameter (I.D.= 4 cm) provided inadequate air mixing and led to poor ink flotation. In order to circumvent this problem a new air-injection section was designed having a similar step-diffuser design as the Sulzer Escher-Wyss injector described in Chapter 2. Figures 2 and 3 below compare the Sulzer Escher-Wyss step-diffuser to the one used for these experiments (pipe diameters in centimeters shown).

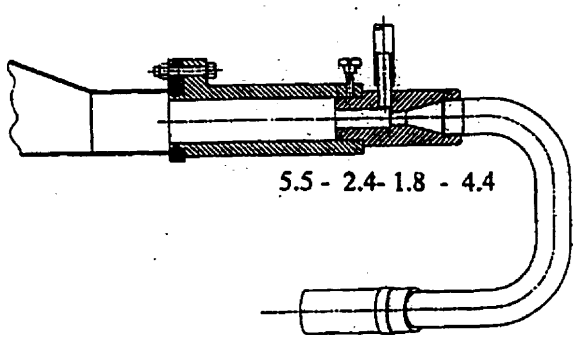

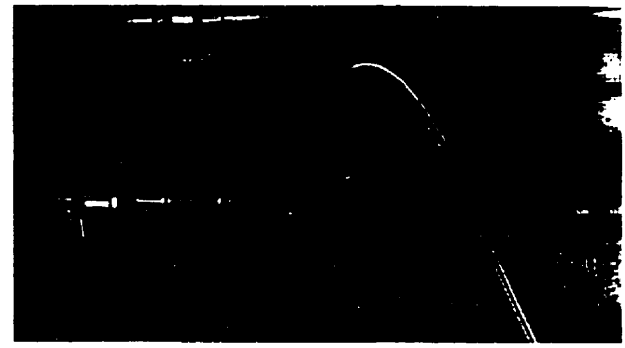

Figure 2. Sulzer Escher-Wyss step-diffuser [102] Figure 3. This study's step-diffuser [103]

The step-diffuser shown in Figure 2 is comprised of four different sized pipes. The internal diameters (I.D.) of these pipes are (progressing counter-clockwise in the flow direction): 4.4, 1.8, 2.4, and 5.5 cm. Air is aspirated through a pipe, which is positioned perpendicularly to the 2.4 cm pipe. The Sulzer Escher-Wyss step-diffuser can aerate a pulp stream with 20 percent volume fraction air and greater.

This study's step-diffuser, shown in Figure 3, is constructed from polyvinylchloide (PVC) piping and is also comprised of different sized pipes. The internal diameters of these pipes are (progressing right to left in the flow direction): 4.0, 1.6, 2.15, and 4.0 cm. Air is aspirated through a ¼ inch two-way ball valve, which is positioned perpendicularly to the 1.6 cm pipe. This step-diffuser can aerate a pulp stream

to a maximum of 10 percent volume fraction air at suspension velocities below 1.5 m/s. In order to operate the cell at higher than 10 percent volume fraction air, air was fed into the flotation cell through the aspiration pipe of the step-diffuser using a compressed air cylinder. The flowrate was regulated using an Omega Rotameter (model FL-1808). Force-feeding the air allowed for runs to be performed at 20 percent volume fraction air.

As was used in the construction of the image cell described in Chapter 2, at either end of the step-diffuser are PVC unions (Nibco 1½ inch) which allow for its quick and easy placement and removal from the loop. The total length of the step-diffuser (including female union-halves) is 59.5 cm, which is the same length as the image cell. For all Chapter 3 experiments, the step-diffuser was positioned in place of the image cell.

3.2.2 Flotation Vessel

The second modification of Chapter 2's experimental set-up is the presence of a custom-built flotation vessel, shown in Figure 4. The flotation vessel is constructed from ¼ inch polycarbonate. The flotation vessel dimensions are as follows : 4.8 inches wide, 20 inches long, and 28 inches high. The vessel is strengthened by the presence of four ½ inch reinforcing bands, which are evenly spaced up the vessel. The vessel's rear wall is equipped with two ball valves at its base which allow for easy drainage. At either end of the flotation vessel are PVC unions (Nibco 1½ inch) which allow for its quick and easy placement and removal from the loop.

The aerated slurry decelerates upon entering the flotation vessel, allowing air bubbles to float to the top of the vessel. A negligible amount of air exits in the outlet pipe (or accepts stream) and is recirculated to the pump. The outlet pipe is situated 1.5 inches below the level of the inlet pipe, which reduces the chances that air entering in the inlet pipe will exit in the outlet pipe.

The flotation vessel is equipped with a removable baffle which can be positioned within the vessel to further prevent air bubbles from exiting in the accepts stream and allows them to rise to the surface of the tank. *Bubble recirculation was not a significant problem for the suspension velocities used in these experiments, thus the baffle was not used.*

The baffle is a rectangular polycarbonate pane that slides vertically down between a set of two polycarbonate tracks to the base of the flotation vessel. The set of two polycarbonate tracks are vertically positioned two-thirds of the way across the vessel (in the flow direction) and are visible in Figure 4 below.

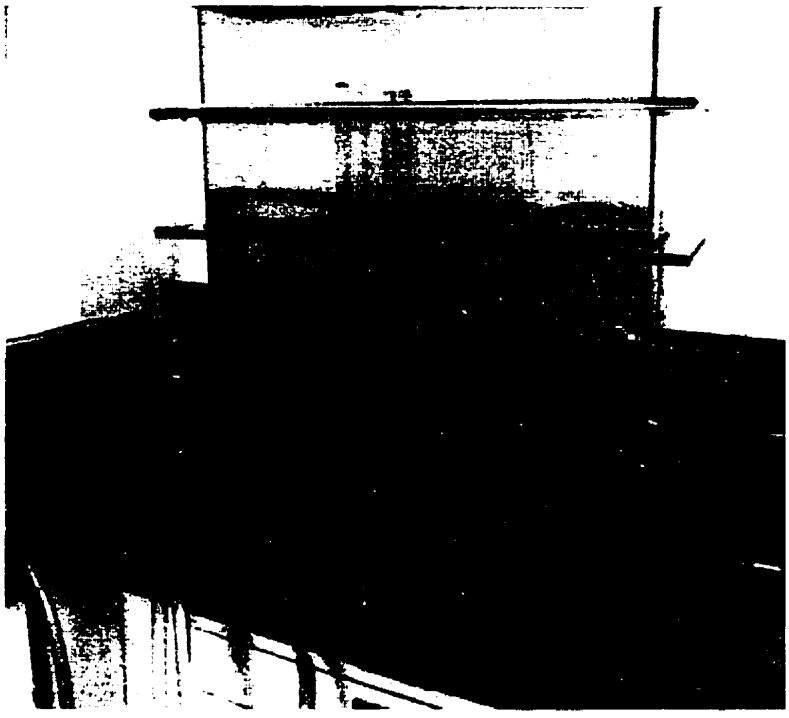

Figure 4. Close-up of the flotation vessel showing vertical baffle tracks [103]

The presence of the baffle strongly affects the flow pattern within the flotation vessel. For more details on the effect of the presence of the baffle on the flow patterns within the flotation vessel, refer to Appendix G.

3.2.3 Closing of the Pump

The third modification of Chapter 2's experimental set-up is that the custom-made centrifugal pump is no longer open to the atmosphere. It was described in Chapter 2 that air bubbles could float up within the pump and be released into the atmosphere. For Chapter 3's experiments, however, a constant fluid level was kept in the flotation vessel which was many inches higher than the top of the pump (refer to the horizontal line on the flotation vessel in Figure 1). This constant fluid level corresponded to a fluid volume

in the flotation cell of 33.9 L for all experiments. In order to prevent an overflow of fluid from the pump, the pump had to be closed to the atmosphere for these experiments. This was easily done using three custom-cut rubber stoppers to plug three pump orifices. Screws were placed into the rubber stoppers to prevent them from accidentally being pushed into the pump. Figure 5 below depicts the closed pump (two of the three rubber stoppers are visible).

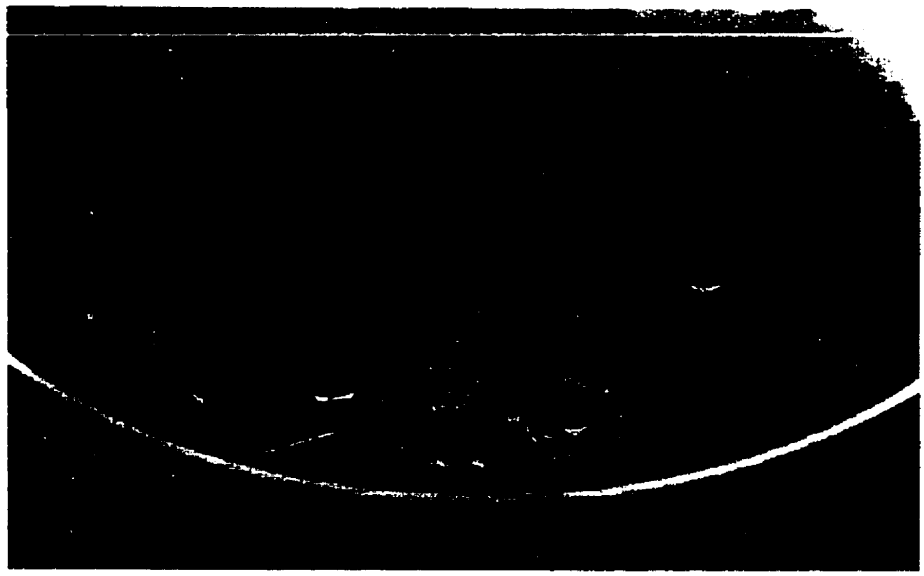

Figure 5. Rubber Stoppers Plug Three Pump Orifices [103]

3.3 MATERIALS

3.3.1 Water Grade

For these experiments tap water was used.

3.3.2 Pulp

Some of the experiments used 100% aged newsprint furnish and others used 70% fresh newsprint and 30% fresh magazine. The pulp temperature was 47 °C. The consistency of the 100% aged newsprint runs was 0.83%, and the consistency of the 70% fresh newsprint and 30% fresh magazine runs was 0.92%. The newsprint source was one particular edition of the Montreal Gazette and the magazine source was one particular pre-bound edition (i.e. no glues or adhesives were present) of Reader's Digest. All

pulpings utilized identical sections of the newspaper and magazine to ensure a constant pulp source.

For the runs which used 100% aged newsprint, the newsprint was place in an oven at 60 °C for 18 hours. This procedure to rapidly age ONP has been previously published in the literature [115]. The purpose of aging the pulp in this manner was to simulate the natural aging process the paper experiences between the time it is fabricated and the time it is eventually deinked during the recycling process. This natural aging period is typically at least a few months in duration.

3.3.3 Deinking Chemicals

Table 1 below indicates all of the deinking chemicals used for these experiments. All of the chemicals listed were added in the pulping stage, except for the $CaCl_2$ which was added in the flotation cell prior to commencing the flotation process.

Table 1. Deinking Chemicals Used

	Amount of Chemical Added	Concentration	Quantity Required for 100 % Aged NP Runs	Quantity Required for 70% Fresh NP : 30% Fresh MG Runs
NP	-	Moisture content : 4.95%	589.9 g	460.3 g
MG	-	Moisture content : 2.59%	0 g	192.5 g
NaOH	1% of pulp mass	100 g/L	59.0 ml	62.5 ml
Na_2SiO_3	0.8% of pulp mass	100 g/L	47 ml	50 ml
Hydrogen Peroxide	1% of pulp mass	0.3 g/L	196 ml	208 ml
DTPA	0.2% of pulp mass	0.4 g/g	2.950 g	3.125 g
Sodium Oleate	0.6% of pulp mass	25 g/L	142 ml	150 ml
Water	Enough to attain 10% consistency pulp in pulper	-	4836 ml	5124 ml
$CaCl_2$	60 ppm (mg/L) added to the flotation cell contents (33.9 L)	30 g/L	11.0 ml	11.7 ml

It should also be noted that prior to the preparation of 3.0 gram Buchner pads, 1 milliliter of 12% Alum solution was added to each pulp sample to help retain the ink particles during pad formation.

3.4 EXPERIMENTAL METHODS

3.4.1 Calibration of Pump RPM and Fluid Velocity

It was discovered that the presence of the air-injection step-diffuser increased the resistance to flow and altered the pump RPM and suspension velocity calibration attained in Chapter 2. In order to recalibrate the pump RPM with the suspension velocity in the

loop, a Doppler flowmeter was used. The velocity calibration data is included in Appendix A. From this data, the following linear relationship with an R^2 value of 0.998 can be obtained which is valid until a fluid velocity of 1.54 m/s:

$$\text{Fluid Velocity [m/s]} = (1.16*10^{-3})\,(\text{Pump RPM}) + 0.055 \quad (1)$$

3.4.2 Air Volume Fraction Control

Table 2 below indicates the air flowrates and corresponding Omega rotameter (FL-1808) levels utilized to attain 10 and 20 percent volume fraction air for both the 1 and 1.5 m/s suspension velocities.

Table 2. Air Flowrates and Corresponding Rotameter Levels for 10 and 20% Volume Fraction Air

Suspension Velocity (m/s)	Pump RPM	Suspension Flowrate (L/min)	Air Flowrate required for 10% volume fraction air (L/min)	Level on Omega Rotameter (FL-1808) for 10% volume fraction air	Air Flowrate Required for 20% volume fraction air (L/min)	Level on Omega Rotameter (FL-1808) for 20% volume fraction air
1.0	814	75.40	7.54	58	15.08	104
1.5	1244	113.09	11.31	82	22.62	144

3.4.3 Pulping Procedure

Paprican's Helico pulper was used for these experiments at Paprican's facility in Pointe-Claire, Quebec. A general schematic of the Helico pulper is shown in Figure 6.

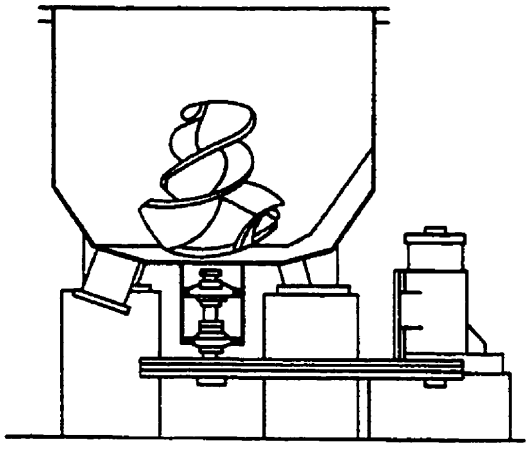

Figure 6. The Helico Pulper [4]

The following ten steps comprise the pulping procedure:

(i) Rip newspaper and/or magazine into small pieces (approximately 2 square inch)
(ii) Heat water to 50 °C
(iii) Ensure that the pulper power switches are off and the drain valve is closed
(iv) Fill the pulper with the required amount of water (see Table 1)
(v) Add all deinking chemicals, except the hydrogen peroxide which is added in step (ix), and the $CaCl_2$ which is added to the flotation cell just prior to flotation
(vi) Start the pulper at 7-8 frequency
(vii) Add all the paper
(viii) Increase the pulper speed to 25 frequency (which corresponds to approximately 806 RPM)
(ix) Add hydrogen peroxide
(x) Pulp for 10 minutes

3.4.4 Buchner Pad Preparation

A simple method was devised to gauge the deinking efficiency for all of the runs after 5, 15 and 30 minutes of flotation. Prior to the flotation process two pulp samples were drawn from the red ball valve located immediately following the flotation vessel. This would be done with the pulp circulating at the desired velocity to ensure thorough mixing within the flotation cell. The consistency of the pulp was then measured using these samples. Two additional pulp samples were then taken which represented the 'before flotation' case. After the flotation process had begun, two pulp samples were taken at the 5, 15 and 30 minute times. *The consistency of the pulp was assumed to be constant throughout the 30 minute flotation process.* With the pulp consistency known, 3.0 gram Buchner pads were prepared from these pulp samples using the CPPA Technical Section Useful Method C.4U. *Prior to the preparation of the pad, 1 milliliter of 12% Alum solution was added to each pulp sample to help retain the smallest of ink particles during pad formation..* The weight of the pads were later measured and they all weighed between 3.0 – 3.2 grams, thus the constant consistency assumption was valid.

3.4.5 Deinking efficiency Measurement Parameters

On the 'screen' side of the Buchner pads the following deinking efficiency parameters were measured at Paprican in Pointe-Claire, Quebec: (i) ISO Brightness

(ii) Effective Residual Ink Count (ERIC) **(iii)** Ink Speck Count [this test provides the Speck Number/cm^2, Percent Coverage, and Average Speck Diameter (μm)].

As was previously mentioned, two pulp samples were drawn for each sample time for all of the runs. Both of the samples were analyzed for the above deinking efficiency parameters. The average of these values is then reported.

3.4.6 Using the Paprican Ink Scanner

The Paprican Ink-Scanner, shown in Figure 7 below, is an image analyzer that measures the amount of ink remaining in paper or board after deinking. The instrument illuminates the specimen with a near IR diffuse source. The instrument incorporates a state-of-the art detector which collects and directly transmits the digital image to the processor for analysis. All adjustments are automatic. This decreases the overall testing time by at least 100 times compared to conventional high magnification image analysis. The minimum particle diameter able to be detected is 8 μm. The user interacts with the software with the use of a touch-screen.

Figure 7. The Paprican Ink-Scanner [119]

The Paprican Ink Scanner was used to measure the Ink Speck Count. This test provides values for the Speck Number/cm^2, Percent Coverage, and Average Speck Diameter (μm).

For each pad analyzed on the 'screen' side, twenty 7.3 mm^2 fields (or sample points) were measured. Sampling twenty different fields ensured less than 3%

uncertainty in the data. This data is then automatically compiled providing the Ink Speck Count. A typical Paprican Ink-Scanner result sheet and plot is shown in Figure 28 of Chapter 1.

3.4.7 Froth Removal

Throughout the flotation process, an inky froth forms at the suspension surface in the flotation vessel. Figure 8 is a typical picture of this froth. The froth was manually removed as it formed using a plastic beaker. The froth was not analyzed to calculate yield losses.

Figure 8. Inky froth forms at the top of the flotation vessel [103]

3.4.8 Typical Experimental Run Procedure

The following thirteen steps comprised a typical experimental run:

(i) Pour the pulp, having a temperature of 47 °C, into the open top of the flotation vessel. Fill the flotation cell with tap water, having a temperature of 47 °C, to the blue line marked on the side of the flotation vessel. The blue line corresponds to a volume of 33.9 litres.

(ii) Turn on the pump's power switch and adjust the pump's RPM until the desired corresponding suspension velocity is reached. *Some air may be trapped in or around the pump which makes it difficult for the pump to circulate fluid. This trapped air can be released by opening the ¼ inch ball valves located immediately before and after the pump. It may require a few minutes to release all of the trapped air.*

(iii) From the red ball valve located immediately following the flotation vessel, take two pulp samples (approximately 250 milliliters each) from which the pulp consistency will be measured. All further pulp samples are taken from this location.

(iv) Take two more pulp samples (approximately 425 milliliters each) which represent the 'before flotation' case. *When the pulp consistency is determined following the completion of the run, the exact pulp volume required to make a 3.0 gram Buchner pad can be calculated.*

(v) Using the peristaltic pump, inject the $CaCl_2$ into the loop through the deinking chemicals injection section. Allow five minutes for homogeneous mixing of $CaCl_2$ to be attained throughout the system.

(vi) Begin the flotation process by injecting air into the loop using a compressed air cylinder. Adjust the flowrate using the rotameter to attain the desired volume fraction air.

(vii) Continually remove the froth as it forms at the suspension surface in the flotation vessel. Use a plastic beaker to manually collect the froth. Attempt to remove as little pulp as possible while removing the froth. The froth was not analyzed to determine yield losses of each run.

(viii) After 5, 15 and 30 minutes of flotation, take two pulp samples (approximately 425 milliliters each). *When the pulp consistency is determined following the completion of the run, the exact pulp volume required to make a 3.0 gram Buchner pad can be calculated.*

(ix) Drain and clean the flotation vessel.

(x) Determine the exact pulp consistency for the run using the first two pulp samples.

(xi) Calculate the exact volume required from the other eight pulp samples to prepare 3.0 gram Buchner pads (the consistency is assumed to be constant throughout the experiment).

(xii) Prepare eight 3.0 Buchner pads for the run following the CPPA Useful Method C.4U.

(xiii) For each pad, measure ISO Brightness, Effective Residual Ink Count (ERIC), and Ink Speck Count. Record the average values of the duplicate samples taken at the three sampling times.

3.5 RESULTS

3.5.1 Experiments Using 100% Aged Newsprint

Two experimental runs (Runs 1 and 2) utilized 100% aged newsprint at 0.83% consistency to gauge the general functionality of this novel flotation deinking cell. The newspaper was aged by being placed in an oven at 60 °C for 18 hours. Table 3 describes the operating conditions for these experiments. These two experiments investigated the effect of Air Volume Fraction on the deinking efficiency. The suspension velocity was held constant at 1 m/s and two air volume fractions were tested, 10 and 20 %.

Table 3. Experimental Run Descriptions for Runs 1 and 2

Run Number	Furnish Type	Pulp Consistency (%)	Suspension Velocity (m/s)	Air Volume Fraction (%)	Suspension Temperature (°C)
1	100% aged NP	0.83	1.0	10	47
2	100% aged NP	0.83	1.0	20	47

The following five parameters were measured: **(i)** Brightness **(ii)** Effective Residual Ink Count (ERIC) **(iii)** Speck Number/cm^2 **(iv)** Percent Speck Coverage **(v)** Average Speck Diameter (μm). These parameters were measured from 3.0 gram Buchner pads prepared before flotation and also 5, 15 and 30 minutes after flotation.

Figures 9 and 10 plot the data attained for Runs 1 and 2.

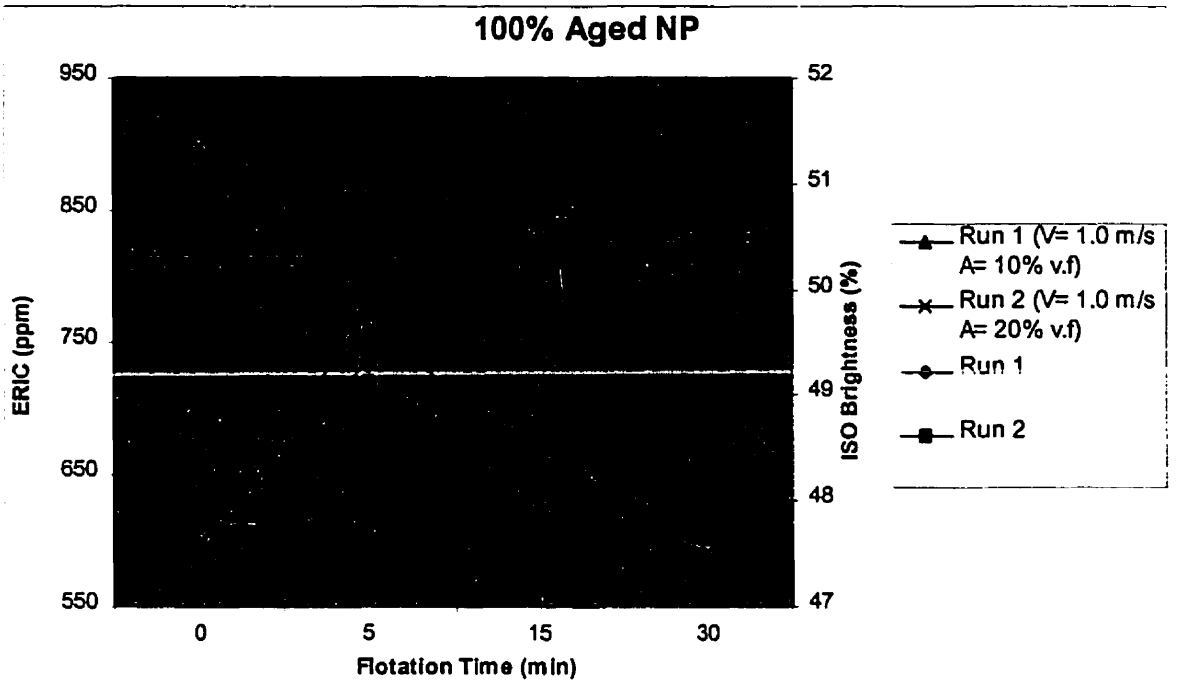

Figure 9. ERIC and Brightness data for Runs 1 and 2. Two different graphical symbols are used for each run, one for each vertical axis.

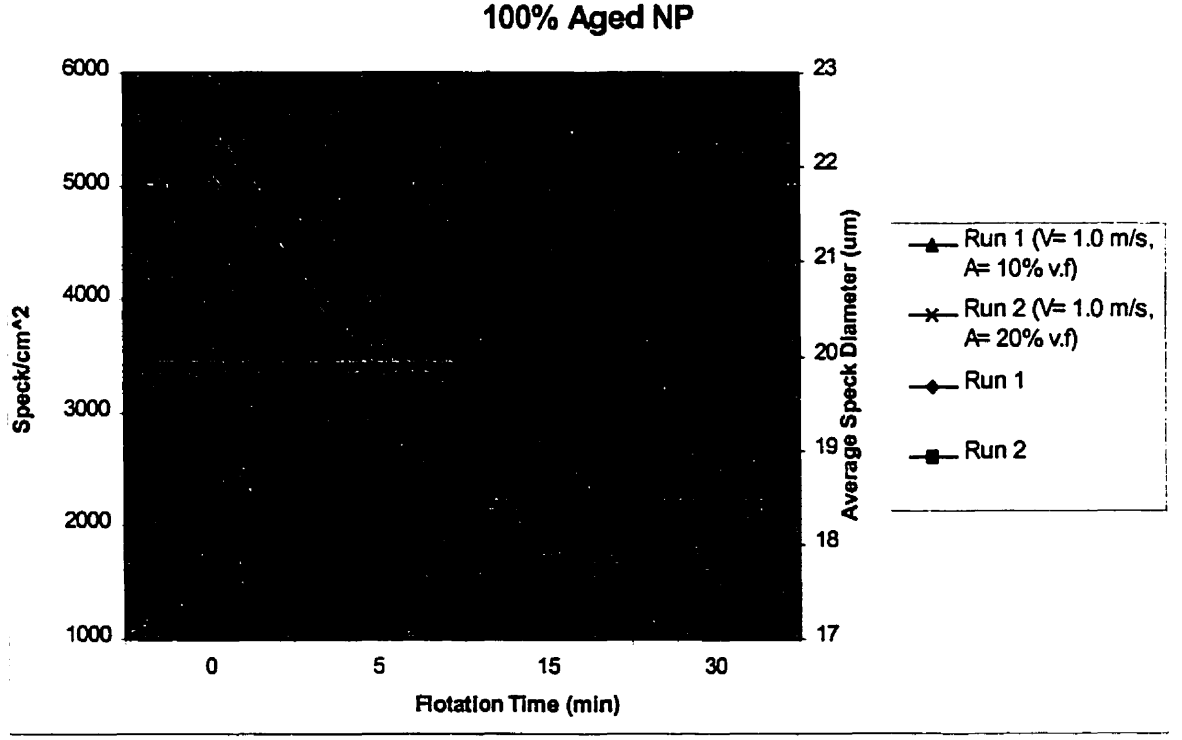

Figure 10. Speck/cm^2 and Average Speck Diameter data for Runs 1 and 2. Two different graphical symbols are used for each run, one for each vertical axis.

In order to express values for the deinking efficiency the following equation was used :

$$\% \text{ Speck Removal} = \frac{(\text{Speck \#/cm}^2 \text{ Before Flotation}) - (\text{Speck \#/cm}^2 \text{ After 30 Min.})}{(\text{Speck \#/cm}^2 \text{ Before Flotation})} * (100) \quad \textbf{(2)}$$

Using Equation 2, the Percentage Speck Removal for Runs 1 and 2 are listed in Table 4 and plotted in Figure 11:

Table 4. Percentage Speck Removal for Runs 1 and 2

Run Number	% Speck Removal After 5 Minutes(%)	% Speck Removal After 15 Minutes(%)	% Speck Removal After 30 Minutes(%)
1	27.1	48.6	53.1
2	29.3	47.6	52.5

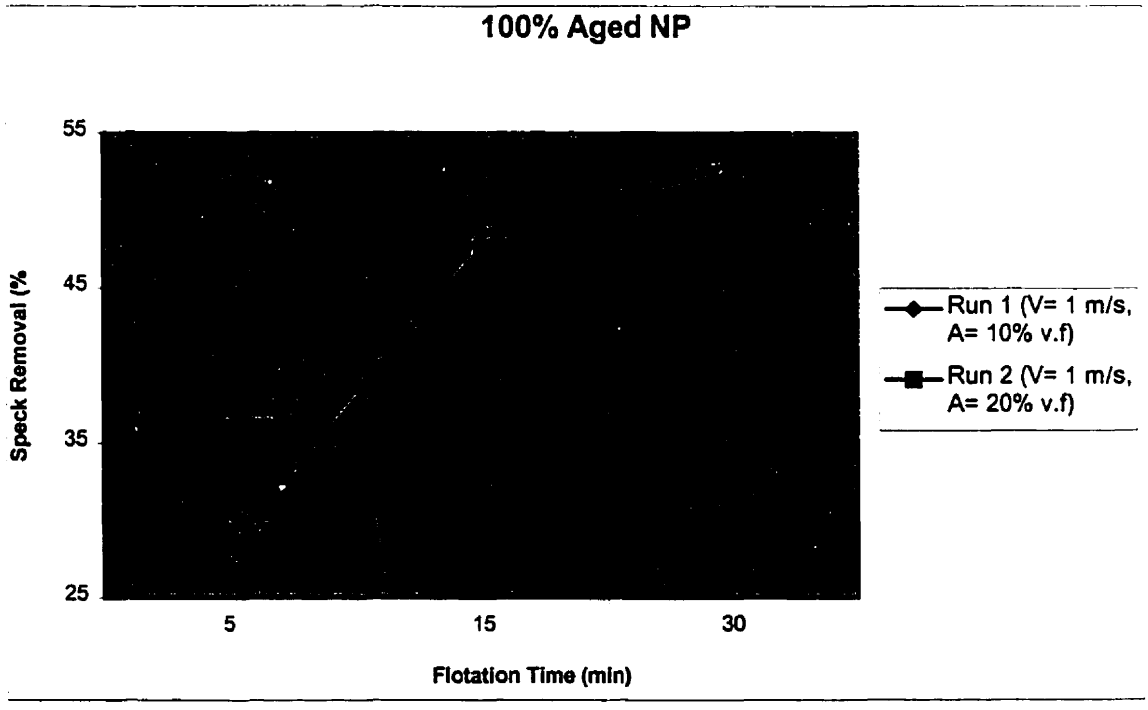

Figure 11. Percentage Speck Removal for Runs 1 and 2.

The low Percentage Speck Removal attained using 100% aged NP, shown in Table 4 and Figure 11, are not due to the functionality of the flotation cell, but rather the nature of the stock used. First of all, the furnish had a low ash content because 100% aged NP was used. As was previously discussed in the Introduction, had a minimum ash content of 8-10 percent been present, improved Percentage Speck Removal would have been expected. In addition, the fact that the NP was aged in a laboratory oven at 60 °C for 18 hours also contributed to the poor Percentage Speck Removal values attained. As discussed in the Introduction section, had fresh NP been used, improved Percentage Speck Removal would have been expected. Based on these findings, it was decided to change furnish type for the remainder of this work in order to better gauge the functionality of this novel cell. A furnish of 70% fresh NP/ 30% fresh MG was chosen due to the fact that such furnish types have been shown in the literature to be effectively deinked.

3.5.2 Experiments Using 70% Fresh Newsprint and 30% Fresh Magazine

Four experimental runs (Runs 3 through 6) utilized 70% fresh newsprint and 30% fresh magazine to gauge the general functionality of this novel flotation deinking cell. Table 5 describes the operating conditions for these experiments. These four experiments investigated the effect of Suspension Velocity and Air Volume Fraction on the deinking efficiency. Using two suspension velocities, 1 m/s and 1.5 m/s, two air volume fractions were tested, 10 and 20 %.

Table 5. Experimental Run Descriptions for Runs 3-6

Run Number	Furnish Type	Pulp Consistency (%)	Suspension Velocity (m/s)	Air Volume Fraction (%)	Suspension Temperature (°C)
3	70% fresh NP 30% fresh MG	0.92	1.0	10	47
4	70% fresh NP 30% fresh MG	0.92	1.0	20	47
5	70% fresh NP 30% fresh MG	0.92	1.5	10	47
6	70% fresh NP 30% fresh MG	0.92	1.5	20	47

Figures 12-16 plot the data attained for Runs 3-6.

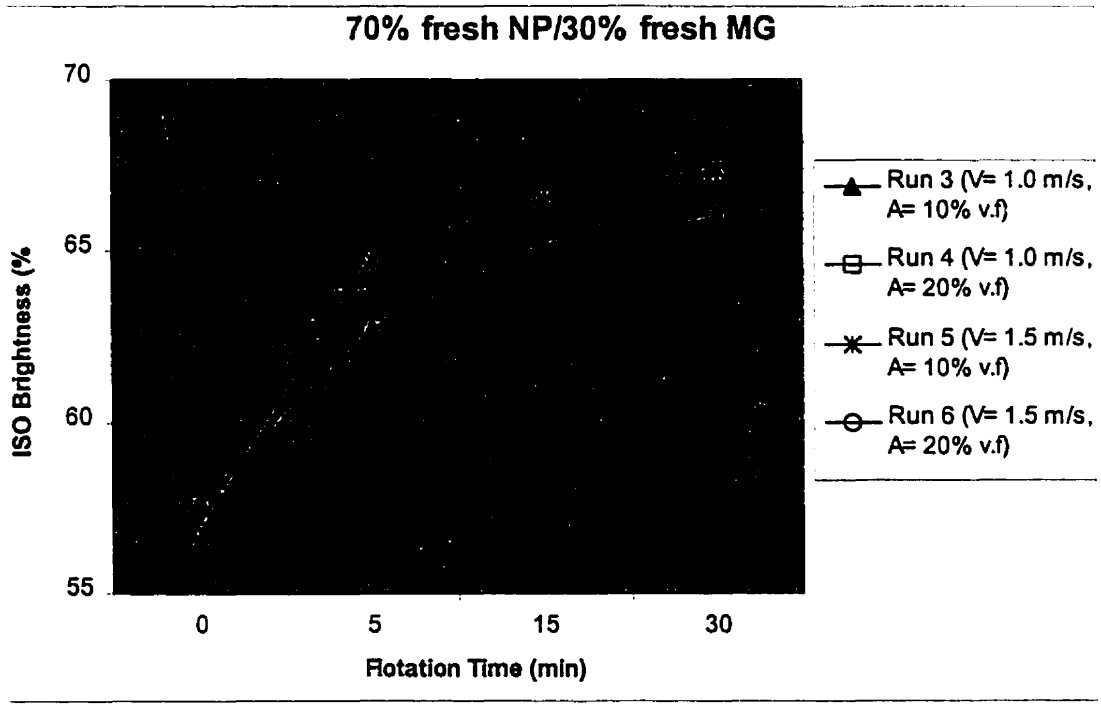

Figure 12. Brightness data for Runs 3-6

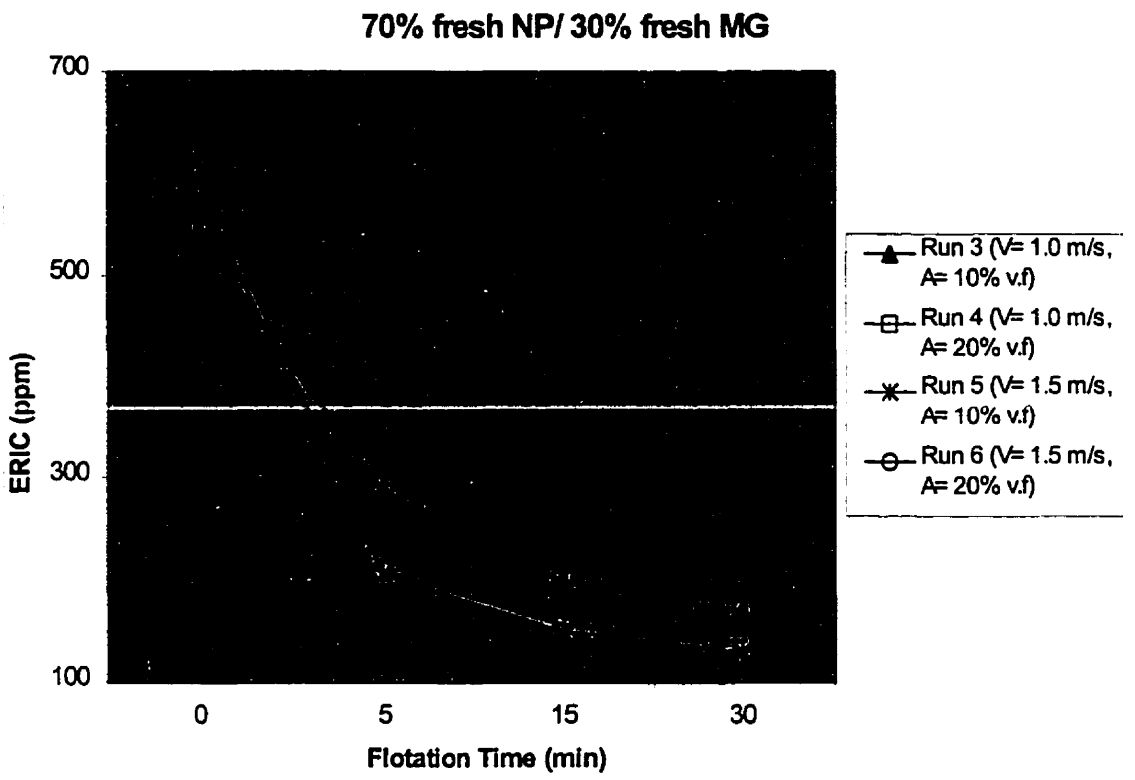

Figure 13. ERIC data for Runs 3-6

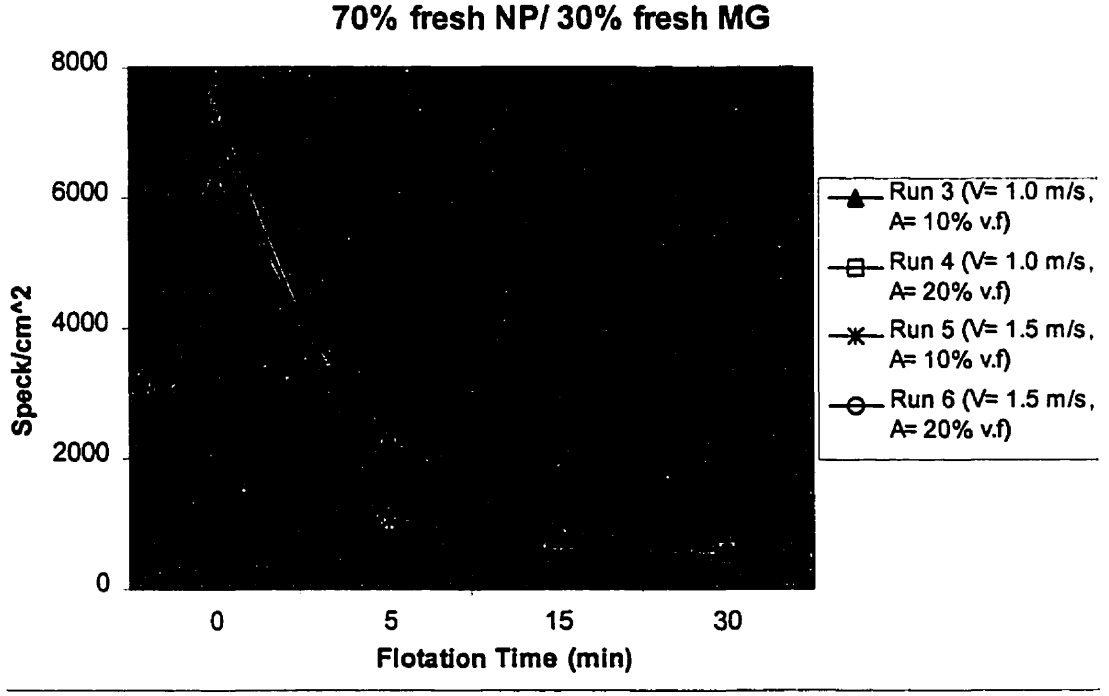

Figure 14. Speck Number/cm^2 data for Runs 3-6

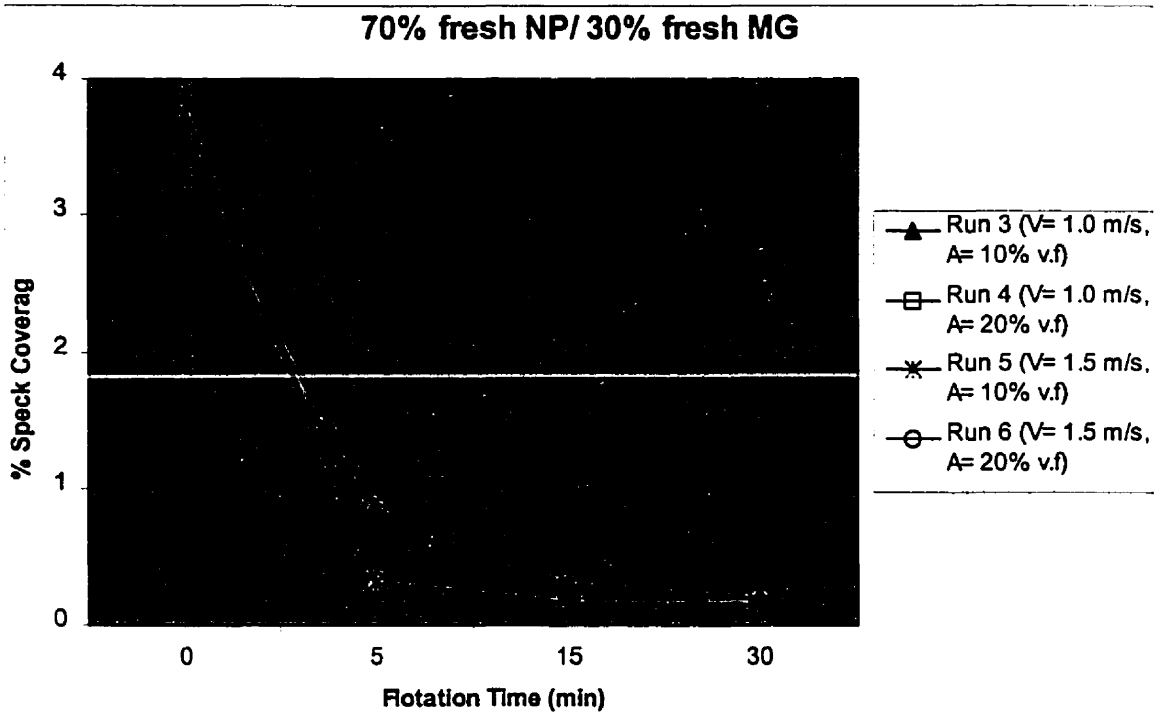

Figure 15. Percent Speck Coverage data for Runs 3-6

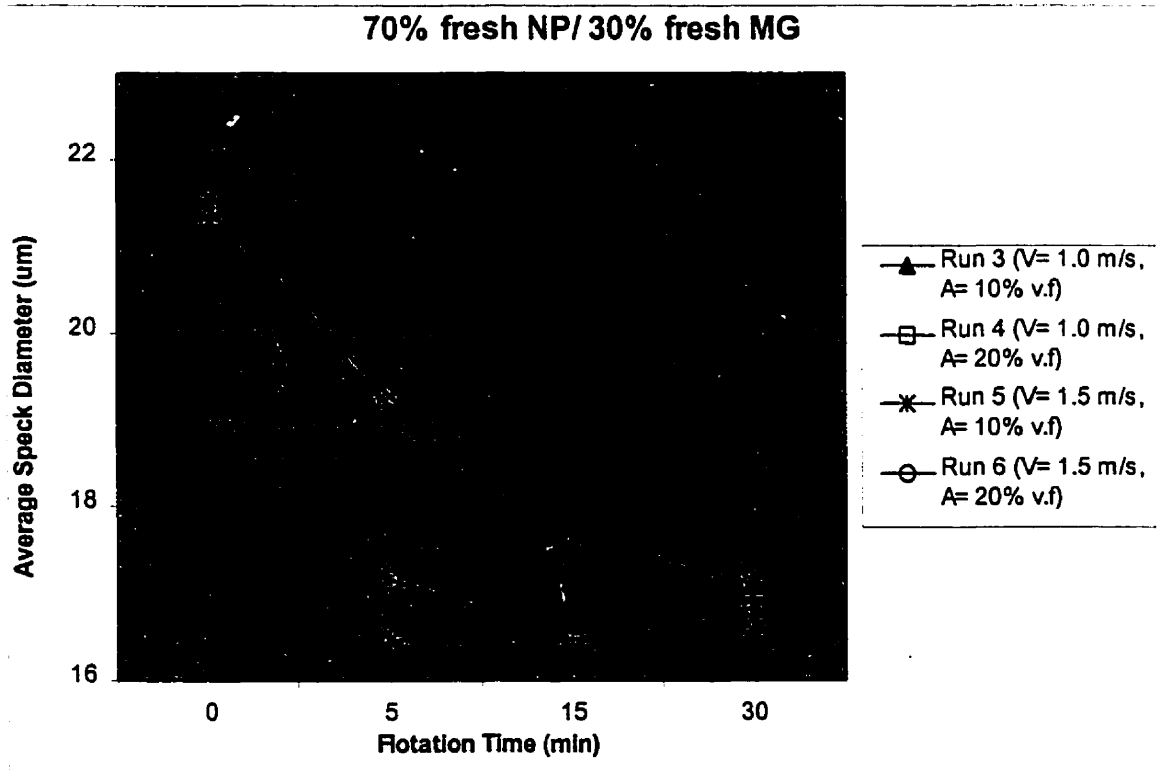

Figure 16. Average Speck Diameter data for Runs 3-6

Using Equation 2, the Percentage Speck Removal for Runs 3-6 are listed in Table 6 and plotted in Figure 17:

Table 6. Percentage Speck Removal for Runs 3-6

Run Number	% Speck Removal After 5 Minutes(%)	% Speck Removal After 15 Minutes(%)	% Speck Removal After 30 Minutes(%)
3	63.8	86.4	90.2
4	65.1	87.3	90.7
5	86.2	93.4	93.7
6	86.1	92.3	93.2

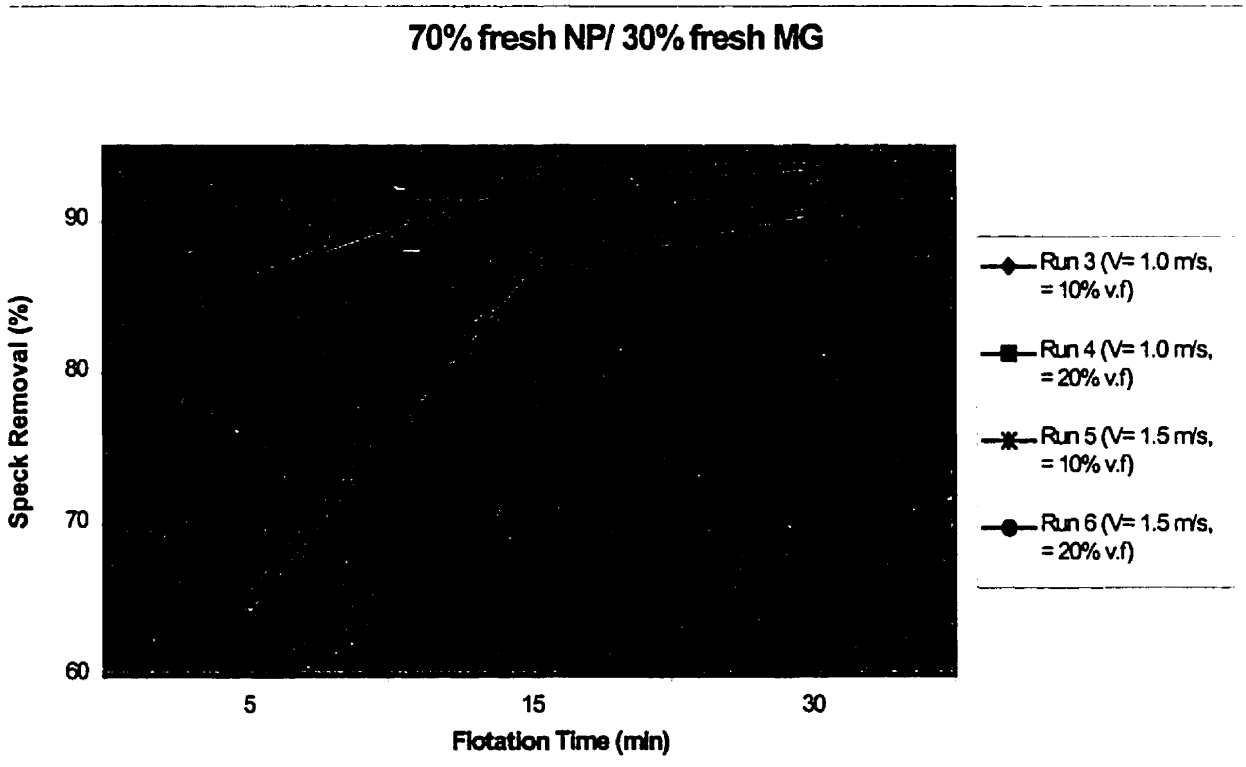

Figure 17. Percentage Speck Removal for Runs 3-6

3.6 DISCUSSION

3.6.1 Effect of Air Volume Fraction

For Runs 1 and 2 using 100% aged NP, increasing the percent volume fraction air from 10 percent to 20 percent resulted in a small improvement in the amount of floated ink up to 15 minutes of flotation. This is evident in Figure 9 by an increase in Brightness (less than 1 point) and a decrease in ERIC (less than 50 points) during the first 15 minutes of flotation. This result was not surprising, since increasing the air volume fraction has been seen in the literature to improve the deinking efficiency [1, 110]. In Figure 10, the 20 percent volume fraction air run (Run 2) did result in lower Speck/cm^2 values after 5, 15 and 30 minutes of flotation, compared to the 10 percent volume fraction air run (Run 1). However, it is difficult to attribute this solely to the increased air volume fraction because Run 2 had a lower initial Speck/cm^2 value prior to flotation (at time 0) as well. After 30 minutes of flotation, utilizing 20 percent volume fraction air over 10 percent led only to a negligible improvement in Brightness, ERIC and Speck/cm^2 values. From this finding , it is hypothesized that at some times between 15 and 30 minutes of flotation, hyperflotation had been achieved for both the 10 and 20 air volume fraction scenarios. Hyperflotation defines the scenario in which all of the free ink in suspension has been floated. Any remaining ink is still attached to fibres and is unavailable for removal by flotation.

For Runs 3 to 6, in which 70 percent fresh newsprint and 30 percent fresh magazine was used, increasing the percent volume fraction air from 10 percent to 20 percent did not result in an appreciable improvement in Brightness, ERIC, Speck/cm^2 and % Speck Coverage (see Figures 12-15). This result was very surprising because the 100% aged newsprint results discussed above, as well as other studies in the literature typically notice improved deinking as the air volume fraction is increased. Based on the different results attained when using 100% aged NP or 70% fresh NP and 30% fresh MG, the effect of air volume fraction on the deinking efficiency may be highly stock dependent. Factors, such as, paper age, ink properties and pulp ash content likely play important roles in the flotation kinetics exhibited.

In regard to the lack of effect of air volume fraction on the deinking efficiency when using the 70% fresh NP and 30% fresh MG, this finding could be predominantly a result of insufficient mixing of air into the stock, which is largely affected by the injector design. One study in the literature, which evaluated the performance of an air-injector having a similar design to ours, found only a small improvement in the deinking efficiency (approximately ½ a brightness point) when the air volume fraction was increased from 40% to 80% [1]. The authors explained the poor brightness increase to be a result of the injector design, which led to insufficient rotation velocity of the suspension in the flotation cell. It is possible that the same phenomenon is being observed in our results. Perhaps increasing the volume fraction of air from 10% to 20% while keeping the suspension velocity (i.e. the shear field) constant, resulted in a larger average air bubble size that was less efficient at floating the ink particles. The degree to which the average air bubble size increased is predominantly characterized by the air injector design which has been shown to highly affect the air to stock mixing. Good mixing is required to ensure a high rate of collision between the bubbles and ink particles. The relative size of the step diffuser segment diameters has been shown to have a large effect on the degree of mixing attained [1]. It is advised that this study's air injector design be optimized in future work to improve the degree of mixing attained.

3.6.2. Effect of Furnish Type

It is interesting to compare the 'before flotation' data (shown on the graphs at a flotation time of 0 minutes). The 100% aged newsprint runs (1 and 2) had considerably lower initial brightness (approximately 10 points) and considerably higher initial ERIC (approximately 320 points) compared to the runs (3-6) using 70% fresh newsprint and 30% fresh magazine. This is likely due to two factors. Firstly, the filler content of the magazine present in Runs 3-6 likely brightened the pulp compared to had no magazine been present [117]. Secondly, aging the newsprint used for Runs 1 and 2 has been shown in the literature to lower brightness and increase ERIC [115].

The furnish type also had an effect on its overall deinkability. For example, Run 1, using 100% aged NP and a suspension velocity of 1 m/s and 10% volume fraction air, attained a Percentage Speck Removal of approximately 53% after 30 minutes of flotation.

Run 3, using 70% fresh NP and 30% fresh MG and a suspension velocity of 1 m/s and 10% volume fraction air, attained a Percentage Speck Removal of approximately 90% after 30 minutes of flotation. The poor Percentage Speck Removal of Runs 1 and 2 can likely be attributed primarily to the fact the newsprint was aged [115], which increased the adhesion of ink to fibre. Thus, the ink was insufficiently separated from the fibre during repulping. Another possible factor involving the poor Percentage Speck Removal of Runs 1 and 2 is that an insufficient amount of ash was present in the pulp. It is commonly believed that ash content has a high impact on the deinking efficiency [112, 113]. This viewpoint is not universal, however. One study found that, based on flotation accepts brightness, OMG addition did not improve deinking efficiency [117]. Flotation accepts brightness with OMG/ONP were not significantly higher than those obtained with ONP alone [117].

3.6.3 Effect of Furnish Velocity

The effect of suspension velocity was investigated only with the 70% fresh NP and 30% fresh MG furnish. Two suspension velocities were used (1 and 1.5 m/s) with 10 and 20% air each, for a total of four runs. The suspension velocity had an effect on the ink size distribution present in the pulp prior to flotation. This can be seen by comparing the 'before flotation' results for Run 3 and Run 5 (similar trends can be attained by comparing the results for Runs 4 and 6 because, as was already discussed, air volume fraction did not have a significant impact on the measured parameters). The only difference between Runs 3 and 5 is that the suspension velocity for Run 3 is 1.0 m/s and for Run 5 is 1.5 m/s.

Increasing the suspension velocity increases the shear forces acting upon the flowing suspension. It is believed that the increased shear forces associated with increasing the suspension velocity from 1 m/s (Run 3) to 1.5 m/s (Run 5) broke-up ink agglomerates that were in suspension into a larger number smaller ink particles. Due to the fact that smaller ink particles have larger specific surface area than larger ink particles, they generally lower Brightness values and increase ERIC values. It is for this reason that prior to flotation (after 0 minutes of flotation), Run 5 is approximately 1 point lower in Brightness and approximately 66 points higher in ERIC than Run 3 (see Figures

12 and 13). In addition, prior to flotation (after 0 minutes of flotation), Run 5 had approximately 1300 more Specks/cm^2 and 0.5% more Percent Ink Coverage than Run 3 (see Figure 14 and 15), and Run 5's Average Speck Diameter was approximately 1 micron smaller than Run 3's (see Figure 16).

It is assumed that hyperflotation had been achieved after 30 minutes of flotation and all of the free ink in suspension available to be floated, had been successfully removed by flotation for Runs 3 and 5. Figures 14 and 15 indicate that Runs 3 and 5 had virtually identical values for Speck/cm^2 and % Speck Coverage. This implies that both runs had virtually the same amount of ink that had not been floated, indicating that increasing the shear by increasing the suspension velocity did not dislodge ink from within fibre flocs, and increase the amount of ink available to be floated.

It is interesting to note that despite the fact that it is believed the same amount of ink was believed to be floated for Runs 3 and 5, Run 5 had approximately 1.4 higher Brightness points (Figure 12) and 40 lower ppm ERIC (Figure 13) than Run 3. If these results are not due to the fact that more ink was floated in Run 5 than Run 3 (for reasons discussed above), perhaps they are a result of less filler loss at the higher suspension velocity (Run 5). This is only speculation, however.

Increasing the suspension velocity increased the collision frequency of air bubbles and ink particles which improves the flotation efficiency. In addition, increasing the suspension velocity is expected to reduce the average air bubble size, which results in a greater overall surface area for floating particles. As a result of these factors the rate of flotation increased for Runs 5 and 6 (both operated at 1.5 m/s) than Runs 3 and 4 (both operated at 1 m/s). This is evident from Figures 14 and 15, in which the Speck Number/cm^2 and the Percent Speck Coverage both reduced at a faster rate for Runs 5 and 6 than did for Runs 3 and 4. After 30 minutes hyperflotation was achieved, however, and all of Runs 3-6 essentially attained the same values for Speck Number/cm^2 and the Percent Speck Coverage.

3.6.4 Functionality of this Novel Flotation Cell

This novel flotation cell functioned very well for these experiments. The greatest increase in Brightness attained was 10.9 points in Run 5, from 56.5 before flotation to 67.4 after 30 minutes of flotation. Figures 18 and 19 below depict scanned images of sections of the before and after flotation Buchner pads prepared for Run 5. These figures give a physical sense for the before and after flotation cleanliness of the pulp.

Figure 18. Buchner pad image from Run 5 – before flotation [120]

Figure 19. Buchner pad image from Run 5 - After 30 minutes of flotation [120]

3.7 CONCLUDING REMARKS

The flotation deinking air-injection unit described in Chapter 2 has been developed into a fully functional laboratory-scale flotation deinking cell for experiments discussed in this chapter. The following are the primary findings of this work:

① Increasing the air volume fraction while keeping the suspension velocity constant, did slightly improve the deinking efficiency for the 100% aged NP case, however, did not result in any significant improvement for the 70% NP/ 30% MG case.

② The 100% aged newsprint runs had considerably lower initial brightness (approximately 10 points) and considerably higher initial ERIC (approximately 320 points) compared to the runs using 70% fresh newsprint and 30% fresh magazine. After 30 minutes of flotation, the 100% aged newsprint runs also achieved much lower Percentage Speck Removal compared to the runs using 70% fresh newsprint and 30% fresh magazine. These findings are likely related to the aging of the newsprint and the low ash content of the 100% aged newsprint runs.

③ It is believed that the increased shear forces associated with increasing the suspension velocity broke-up ink agglomerates that were in suspension into a larger number smaller ink particles. It is for this reason that prior to flotation, lower Brightness and higher ERIC values were attained for the runs operating at higher suspension velocities. Hyperflotation results indicate that virtually identical values for Speck/cm^2 and % Speck Coverage for runs operating at 1 and 1.5 m/s. This infers that both runs had virtually the same amount of ink that had not been floated, indicating that increasing the shear by increasing the suspension velocity did not dislodge ink from within fibre flocs, and increase the amount of ink available to be floated.

④ Increasing the suspension velocity increased the rate of flotation.

3.8 RECOMMENDATIONS FOR FUTURE WORK

The following types of experiments are interesting possibilities for continued work concerning the effect of flotation deinking process parameters on the deinking efficiency:

- continue investigating the effect of air volume fraction and suspension velocity on the deinking efficiency
- investigate the deinkability of 100% non-aged newsprint
- the effect of suspension temperature on the deinking efficiency
- the effect of air injector design on the deinking efficiency
- the effect of surfactant type and concentration on the deinking efficiency
- the effect of consistency on the deinking efficiency

REFERENCES

1. ACKERMANN, C. and GOTTSCHING, L. and MULLER, J. and PUTZ, H.J., "Injector Aerated Laboratory Flotation Cell", *Wochenbl. Papierfabr, 120(21)*: 869-874 (mid Nov. 1992).
2. GOTTSCHING, L. and HUNOLD, M. and KRAUTHAUF, T. and MULLER, J. and PUTZ, H.J., "Effect of Air Volume and Air Bubble Size Distribution on Flotation in Injector Aerated Deinking Cells", *3rd Research Forum on Recycling Proceedings*, Vancouver, BC, November 20-22 (1995).
3. BIERMANN, C.J., "Handbook of Pulping and Papermaking, Second Edition", ACADEMIC PRESS, San Diego, CA (1996).
4. DORRIS, G. et al, "Deinking and Wet End Chemistry", *Recycling and the Canadian Pulp and Paper Industry, Research Program Committee of Paprican Report*: 1-42 (1989).
5. CROW, D.R. and SECOR, R.F., "The Ten Steps of Deinking", *TAPPI, 70(7)*: 101-106 (1987).
6. BORCHARDT, J.and TUTUNJIAN, P.and PRIETO, N., "Possible Deinking Mechanisms and Potential Analogies to Laundering", *Progress in Paper Recycling*: 47-53, February (1993).
7. WEED, D.C., "Deinking Chemicals-Selection Factors and Criteria", *Developments in Wastepaper Technology Conference Proceedings*, March 24-25 (1993).
8. KOFFINKE, R.A., *TAPPI, 63(11)*:51 (1980).
9. BLAIN, T.J., "The Process of Flotation Deinking", *1992 Contaminant Problems and Strategies in Wastepaper Recycling Seminar Proceedings*: 113-120, Cincinnati, Ohio, 28-30 April (1992).
10. POVRY, J., "Recycled Fibre - An Underutilised Opportunity, Report No.3": 95 (1990).
11. SPANGENBERG, J., "Secondary Fibre Recycling", TAPPI PRESS, Chapter 15 (1993).
12. ORTNER, H.E., "Recycling of Papermaking Fibres" , TAPPI PRESS, Atlanta, (1981).

13. ORTNER, H.E., in Pulp and Paper Manufacture, *CPPA/TAPPI Joint Textbook Committee of the Paper Industry*, Paprican, Pointe-Claire, (1987).
14. PAPRICAN, "Recycling and the Canadian Pulp and Paper Industry", Paprican, Pointe-Claire.
15. FERGUSON, L.D, *Progress in Paper Recycling* 1(1): 17 (1991).
16. ORTNER, H.E., in *Pulp and Paper Manufacture, Vol. 3, Secondary Fibres and Non Wood Pulping*, M.J. Kocurek Ed.: 206-220 (1987).
17. SMOOK, G.A., "Handbook for Pulp and Paper Technologists: Second Edition": 215-219.
18. FERGUSON, L.D., "A Review of Flotation Deinking Technology", *Recycled Paper Technology: An Anthology of Published Papers* (1994).
19. PERRY, R.H. and GREEN, D., "Perry's Chemical Engineer's Handbook, Sixth Edition", McGraw Hill Book Company (1984).
20. SCHUMANN, R., "Flotation Kinetics", *J. phys. Chem.*, 46: 891 (1942).
21. GAUDIN, A.M., "Flotation", Chapter 6, McGraw Hill Book Company, New York (1932).
22. TOMLINSON, K.I. and DOLOTOVA, I.A. and LITOVKA, V.G., promyslennom vnedrenii masiny instituta gasgorchimproekt margancevych obogatitel'nych fabrikach. - Obogascenie rud (Mechanobr.) 17: 19 (1972).
23. DORRIS, G.M. and NGUYEN, N., "Flotation of Model Inks. Part 2. Flexo Ink Dispersions Without Fibres", *2nd Research Forum On Recycling Proceedings*: 13-22 (1993).
24. JANCAREK, J., Der Einflu der Flotationsmaschinen verschiedener Bauart auf die Magnesitflotation. - Freiberger Forschungsh. A. 446:39 (1968).
25. JANCAREK, J.: Ein Beitrag zur Theorie der Flotationsgeschwindigkeit. - Bergakademie 16 4/5: p.257 (1964).
26. LENGLER, P. and HOFMANN, H.: Eine neue Modellvorstellung zur Kinetik der Flotation. Entwicklung der Grundgleichungen. - VDI-Ber. 182: p.123 (1972).
27. SCHULZE, H.J., "The Fundamentals of Flotation Deinking In Comparison To Mineral Flotation", *1st Research Forum on Recycling Proceedings*: 161-167, October 29-31 (1991).

28. SCHULZE, H.J., "Physio-Chemical Elementary Processes In Flotation", VEB Verlag der Wissenschaften, Berlin (1983).
29. PAN, R. and PAULSEN, F.G. and JOHNSON, D.A. and BOUSFIELD, D.W., "A Global Model For Predicting Flotation Efficiency. Part I: Model Results and Experimental Studies", *Tappi J.*, 79(4):177-185 (1996).
30. PAN, R. and PAULSEN, F.G. and KOCER, H. and NEREZ, R and JOHNSON, D.A. and BOUSFIELD, D.W., "A Global Model For Predicting Flotation Efficiency. Part II: Particle Size and Flotation Rate Predictions, and Experimental Studies and Comparisons", *1994 Recycling Symposium Proceedings*: 291-301, 15-18 May (1994).
31. PAN, R. and BOUSFIELD, D.W. and JOHNSON, D.A., "Modelling Particle-Bubble Dynamics and Adhesion in Air Bubble/Solid Particle/ Liquid Systems", *1992 Pulping Conference Proceedings*: 941-956, 1-5 November (1992).
32. SILVERI, L., "1989 TAPPI Annual Meeting Proceedings", TAPPI PRESS, Atlanta: 59 (1989).
33. RODDA, M.E., *Pulp Paper, 55(7)*: 128 (1981).
34. LeBLANC, P.E and McCOOL, M.A, "1988 TAPPI Pulping Conference Proceedings", TAPPI PRESS, Atlanta: 661 (1988).
35. DARMSTADT, W., "IFRA Special Report on Deinking of Wood-Containing Secondary Fibres", Germany (1988).
36. MCCOOL, M.A and CARROLL, W.P., "Pressurized Deinking Module", *1990 TAPPI Pulping Conference Proceedings*: 145-152 (1990).
37. Shinama Technical Brochure, 1991.
38. CARLETTI, C. and WOOD, R.J., "Spidercel Reactor Technology Improves Flotation Deinking Efficiency. New Cell Design Permits Use of Variable-Quality Recovered Paper Grades", *82nd Annual Meeting of the Technical Section Proceedings*: A293-A296 (1996).
39. "Spidercel Deinking Cell", Comer Technical Brochure.
40. DESSUREAULT, S. and BARBE, M.C. and LEVESQUE, M., "Column Flotation: A New Technology For Deinking Recycled Pulp".
41. CARABIN, P. and DESSUREAULT, S. and BARBE, M.C. and KLEUSER, J. and WARD, K., and MAGNY, R., "Flotation Column Deinking of MOW".

42. "MAC Cell-Deinking Cell", Thermo Black Clawson Inc, Technical Brochure.
43. "Deinking Ecocell Flotation Cells", Voith Sulzer Technical Brochure (1996).
44. JAMIESON, G.J., NAM, S. and MOO YOUNG, *M., Minerals Sci., Engng. 9(3)*:103 (1977).
45. MILANOVA, E. and DORRIS, G.M, "Flotation of Model Inks, Part 1: Experimental Methods", *79th CPPA Conference Proceedings*, January 26-29: A85-A95 (1993). 45
46. BORCHARDT, J.K., "Effect of Process Variables in Laboratory Deinking Experiments", *1992 Pulping Conference Proceedings*: 749-763, November 1-5 (1992).
47. Voith, technical brochure.
48. Adirondack Machine Corporation, technical brochure.
49. Courtesy of http: www.mm.mtu.edu/test/teisele.html
50. LINCK, E. and Britz, H., "Ink and Speck Removal Efficiency - A Matter of the Right Flotation Cells", *1990 TAPPI Pulping Conference*: 123-131, (1990).
51. PFALZER, L., "Deinking Technology and Its Application in Waste Paper Recycling", Voith Inc., Appleton, WI, USA, Technical Literature.
52. PFALZER, L., "Flotation Deinking and Waste Paper Recycling Systems", *1989 TAPPI Pulping Conference Proceedings* : 43-47 (1989).
53. HARRISON, A., "Flotation Deinking is Critical in Unit Process Method of Deinking", *Pulp Paper 3, no.3*: 60-65, March (1989).
54. SZATKOWSKI, M. and FREYBERGER, W.L., "Model Describing Mechanism of the Flotation Process", *Trans. Instn. Min. Metall. (Sect. C: Mineral Process Extr. Metall.) 94*: C129-135, September (1985).
55. MARCHILDON, L. and LAPOINTE, M., and CHABOT, B., "The Influence of Particulate Size in Flotation Deinking of Newsprint", *1988 CPPA Annual Meeting Technical Section: B61-65* (1988).
56. ORTNER, H.E., "Flotation Deinking", *Recycling of Papermaking Fibres:* 1-33 (1981).
57. ACKERMANN, C. et al, "Deinkability of Waterborne Flexo Inks by Flotation", *2nd Research Forum on Recycling, CPPA*: 201-215 (1993).
58. SCHULZE, H., "The Elementary Steps of Particle/Bubble Interaction in Flotation and

Some Ideas to Increase Its Efficiency by External Energy", *8th International Conference on Surface and Colloid Science, Abst. E37*, February (1994).

59. READ, B., "The Chemistry of Flotation Deinking", 1991 TAPPI Pulping Conference: 851-856, TAPPI Proceedings (1991).
60. DORRIS, G.M., "Chemistry and Technology of Deinking Processes", *Course notes for course 302-538B given at McGill University, Montreal, Quebec.*
61. JARREHULT, B. and HORACEK, R.G. and LINDQUIST, M.L., "Deinking of Wastepaper Containing Flexographic Inks", *1989 Tappi Pulping Conference Proceedings* (1989).
62. LARSON, A. and STENIUS, P. and ODBERG, L., *Svensk Papperstidn., 87(18)*: R158 (1984).
63. LARSON, A.and STENIUS, P. and ODBERG, L., *Svensk Papperstidn., 87(18)*: R165 (1984).
64. BLECHSCHMIDTH, J. and NAIYOCK, H-J., *XX Eucepa Conference*, Budapest, I-4, (1982).
65. ISLER, W. Entstehung und abscheidung von luftblasen in technischen papierstoffsuspensionen. Thesis no. 6063, ETH, Zurich, Germany, (1978).
66. DONGMING, L.and FITZPATRICK, J. A.and SLATTERY J.C., "Rate of Collection of Particles by Flotation", *Ind. Eng. Chem. Res. 29, no. 6*: 955-967 (1990).
67. MARCHILDON, L. and CASTRO, C. and DANEAULT, C. and LAPOINTE, M., "Comparison Between Carbon Dioxide and Air in the Batch Flotation", *1992 Pulping Conference Proceedings*: 957-962, 1-5 November (1992).
68. FERGUSON, L.D., "Deinking Chemistry", *1995 Deinking Short Course*, Vancouver, WA, USA, 4-7 June (1995).
69. READ, B.R., "1991 Pulping Conference Proceedings"., TAPPI PRESS, Atlanta: 851 (1991).
70. MAK, N., "Characteristics of Fatty Acids as an Effective Flotation Deinking Collector", *CPPA 2nd Research Forum on Recycling*: 145-146 (1993).
71. MORELAND, R., "Changes in Deinking Chemistry", *PIMA Magazine*: 50-52, June (1992).
72. PUTZ, H.J. and Schaffrath, H.J. and Gottsching, L., "CPPA Recycling Forum

Proceedings": 183 - 190, October (1991).

73. BECHSTEIN, G., *Das Osterreichishe Papier 12 (4) 16* (1975).
74. HORACEK, R.G. and JARREHULT, B., *Pulp and Paper 63(3)*: 97 (1989).
75. BORCHARDT, J.K, "An Introduction To Deinking Surfactants", *1993 Recycling Symposium Proceedings,* New Orleans, USA, February 28-March 4 (1993).
76. Temanex Consulting Inc., "Fibre Deterioration from Repeating Recycling and Paper Recycling Simulation Model: Executive Summary", *Progress in Paper Recycling*: 61-63, August (1993).
77. GOSS, R.B. and JOHNSON, A.E., "Polysolv Process Proceedings", *1969 TAPPI Secondary Fibre Conference,* Syracuse, NY, September 24-26 (1969).
78. ALDRICH, L.C., "A New Look at Deinking With Solvents", *TAPPI 60(8)* (1977). 78
79. HOWARD, R.C, "Effect of Recycling on Paper Quality", *Recycling and the Canadian Pulp and Paper Industry, Research Program Committee of Paprican Report*: 2-5, September (1989).
80. WULTSCH, F. and MAIER, K., *Das Papier 16(10A)*:533-540 (1962).
81. ERIKSSON, E., Paper presented at the Symposium Deinking of Waste Paper, Soc. Chem. Ind., Paper & Textile Chelicals Group and Technical Div. BPBIF, London, April 19-20 (1979).
82. HOWARD, R.C, "Effect of Recycling on paper quality", *Recycling and the Canadian Pulp and Paper Industry, Research Program Committee of Paprican Report*: 5-10, September (1989).
83. MINOR, J., "Hornification: Its Origin and Meaning", *Progress in Paper Recycling*: 93-95 February (1994).
84. KOFFINKE, R.A., "Pulping Developments in the Secondary Fibre Field", *TAPPI 63(11), November* (1980).
85. CARR, W.F., "Many Problems Involved in Increasing Utilization of Waste Paper", *Paper Trade J.* (May 17, 1971).
86. BAXTER, J., Jr., "A Solid Waste Disposal System - Fibreclaim", *1970 TAPPI Secondary Fibre Pulping Conference Proceedings* (1970).
87. MAK, N., "Characteristics of Fatty Acid as an Effective Flotation Deinking Collector", *2nd Research Forum on Recycling, CPPA*: 145-152 (1993).

88. SCOTT, DON L., "Ask Your Question", *Progress in Paper Recycling*: 106-109, August (1993).

89. DEXTER, R.J., "Field Uses of Scanning Dirt Counter Technology", *Progress in Paper Recycling*: 40-41, August (1993).

90. MCCOOL, M.A., and TAYLOR, C.J., *TAPPI J., 66(8); 69* (1983).

91. NGUYEN, N.G. and O'NEILL, M.A. and WORDAN, B.D. and DORRIS, G.M., *1991 Recycling Forum Proceedings*, CPPA, Ponte-Claire: p.169 (1991).

92. SCHRIVER, K.C. and VOOSEN, L.L and BINGHAM, S.J., *1991 Pulping Conference Proceedings*, TAPPI PRESS, Atlanta: p.1009 (1991).

93. SCOTT, D. and BLISS, T.L., *1991 Pulping Conference Proceedings*, TAPPI PRESS, Atlanta: p.988 (1991).

94. Laboratory test results obtained from Paprican, Pointe-Claire.

95. SCHULZE, H.J., *Mineral Processing and Extractive Metallury Review* 5:43 (1989).

96. AHMED, N. and JAMESON, G.J., "Flotation Kinetics", *Mineral Processing and Extractive Metallury Review*: 5:77-79 (1989).

97. RAO, R. and STENIUS, P., "The Effect of Flotation Deinking Chemicals on Bubble Formation", *4th Research Forum on Recycling* : 11-16 (1997).

98. WALMSLEY, M.R.W., "Air Bubble Motion in Wood Pulp Fibre Suspension", *APPITA* '92: 509-515 (1992).

99. AJERSCH, M. and PELTON, R., "The Growth of Bubbles on Pulp Fibres and on Carbon Black Dispersed in Supersaturated Carbon Dioxide Solutions", *Nordic Pulp and Paper Research Journal*: 2: 129-135 (1994).

100. DRABEK, O. and STERNE, J. and VAN DE VEN, T.G.M., "Effect of Deinking Chemicals on the Deposition of Fines and Fillers on an Air-Water Interface", JPPS, 24(4): 116-120 (1998).

101. Personal photograph taken in 1997 at Perkins Paper Ltd. (Candiac, Quebec, Canada).

102. Sulzer Escher Wyss manual.

103. Personal photograph taken at Dr. Theo van de Ven's laboratory of the Pulp and Paper Research Centre of McGill University.

104. Photograph taken by Paprican Machine Shop personnel at Paprican (Pointe-

Claire, Quebec, Canada).

105. CLIFT, R. and GRACE, J.R. and WEBER, M.E., *Bubbles, Drops and Particles*, Academic Press, New York (1978).

106. VAN DE VEN, T.G.M., *Colloidal Hydrodynamics*, Academic Press, New York (1988).

107. LUO, H. and SVENDSEN, H.F., "Theoretical Model for Drop and Bubble Breakup in Turbulent Dispersions", *AIChE Journal* 42(5):1225-1233 (1996).

108. HESKETH, R.P. and ETCHELLS, A.W. and RUSSELL, T.W.F, "Bubble Breakage In Pipeline Flow", Chemical Engineering Science 46(1):1-9 (1991).

109. MODARESSI, H., "Hydrodynamics of a Loop Bioreactor Using a Spinning Sparger", Master of Science in Chemical Engineering Thesis from the University of Saskatchewan (1996).

110. KOCER, H.; JOHNSON, D.; and THOMPSON, E., "Influence of Air Flow Rate, Time and Total Air Volume on Efficiency of Toner Removal in Mixed Office Waste Flotation", *1995 Recycling Symposium Proceedings*, pp. 65-72 (1995).

111. YU, C., "Effect of Consistency, Volume and Residence Time on Laboratory Flotation Performance", *1994 Recycling Symposium Proceedings*, pp. 393-397 (1994).

112. ZABALA, J. and MCCOOL, M., *TAPPI J.*, 71 (8): 62 (1988).

113. IONIDES, G.N., "Trip Report From European Deinked Newsprint Mill Visits", Temanex Consulting Report.

114. RAIMONDO, F.E., "Deinking of Printed Wastepapers by Flotation", *TAPPI J.*, 50 (9): 69A (1967).

115. DORRIS, G., "Ink Detachment and Flotation Efficiency in ONP/OMG Blends. Part 1: Effect of Specimen Preparation Procedure on Estimates", JPPS 25 (1): 1-9 (1999).

116. BORCHARDT, J.; MATALAMAKI, D.; LOTT, V.; and RASK, J., "Pilot Mill and Laboratory Deinking Studies Using Office Paper Furnishes Containing Photocopied and Laser-Printed Papers", *1994 Recycling Symposium Proceedings*, pp. 449-475 (1994).

117. LETSCHER, M. and SUTMAN, F., "The Effects of Magazine and Filler on the Flotation Deinking of Newsprint", JPPS, 18 (6): J225-J230 (1992).
118. HARWOT, P. and VAN DE VEN, T.GM., "Effects of Sodium Oleate and Calcium Chloride on the Deposition of Latex Particles On An Air-Water Interface", Colloids and Surfaces, **A121**: 229-237 (1997).
119. Paprican Ink Scanner brochure.
120. Scanned images attained using the Paprican Ink Scanner.

APPENDIX A

PUMP BLUEPRINT

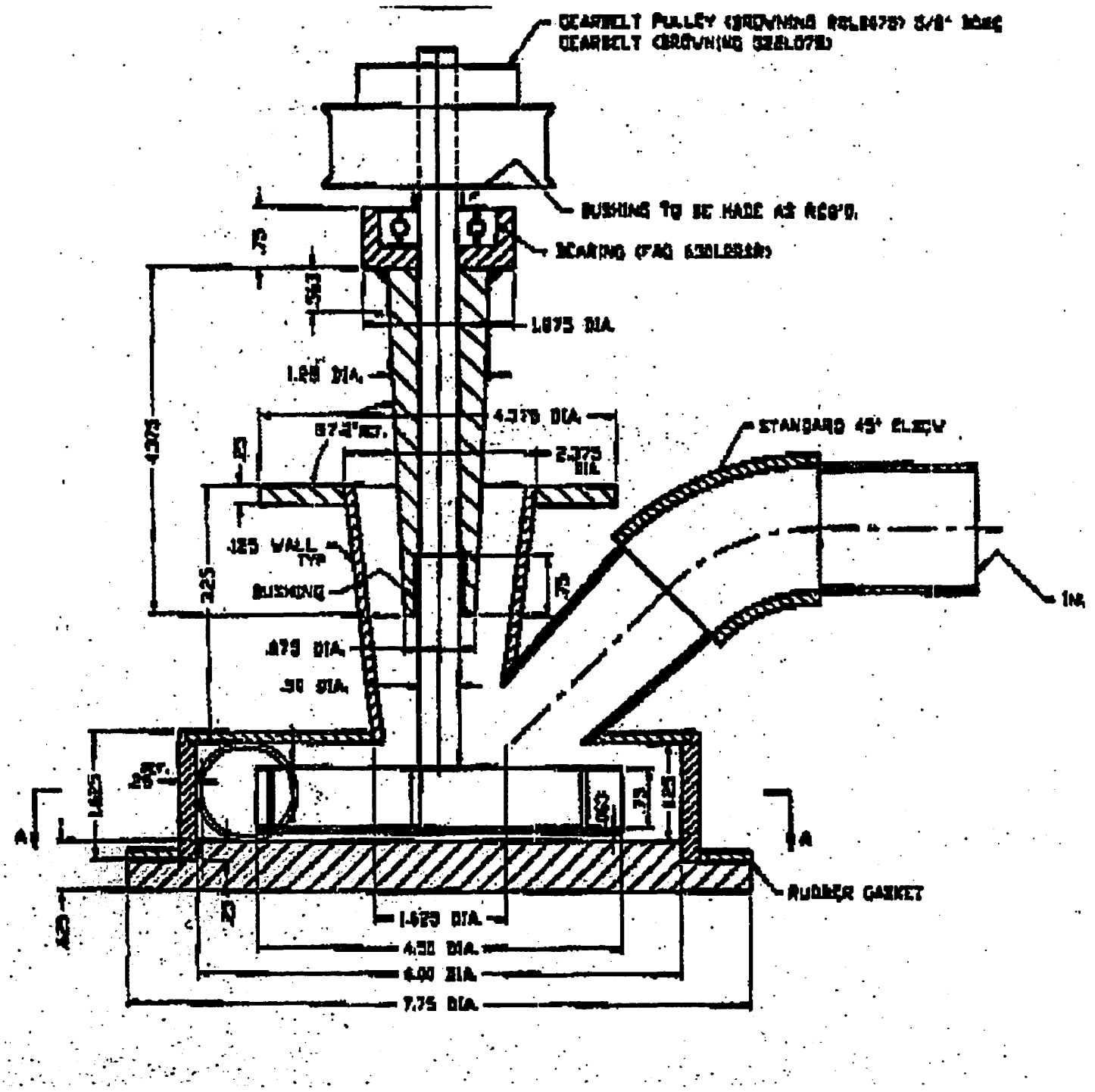

Figure A.1. Cross-Sectional Blueprint of the Pump (reservoir section not shown)

APPENDIX B

OTHER LOOP CONFIGURATIONS

The air-injection unit has a versatile design in that it can be dismantled or pieced-together quickly and easily due to its modular construction made possible with the use of PVC unions. Two larger loop-configurations, shown below in figures B.1 and B.2, can be constructed but were not discussed in Chapter 2. In figure B.2 the image cell is positioned 81.5 cm further downstream from the pump. These configurations are constructed by adding two 81.5 cm lengths of 4 cm I.D. PVC pipe. These extension pieces add 2048 ml to the loop bringing its total volume to 8660 ml at the 4.5 cm mark on the pump reservoir measuring tape.

Figure B.1. Large Loop Configuration

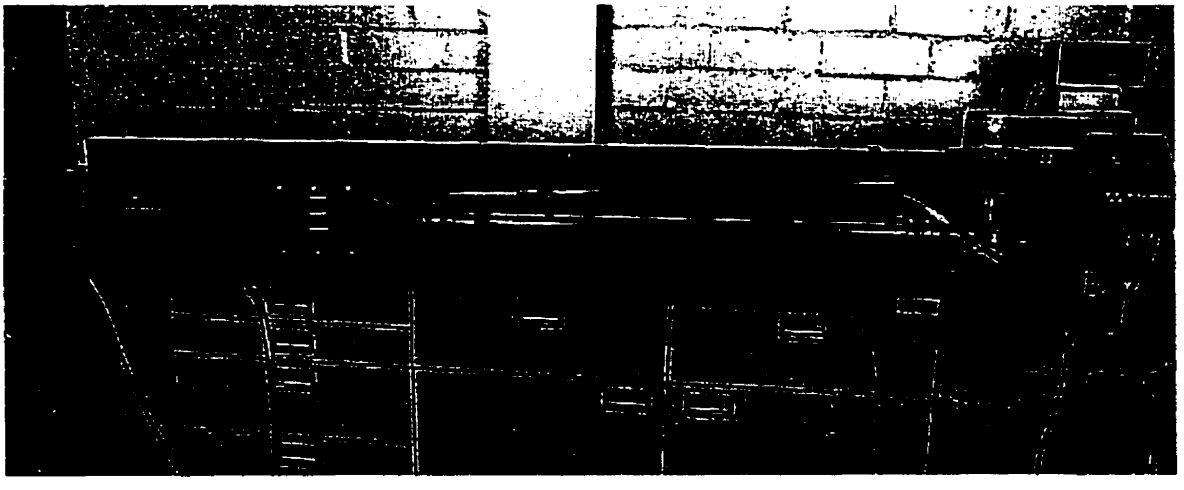

Figure B.2. Large Loop Configuration With the Image Cell Positioned Further From the Pump

APPENDIX C

LOOP VOLUME CALIBRATION DATA

Table C1. Small Loop Volume Calibration Data

Loop Volume (ml)	Level on Tape Measure (cm)	Loop Volume (ml)	Level on Tape Measure (cm)
5950	2.32	6850	5.31
6000	2.41	6900	5.49
6050	2.55	6950	5.67
6100	2.75	7000	5.80
6150	2.88	7050	5.99
6200	3.07	7100	6.18
6250	3.33	7150	6.32
6300	3.48	7200	6.50
6350	3.60	7250	6.68
6400	3.79	7300	6.89
6450	3.96	7350	7.05
6500	4.18	7400	7.23
6550	4.29	7450	7.38
6600	4.46	7500	7.58
6650	4.63	7550	7.75
6700	4.81	7600	7.90
6750	4.98	7650	8.13
6800	5.15		

Note: For the large loop configuration volume calibration, add 2048 ml to the volume data in Table C.1.

APPENDIX D

FLYGT "FLOAT-WASH" FRACTIONATOR SCHEMATIC AND OPERATING PROCEDURE

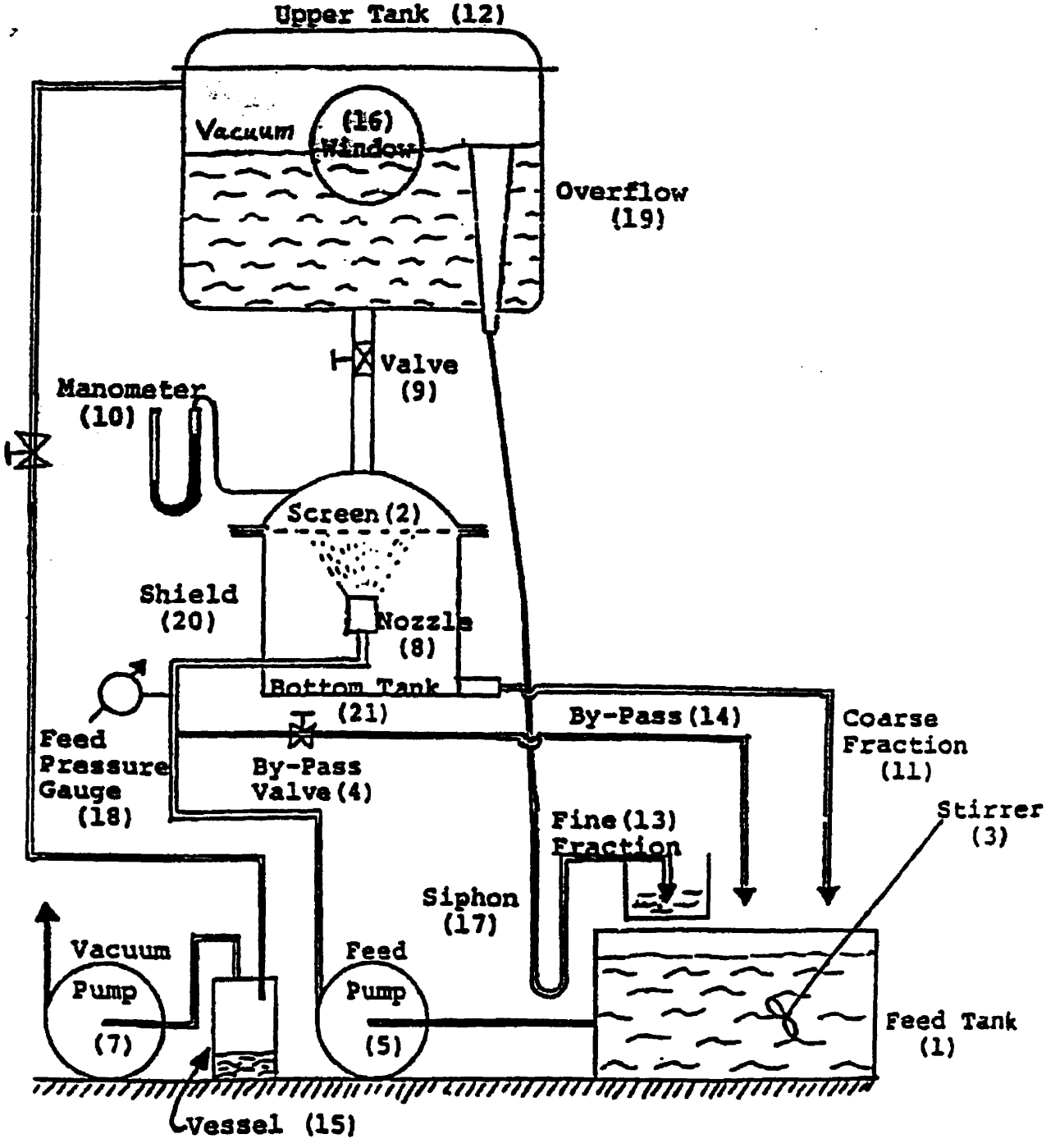

Figure D.1. Flygt "Float-Wash" Fractionator Schematic

Fibres/Fines Separation Procedure Using The Float-Wash

1. Install the 150 micron (100 mesh) screen. Be sure to use a reinforcing coarse screen backing.

2. Fill the accept reservoir (also called the "upper tank") with water to equalize the separating conditions at start-up.

3. Put the disintegrated pulp in the reservoir (also called the "feed tank") and dilute to approximately 0.15 - 0.20 % consistency; start the mixer.

4. Make sure that all the valves are in the desired positions.

5. Start with the accept valve set to return fines to the feed tank. Leave it this way long enough to replace the water with fines.

6. Close the pump bypass to obtain 20 kPa (3 psi) at the spray.

7. Carefully open the valve over the screen after having started the vacuum pump (only a differential of 2 to 5 mm of water is necessary which is measured by a manometer); adjust the vacuum slowly to increase the visually observed consistency of the retained long fiber.

8. Set the fines return valve to recover the fines in the collecting tanks.

9. Stop when the main reservoir is at 1/3 of the initial volume or when the consistency of the feed is too high.

10. Dilute again to approximately 2/3 of the initial volume and recover fines in a second pass.

11. After the run is complete, do not forget to transfer the fines remaining in the upper tank to the collecting tanks.

12. After no less than 16 hours decant the clear supernatant from the tanks containing the settled fines.

13. You should now have between 60 to 80 grams (oven dried) of fines from a starting weight of 300 to 400 grams (oven dried) of Thermal Mechanical Pulp (TMP) in a 200 liter tank.

14. Clean all the parts of the Float Wash thoroughly.

APPENDIX E

AIR BUBBLE SIZE DISTRIBUTION HISTOGRAMS (CHAPTER 2 - RUNS 2-5 and 7)

Figure
movin

Figure
movin

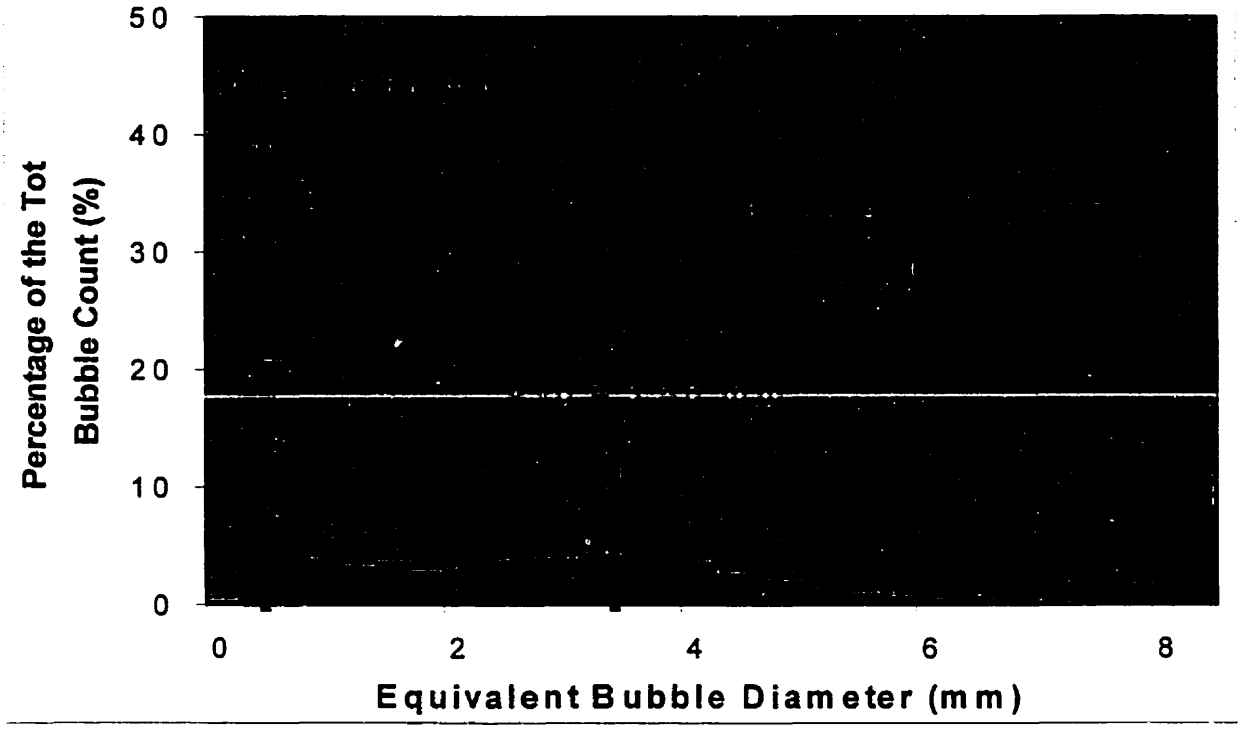

Figure E3. Bubble Size Distribution Histogram for Run 4 (Tap water moving at 1 m/s with 0.2% consistency TMP fibres and 6% volume fraction air)

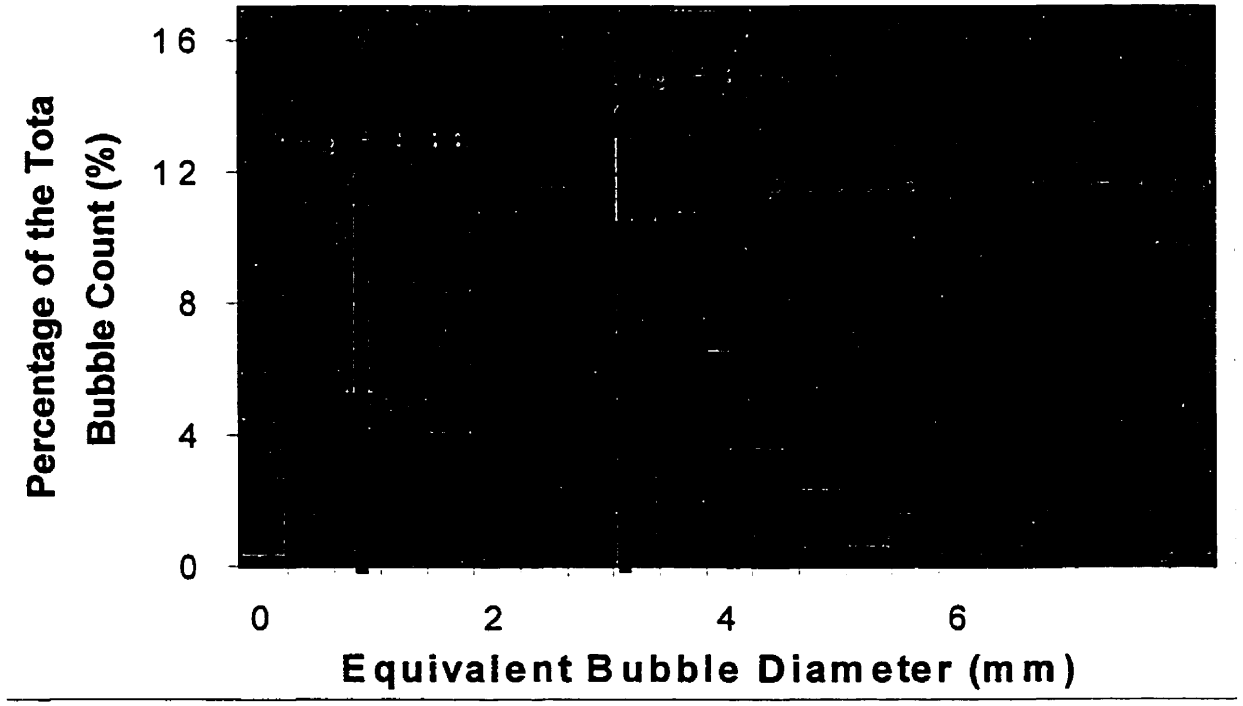

Figure E4. Bubble Size Distribution Histogram for Run 5 (Tap water moving at 1 m/s with 0.2% consistency TMP fines and 6% volume fraction air)

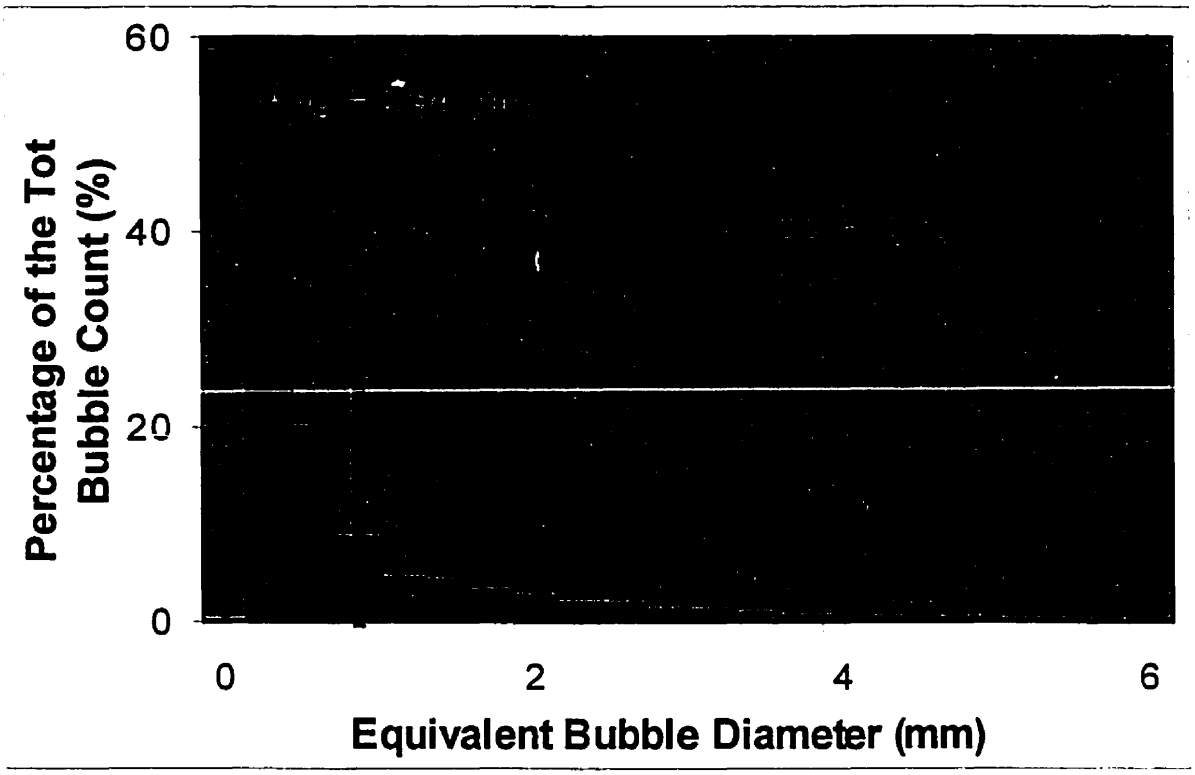

Figure E5. Bubble Size Distribution Histogram for Run 7 (Tap water moving at 1 m/s with 0.2% consistency TMP fibres, 0.07 mmol/L Sodium Oleate, 0.09 mmol/L Calcium Chloride, and 6% volume fraction air)

APPENDIX F

CALIBRATION OF PUMP RPM and FLUID VELOCITY USING A DOPPLER FLOWMETER

Table A1. Calibration of Pump RPM and Fluid Velocity

Pump RPM	Doppler Velocity Measurement (m/s)
350	0.424
400	0.515
450	0.588
500	0.629
526	0.642
550	0.698
600	0.748
650	0.822
700	0.888
738	0.927
750	0.93
800	1.001
850	1.058
900	1.110
949	1.174
1000	1.225
1050	1.274
1100	1.337
1150	1.382
1200	1.435
1250	1.493
1300	1.542

APPENDIX G

FLOW PATTERNS IN THE FLOTATION VESSEL WITH AND WITHOUT THE 6 INCH HIGH BAFFLE

Flow Patterns In the Flotation Cell With and Without the 6 Inch High Baffle

The following six pictures (Figures B1 – B6) illustrate how the presence of the baffle in the flotation vessel affects the flow pattern. The fiber consistency in the flotation cell was 2 percent. The flotation cell was operated with and without the 6 inch high baffle at three different suspension velocities (0.5, 1.0 and 2.0 m/s) for 10 minutes, in order for an equilibrium flow pattern to be attained. *The presence of the baffle increased the resistance to flow within the cell and decreased the suspension velocity within the flotation cell pipes by 2-3 percent, as measured with a Doppler flowmeter.*

The natural circulation pattern in the cell without the presence of the baffle is a clockwise flow pattern. The presence of the baffle forces the flow to pass up and over the baffle strongly changing the natural flow pattern.

Considering the 0.5 m/s cases, the scenario with the baffle (Figure B1) led to more symmetric fiber settling on the right and left sides of the vessel. The scenario without the baffle (Figure B4) led to settling primarily on the right side of the vessel due to the strong clockwise circulation pattern within the cell.

Considering the 1.0 m/s cases, the scenario with the baffle (Figure B2) led to some settling throughout the cell (particularly in the center). The scenario without the baffle (Figure B5) experienced superior mixing within the flotation vessel and led to a small amount of settling on the right side of the vessel.

Considering the 2.0 m/s cases, both scenarios with and without the baffle (Figures B3 and B6) led to intense mixing throughout the cell with negligible amount of fiber settling.

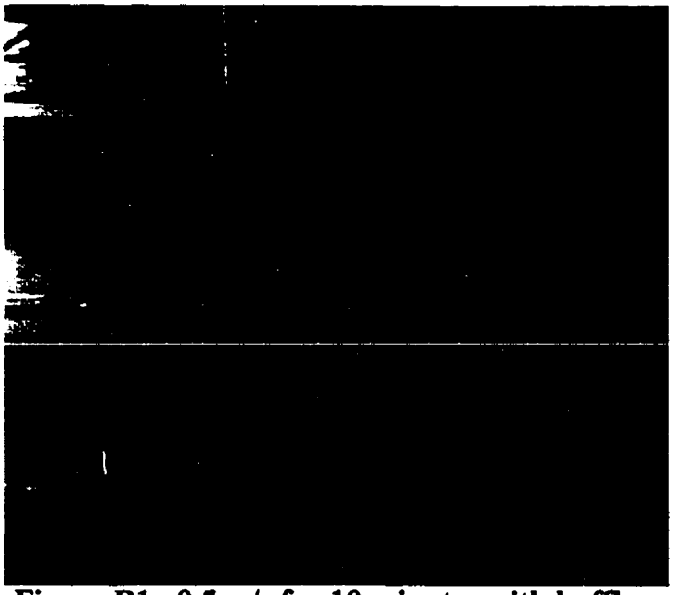

Figure B1. 0.5 m/s for 10 minutes with baffle

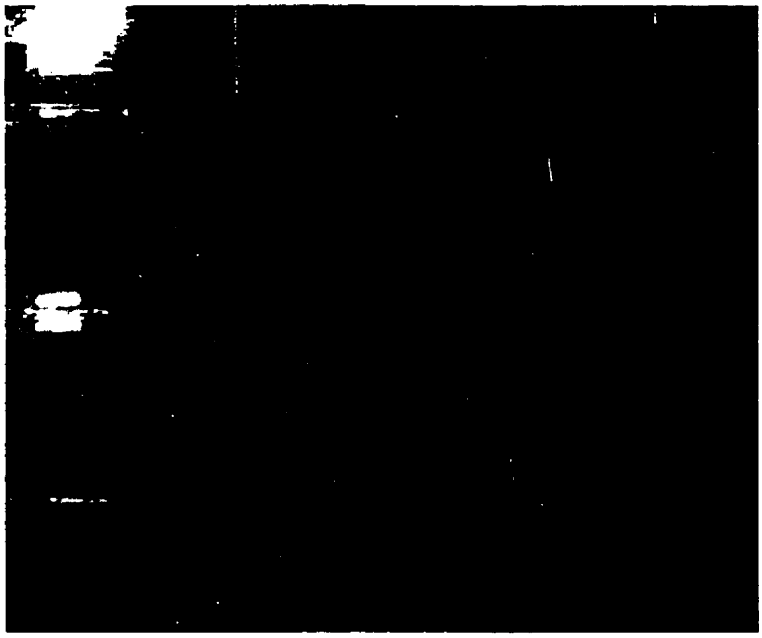

Figure B2. 1.0 m/s for 10 minutes with baffle

Figure B3. 2.0 m/s for 10 minutes with baffle

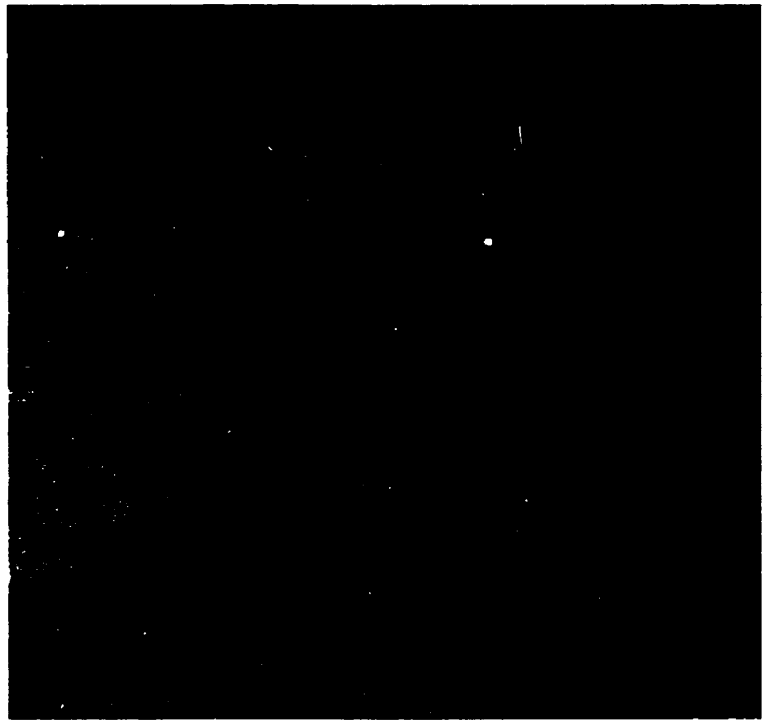

Figure B4. 0.5 m/s for 10 minutes without baffle

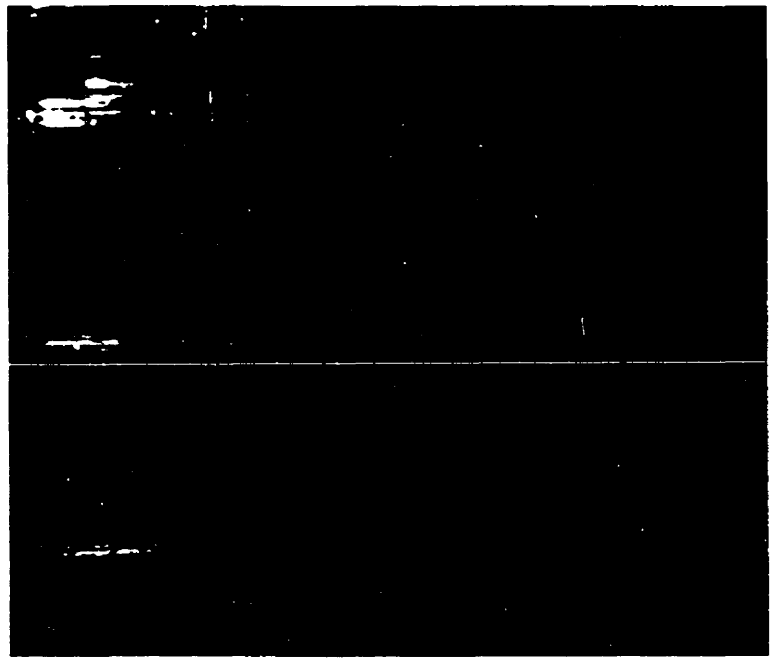

Figure B5. 1.0 m/s for 10 minutes without baffle

Figure B6. 2.0 m/s for 10 minutes without baffle

APPENDIX H

TABULATED RESULTS FOR CHAPTER 3 (RUNS 1-6)

Tabulated Results For Runs 1 - 6

Table C1. Run 1 Results

	Speck #	Speck #/cm2	Average Speck Diameter (μm)	% Coverage	Brightness	ERIC
BF #1	8130	5576	22.00	3.172	47.38	913.71
BF #2	7831	5371	22.05	3.129	47.60	904.43
Average BF	7980.5	5473.5	22.02	3.150	47.49	909.07
5 min	5816	3989	19.40	1.724	49.33	761.16
15 min #1	4186	2871	17.78	1.060	50.50	670.30
15 min #2	4014	2753	18.19	1.040	50.71	661.11
Average 15 min	4100	2812	17.985	1.050	50.60	665.70
30 min #1	3885	2665	17.51	0.931	51.68	602.45
30 min #2	3593	2464	17.77	0.867	51.79	588.55
Average 30 min	3739	2564.5	17.64	0.899	51.73	601.00

Table C2. Run 2 Results

	Speck #	Speck #/cm2	Average Speck Diameter (μm)	% Coverage	Brightness	ERIC
BF #1	7576	5196	22.54	3.140	47.57	903.72
BF #2	7266	4984	22.87	3.060	47.61	894.00
Average BF	7421	5090	22.705	3.100	47.59	898.86
5 min #1	5293	3630	19.17	1.552	49.82	724.13
5 min #2	5206	3571	19.50	1.559	49.69	730.47
Average 5 min	5249.5	3600.5	19.34	1.540	49.76	727.30
15 min #1	3817	2618	17.76	0.923	51.30	624.54
15 min #2	3961	2717	17.87	1.006	51.13	629.68
Average 15 min	3889	2667.5	17.82	0.964	51.22	627.11
30 min #1	3602	2471	17.39	0.859	51.89	587.92
30 min #2	3453	2368	18.01	0.966	51.75	595.19
Average 30 min	3527.5	2419.5	17.7	0.912	51.82	591.56

Table C3. Run 3 Results

	Speck #	Speck #/cm2	Average Speck Diameter (μm)	% Coverage	Brightness	ERIC
BF #1	9092	6236	22.24	3.512	57.48	548.75
BF #2	8832	6058	22.28	3.467	57.67	539.94
Average BF	8962	6147	22.26	3.4895	57.58	544.34
5 min #1	3398	2331	18.86	0.873	62.69	288.76
5 min #2	3095	2123	18.97	0.829	62.69	287.83
Average 5 min	3246.5	2227	18.915	0.851	62.69	288.30
15 min #1	1241	851	17.52	0.293	64.95	202.59
15 min #2	1193	818	17.56	0.294	65.06	199.45
Average 15 min	1217	834.5	17.54	0.294	65.00	201.02
30 min #1	888	609	17.27	0.205	66.05	167.61
30 min #2	860	590	16.96	0.185	65.90	170.03
Average 30 min	874	599.5	17.117	0.195	65.98	168.82

Table C4. Run 4 Results

	Speck #	Speck #/cm2	Average Speck Diameter (μm)	% Coverage	Brightness	ERIC
BF #1	9623	6600	21.55	3.462	57.38	552.13
BF #2	8862	5941	21.28	3.029	57.74	534.47
Average BF	9242.5	6270.5	21.42	3.2455	57.56	543.30
5 min #1	3176	2178	19.27	0.899	62.64	286.37
5 min #2	3211	2202	19.30	0.889	62.88	284.14
Average 5 min	3193.5	2190	19.285	0.894	62.76	285.26
15 min #1	1152	790	17.49	0.267	65.11	198.55
15 min #2	1114	798	17.49	0.272	65.19	196.67
Average 15 min	1158	794	17.49	0.2695	65.15	197.61
30 min #1	808	554	17.50	0.188	66.09	170.55
30 min #2	889	610	17.08	0.195	66.13	170.73
Average 30 min	848.5	582	17.29	0.192	66.11	170.64

Table C5. Run 5 Results

	Speck #	Speck #/cm2	Average Speck Diameter (μm)	% Coverage	Brightness	ERIC
BF #1	11422	7834	21.30	3.988	56.33	617.95
BF #2	10866	7453	21.29	3.814	56.68	603.43
Average BF	11144	7643.5	21.30	3.901	56.50	610.69
5 min #1	1537	1054	16.51	0.306	64.64	209.19
5 min #2	1545	1060	16.41	0.296	64.87	203.99
Average 5 min	1541	1057	16.46	0.301	64.75	206.59
15 min #1	708	486	16.47	0.139	66.13	152.78
15 min #2	754	517	16.26	0.141	66.86	145.52
Average 15 min	731	501.5	16.36	0.140	66.50	149.15
30 min #1	682	468	16.16	0.125	67.36	129.94
30 min #2	719	493	16.95	0.164	67.37	128.91
Average 30 min	700.5	480.5	16.56	0.1445	67.36	129.43

Table C6. Run 6 Results

	Speck #	Speck #/cm2	Average Speck Diameter (μm)	% Coverage	Brightness	ERIC
BF #1	10862	7450	21.64	3.844	56.64	605.68
BF #2	10289	7057	21.75	3.699	56.90	589.92
Average BF	10575.5	7253.5	21.70	3.772	56.77	597.80
5 min #1	1487	1020	17.33	0.331	64.79	210.40
5 min #2	1461	1002	17.00	0.297	64.85	208.07
Average 5 min	1474	1011	17.16	0.314	64.82	209.24
15 min #1	821	563	16.36	0.164	66.56	157.39
15 min #2	803	551	16.58	0.164	66.48	156.84
Average 15 min	812	557	16.47	0.164	66.52	157.12
30 min #1	724	497	17.13	0.161	67.37	137.61
30 min #2	719	493	16.54	0.140	67.13	139.50